THE LONGITUDINAL EFFECTS OF HIV AND ART ON THE DEVELOPING BRAIN: A STRUCTURAL MRI STUDY USING MANUAL SEGMENTATION

By Candidate

Steven Ronald Randall

Dissertation presented for the degree of

Doctor of Philosophy in Neuroscience

Faculty of Health Sciences

University of Cape Town

Date of Submission: August 2023

Supervisor: Dr Martha J Holmes

Co-supervisors: Prof Ernesta M Meintjes

Dr Christopher M Warton

PLAGIARISM DECLARATION

I, STEVEN RONALD RANDALL, hereby declare that the work on which this dissertation is based is my original work (except where acknowledgements indicate otherwise) and that neither the whole work nor any part of it has been, is being, or is to be submitted for another degree in this or any other university.

I authorise the University to reproduce for the purpose of research either the whole or any portion of the contents in any manner whatsoever.

ACKNOWLEDGEMENTS

I would like to acknowledge the parents and children who participated in the study.

I offer my gratitude to my supervisor Dr Martha Holmes, for her patience and understanding throughout the difficult years. I would like to thank my co-supervisors Professor Ernesta Meintjes, for the skills that I have learned under her guidance; Dr Christopher Warton, who has provided me with an immeasurable amount of knowledge. His wisdom and support was always be appreciated.

I would like to thank my co-authors Dr Barbara Laughton and Prof Andre van der Kouwe principal investigators of the neuroimaging study. Prof Mark Cotton for access to the clinical and demographic data. Professor Francesca Little for her extremely valuable statistical insights and consults. Dr Shalena Naidoo for immunological blood sample data and her valuable insights into helping me understand effects of some cytokines. Dr Allison Moreau and Leah Morgan for data pertaining to the FreeSurfer longitudinal pipeline. I further extend our gratitude to Kennedy Otwombe from the Perinatal HIV Research Unit and Christie Heiberg formerly of the Desmond Tutu HIV Foundation for assisting with clinical data requests; the CUBIC radiographers Marie-Louise de Villiers and Nailah Maroof; research staff Thandiwe Hamana, Rosy Khethelo and Anita Janse van Rensburg for assisting with data collection, study paediatrician Dr Els Dobbels, and Shabir A Madhi for facilitating the study.

A thank you to all students and postdoctoral fellows in the MRI laboratory who have been involved in data acquisition, management and image processing, and always open to discuss findings. Dr Natalie Strickland for her immunological expertise, Dr Catherine Riou for her invaluable insight and teaching of inflammatory processes and inference. To the people who have pulled me through, the past years have not been easy, since even before the pandemic, without your support I wouldn't be here, in no particular order but first on the list Chandra, Devin, Rob, Alicia, Claire, Carly.

A further heart-felt thank you to my parents Greg and Theresa Randall for their steadfast and endearing support throughout all my studies, I'm finally at the last step. In memorial of Troroy Carlos and Sheila Randall.

FUNDING AND AID

Support for this study was provided by NRF/DST South African Research Chairs Initiative; US National Institute of Allergy and Infectious Diseases (NIAID) through the CIPRA network, Grant U19 AI53217; NRF grant CPR20110614000019421, and the Medical Research Council (MRC). As well as my personal NRF PhD Scholarship. South African National Research Foundation (NRF) grants 48337, 99069 and 78737; NIH/NICHD grants R01 HD099846, R01 HD071664 and R01 HD093578; NIH/NIMH grants R21 MH096559 and R21 MH108346; NIH/National Institute of Allergy and Infectious Diseases (NIAID) Our thanks to GSK/Viivhealthcare for supplying of ARVs.

ABSTRACT

Background:

Previous neuroimaging research into the effects of HIV in paediatric populations receiving treatment has reported brain abnormalities across a variety of ages and modalities. There are limited longitudinal studies, which would clarify if the observed changes represented developmental delay or ongoing damage. In addition, most neuroimaging studies do not include links to functional, immunological, or genetic outcomes which aid in understanding the consequence, mechanisms and factors underlying the brain imaging abnormalities. There is a need for longitudinal work and interdisciplinary cross-sectional imaging studies to comprehend the consequences of the current literature.

To address literature gap, this thesis builds on a cross-sectional study, by the same author, of this group of 106 children who were perinatally infected with HIV (PHIV), and form part of "Children with HIV early antiretroviral"(CHER) trial who have been followed since birth (Violari et al. 2008; Laughton et al. 2012; Cotton et al. 2013). The study showed larger subcortical gray matter and smaller white matter in children with perinatal HIV infection compared to controls, at 5 years of age. This thesis presents a longitudinal follow-up to assess whether these morphometric differences persisted into later childhood, as well as assess possible early contributors that may exacerbate or predict certain highlighted disturbances observed from 5 to 10 years of age. We aim to determine if the volumetric abnormalities observed at age 5 years represent developmental delay or ongoing injury due to HIV infection. In addition, we seek to identify potential early immune markers and the 5-year-old volume changes to better understand contributing factors.

Methods:

MRI scans were obtained at ages 5, 7, and 9 years, on a 3 T Allegra MRI (Siemens, Erlangen, Germany), and 10 years 3 T Skyra Siemens. Images were manually traced, by the author, for volumes of basal ganglia structures and corpus callosum using MultiTracer. Twenty-seven individuals were rescanned to assess whether incorporation and integration of 10 year old scanner data with scans from previous ages on a different scanner was possible, as a result of decommissioning the 3 T Allegra scanner. Volumetric growth curves were fit for forty children using mixed effects models with subject-specific random effects, with adjustment for possible two-way interactions between age and diagnosis. We investigated linear, quadratic, cubic and logarithmic fits for each volume. A panel of 44 soluble blood biomarkers were obtained at enrolment for a small sample of infants living with HIV. Cytokine concentrations were Z-score transformed and principle component analysis (PCA) performed.

Results:

Manual segmentation was reproducible across the different 3 T scanners within this pediatric sample allowing for volumetric data to be combined into one model without a scanner confounder. Across volumes, logarithmic models performed best. Age-related decreases were observed across children in the bilateral caudate and globus pallidus, as well as the corpus callosum. HIV-related alterations to growth trajectories were observed in the right nucleus accumbens and bilateral putamen, driven by volume abnormalities reported at 5 years. HIV-related corpus callosum reductions previously reported at age 5 did not alter the growth trajectories.

PCA analysis identified a component associated negatively with subcortical volumes. Association with the derived component variable suggest that during the period of initial infection, in infancy, an increase of IL-10, IP-10, LBP and IFN-α, and accompanying decrease in IL-17F and CD40L contribute to smaller basal ganglia volumes at 5 years.

Conclusions:

This thesis expands cross sectional volumetric work which identified basal ganglia and corpus callosum volume abnormalities in 5-year-old PHIV children. Longitudinal analysis found the 5-year-old volumetric changes were likely HIV-related developmental delays, as volumes differences did not persist. The volume increases in the putamen affected the growth trajectories in PHIV and were related to early immunological factors associated with proinflammatory effects, immune activation and immune dysfunction. The volume decreases in the corpus callosum did not affect the age-related trajectory, and no cytokines related to volume abnormalities at 5 years. While cross sectional HIV-related results in PHIV are concerning, more work is needed to contextualize their consequences on growth and function.

Table of Contents

LIST OF FIGURES

LIST OF TABLES

LIST OF ABBREVIATIONS

TABLE OF ABBREVIATIONS

Abbreviation	-	Full Term
General		
SA	-	South Africa
SSA	-	Sub-Saharan Africa
AIDS	-	Acquired Immunodeficiency Syndrome
HIV	-	Human Immunodeficiency Virus
ART	-	Antiretroviral Therapy
ARV	-	Antiretroviral
HAART	-	Highly Active Antiretroviral Therapy
CHER	-	Children With HIV Early Antiretroviral Therapy
CIPRA	-	Comprehensive International Program For Research On AIDS In South Africa
CLWH	-	Children Living With HIV
CUBIC	-	Cape Universities Brain Imaging Centre
FAMCRU	-	
GMDS	-	Griffiths Mental Development Scales
HPE	-	HIV-Associated Progressive Encephalopathy Of Childhood
KID-CRU	-	Children's Infectious Diseases Clinical Research Unit
MeSH	-	Medical Subject Headings
MTCT	-	Mother-To-Child Transmission
PMTCT	-	Prevention Of Mother-To-Child Transmission
Immunological		
ATP	-	Adenosine Triphosphate
B-Cell	-	Bone Marrow Cell
CD#	-	Cluster Of Differentiation (4) E.G. CD4, CD8 T-Cells
CD4%	-	CD4 Percentage
DNA	-	Deoxyribonucleic Acid
gp	-	Glycoprotein
GM-CSF	-	Granulocyte-macrophage colony-stimulating factor
IL	-	Interleukin
MCP-1	-	Monocyte Chemoattractant Protein-1
LBP	-	Lipopolysaccharide Binding Protein
LTR	-	Long Terminal Repeats
MHC	-	Major Histocompatibility Complex
M-tropic	-	Macrophage Tropic
PCR	-	Polymerase Chain Reaction
PDGF-BB	-	Platelet Derived Growth Factor-BB
PVL	-	Plasma Viral Load
RANTES	-	Regulated upon Activation, Normal T Cell Expressed and Presumably Secreted
RNA	-	Ribonucleic Acid
mRNA	-	Messenger RNA
ssRNA	-	Single Stranded RNA
vRNA	-	Viral RNA
RT	-	Reverse Transcriptase
T-Cell	-	Thymus Cell
TNF	-	Tumor necrosis factor
VL	-	Viral Load
Imaging		
3 T	-	3 Tesla
AAM	-	Auto-Assisted Manual
aparc	-	Automatic Parcellation

aseg	-	Automatic Subcortical Segmentation
BOLD	-	Blood Oxygen Level Dependent
CT	-	Computerized Tomography
DTI	-	Diffusion Tensor Imaging
EPI	-	Echo-Planar Imaging
IBASPM	-	Individual Brain Atlases Using Statistical Parametric Mapping
MEMPRAGE	-	Multi Echo Magnetization Prepared Rapid Gradient Echo
MR	-	Magnetic Resonance
MRI	-	Magnetic Resonance Imaging
MRS	-	Magnetic Resonance Spectroscopy
fMRI	-	Functional Magnetic Resonance Imaging
PET	-	Positron Emission Tomography

Neuroanatomical

AC-PC	-	Anterior and Posterior Commissure
BBB	-	Blood-Brain-Barrier
Caud	-	Caudate
CC	-	Corpus Callosum
CNS	-	Central Nervous System
CSF	-	Cerebrospinal Fluid
GM	-	Grey Matter
GP	-	Globus Pallidus
ICV	-	Intracranial Volume
L	-	Left
R	-	Right
NA	-	Nucleus Accumbens
Pu	-	Putamen
ROI	-	Region Of Interest
TIV	-	Total Intracranial Volume
WM	-	White Matter

Statistical

ANCOVA	-	Analysis Of Covariance
ANOVA	-	Analysis Of Variance
BIC	-	Bayesian information criterion
CV	-	Coefficient of Variation
ICC	-	Intraclass Correlation
LME	-	Linear Mixed Effect
ME	-	Mixed Effect
N	-	Total Sample Size
n	-	Sub-sample/Subgroup Size
p.a.	-	Per Annum
SD	-	Standard Deviation
Wks	-	Weeks
Yrs	-	Years

THESIS OUTLINE

Note that chapters 5, 6 and 7 are presented in journal article format, with their own introduction and literature review.

- **Chapter 1** Introduces the research setting and provides motivation for the study in question.
- **Chapter 2** includes a brief background and literature review for the relevant topics of interest.
- **Chapter 3** Provides a cohort background and outlines previous findings relating to the cohort.
- **Chapter 4** Lists research aims and objectives.
- **Chapter 5** Presents inter-scanner reproducibility at 9 – 10 years of age, contrasting manual and automated segmentation. Chapter 6 provides evidence supporting the approach presented in Chapter 7.
- **Chapter 6** Includes a longitudinal assessment of growth trajectory, in both children living with HIV and uninfected controls.
- **Chapter 7** From findings gathered through longitudinal assessment, we present an assessment of blood sample derived immunological biomarkers and their association to subcortical volumes at 5 years of age.
- **Chapter 8** Provides a discussion and conclusions of core findings observed in chapters 5, 6 and 7 and their relevant limitations and impact.

Work presented in this dissertation has been written toward journal publication, chapters 5 and 6 have been reviewed and approved by relevant co-authors and submitted for publication, to date both articles are still under review and unpublished.

CHAPTER 1 INTRODUCTION

The Human Immunodeficiency Virus (HIV-1) is still of great concern to developing countries as well as worldwide. The WHO UNAIDS currently estimates between 5 and 10 million individuals are living with HIV in South Africa (WHO-UNAIDS 2020). Approximately 310 000 of these cases are children. The epidemic also accounted for between 1200 and 11000 child mortalities linked to HIV in South Africa, with 12000 newly infected cases in 2020 alone (WHO-UNAIDS 2020). The rate of new infections in children is not expected to slow, based on two main factors. Firstly, women of childbearing ages (15 to 49 years) account for 24.7% of total infections. These women pose potential infection risk to possible offspring. Mother-to-child-transmission (MTCT) contributes to a vertical transmission rate of 3.91, despite an approximate antiretroviral coverage and prevention of mother-to-child-transmission therapy (PMTCT) of 97% (WHO-UNAIDS 2020). Although, there were high hopes for South Africa to improve the availability of treatment, there are many challenges limiting supply and access to medicines to the public (Barron et al. 2013).

The advent of highly active antiretroviral treatment (HAART) means the prognosis is less likely to be fatal and more in-line with a chronic condition. That said, HIV-1 is still a chronic infection of the body including the central nervous system (CNS). The HIV-1 virus is capable of traversing the blood-brain barrier (BBB), where penetration by ART is limited, and the brain becomes a reservoir for the virus. (van Rie et al. 2007). As children are still developing, neurosystem infection may be more severe than in adults. A certain caveat is the knowledge that HAART itself may cause neurodevelopmental impairment despite virologic suppression in the CNS (van Rie et al. 2007; Tardieu et al. 2005). Treatment recommendation regarding PMTCT was adopted in the 2015 WHO UNAIDS treatment recommendations and guidelines (WHO 2013; WHO UNAIDS & World Health Organisation 2014). The guidelines suggest immediate use of ART, following birth, for children born to mothers living with HIV irrespective of current CD4+ T-cell count and viral load. Indefinite use of antiretroviral therapy is needed to preserve clinical benefits.

As HIV still may influence the developing brain despite early ART initiation, more research is needed to follow infants and children living with HIV throughout childhood. Many brain imaging studies have been performed in children living with HIV, however few in children who

initiated ART in infancy. In addition, neuroimaging studies of children with HIV often span a wide range of ages and treatment regimens as well as imaging modalities and study designs, making the long-term consequences of effects of ARV and HIV on the developing brain unclear (Hoare et al. 2014; Van Den Hof et al. 2019; Musielak & Fine 2016). Lastly, longitudinal studies are needed to better understand whether the HIV-related abnormalities reported represent developmental delay or damage to the paediatric brain.

While neuroimaging is ideally suited to identify structural abnormalities in the brain, it may not provide insight into the mechanisms involved in pathology changes. Combining imaging outcomes with other data, such as immunological and clinical outcomes, allows for a deeper understanding of changes in the brain.

The proposed study seeks to advance knowledge of the effects of HIV on brain development in young children who initiated ART in infancy. Within a well characterised cohort of Southern African children living with and without HIV, this study examines possible links between immune markers in infancy on subcortical volumes at 5 years, as well as the long-term consequences of HIV-related subcortical volumetric changes from 5 to 10 years. In addition, this study will provide insights into combining paediatric data across multisite scanners.

Early immunological associations with later brain structure measures will provide knowledge into the long-term consequences of early immune health on brain development. The longitudinal nature of this project will inform the clinical community on developmental changes which differ as a result of HIV pathology. Pathology aside, this is the largest cohort of healthy children with manually segmented subcortical structures across the age range of 5 to 9 years, providing valuable insight into the current literature of normal brain development within this critical stage of learning and growth (Durston et al., 2001; Sowell et al., 2003, 2004).

CHAPTER 2 BACKGROUND AND LITERATURE REVIEW

2.1 The Immune System and Inflammation

The body strives to maintain homeostasis. The inflammatory response is an attempt by the body to restore and maintain homeostasis, following invasion of a pathogen or injury. The body's inflammatory response is predominantly deployed from within the blood, as it is constantly circulating. Inflammation is the necessary process allowing and recruiting inflammatory cells and chemicals to enter infected/injured areas. The process of inflammation favours quickest return to homeostasis, which can lead to scar formation and loss of function (Martin & Leibovich 2005). In addition, periods of prolonged or chronic inflammation can lead to adverse effects (Pérez-Cerdá, Sánchez-Gómez & Matute 2016).

The process of inflammation is triggered by disruption from injury or infection. The stimulus elicits the release of numerous mediators by the affected tissue or patrolling inflammatory cell. These chemical mediators bind to their respective receptors on endothelial cells causing vasodilation, as well as increasing permeability between endothelial linings of blood vessels, and promoting migration of inflammatory cells and macromolecules into the affected area. The inflammatory cells then migrate towards chemotactic agents released by the disrupted tissue (Kaiser 2019). Once activated, the recruited immune cells release additional cytokines recruiting additional immune cells. This is only the beginning of a proinflammatory process and involves a complex cascade of chemical release promoting migration, replication, capillary invasion and removal.

The process of inflammation, much like its intention to return the body to homeostasis, is also carefully regulated by additional cytokines which act as anti-inflammatory molecules. Thus, proinflammatory products promote inflammation, whilst anti-inflammatory products inhibit or reduce inflammation.

Chronic inflammation involves prolonged exposure to an inflammatory response, either through a prolonged infection, or autoimmune troubles. Prolonged exposure of a tissue to inflammatory cytokines leads to increased blood vessel permeability and inflammatory cell accumulation – due to continued recruitment. Which in turn leads to accumulation and long

term exposure of waste products in the tissue, which may in itself be toxic and cause further disruption(Kaiser 2019).

We have covered the outline of a basic generalized immune response, however these responses are still broken down into two systems, Innate and Adaptive immunity.

Innate immunity is non-specific. Innate pathways are prompted by the first interaction to injury or unique pathogen. The process involves the recruitment of circulating phagocytic cells: neutrophils, eosinophils, and monocytes, microglia and macrophages. These cells specialise in recognizing and eliminating foreign pathogens.

The adaptive immune system is more specialized. Adaptive immunity is created following an innate response. It serves as a specialized memory to specific pathogens and provides an enhanced immune response during subsequent encounters of a pathogen. This forms the basis of immunity and is the process used by vaccines. Adaptive immunity can further be broken into humoral immunity and cell-mediated immunity. Humoral immunity involves the production of antibody molecules by B-lymphocytes. Whereas, cell-mediated immunity involves the production of phagocytic cells and cytokines by T-lymphocytes.

2.2 Human immunodeficiency virus (HIV)

HIV-1 is composed of nine genes, assembled to form a linear single stranded RNA (ssRNA). These genes are divided into three standard genes in the retrovirus family, namely *gag, pol,* and *env,* which is flanked by long terminal repeats (LTRs) and six accessory genes*, vif, vpr, tat, rev, vpu,* and *nef* (in the form: 5' LTR-*gag-pol-vif-vpr-tat-rev-vpu-env-nef*-LTR 3') (Cullen 1992; Ochsenbauer et al. 2012).

2.3 Innate immune response to HIV

The innate immune system is the first to encounter HIV. Once entering the body, infection of a target cell occurs when the surface glycoprotein of HIV (gp120), binds to a CD4 receptor on the target cell (Musich et al. 2011). Unfortunately, these target cells expressing the CD4 receptor are inherently immune cells such as T-cells, macrophages/monocytes, and microglia. This leads to a process of fusion of the virus to the host cell accompanied by insertion of the viral contents into the host cell (Pollard & Malim 1998). The viral RNA is incorporated into the infected cell's genome forming a provirus (Brik & Wong 2003; Pollard & Malim 1998). Macrophages are a target for HIV, as they have CD4 receptors on their surface. Additionally, we have dendritic cells with dendritic cytoplasmic extensions. Once exposed to a pathogen, these cells present antigen to T lymphocyte cells in lymph nodes and form the integral pathway toward adaptive immunity. These are the most likely cells to make first contact with HIV at the mucosal surface (Kaiser 2019; Shokouh 2021). Once these cells arrive at lymph nodes, they provide signals for the activation of B lymphocytes. Lastly, we have natural killer (NK) cells who are important should HIV escape other cellular immune responses. When dendritic cells are activated, they release interferon, which causes NK cells to proliferate. Once proliferated and activated these NK cells release cytokines, such as interferon-γ, tumour necrosis factor α (TNF-α), as well as chemokines which serve to inhibit viral replication, and recruit and activate further T lymphocytes. Viral replication occurs when the host cell is activated (Brik & Wong 2003). HIV-1 activates host T-lymphocyte cells via nef which in turn allows for viral replication (Cullen 1991). Macrophages express low levels of CD4 on their surface. However macrophages are of particular importance as they have a long lifespan and the ability to traverse compartments like that of the CNS. (Mlcochova et al. 2014).

2.4 Adaptive immune response to HIV

Once the virus is contained within an infected phagocytic cell, major histocompatibility complex (MHC) class 1 is displayed on the cell surface alongside degraded HIV peptide fragments for recognition by T-cell receptors on CD8+ T cells (Shokouh 2021). CD8+ T lymphocyte cells then release cytokines and chemokines that inhibit viral replication and block viral entry into CD4+ T lymphocytes (Shokouh 2021). CD8+ T-lymphocyte cells can innately kill infected cells (Kirchhoff 2010). CD8+ T-lymphocytes produce chemokines (RANTES/ CCL5) and macrophage inflammatory proteins MIP-1α and MIP-1β), which inhibit HIV-1 infection (Zhang et al. 2002). By infecting predominantly CD4+ T lymphocyte cells, it affects the very function of the cells needed to control viral spread. HIV-1 is also capable of evading CD8+ T-lymphocytes through periods of apparent latent infection in CD4+ cells.

In adults, disease progression once infected is primarily monitored by 3 main measures. These measures include CD4 T-cell count, CD8 T-cell count and viral load (VL) within the blood.

Children have higher CD4 T-cell count that decreases with age (Shearer et al. 2007). High CD8 T-cell count in children living with HIV has been associated with disease progression (Paul et al. 2005). CD4 percentage (CD4%) and CD4/CD8 ratio are more reliable measures of HIV-1 infection and disease progression in children. CD4% is the relative percentage of CD4 cells amongst other lymphocytes in a blood sample. CD4/CD8 ratio is the amount of CD4 T-cells relative to a single CD8 T-cell. In infants, CD4/CD8 ratio has been described as the more reliable diagnostic marker (Shearer et al. 2007).

2.5 Cytokines in inflammation

As stated, immune responses are complex, at the same time the immune cells and cells aiding in the inflammatory process require coordination to mount an effective attack. The release of cytokines is the mechanism used to facilitate the communication between cells and other tissues. Cytokines are large protein/glycoprotein molecules. Although not strictly for immune activation, they also are involved in various developmental and cellular differentiation and migration processes. Cytokines are primarily produced by T-lymphocytes cells, epithelial cells, and macrophages.

Cytokines have various modes to which they can affect surrounding cells. Their actions can be pleiotropic, redundant, synergic, antagonistic and cascade induction. Pleiotropic action allows for different effects dependent on target cell/target cell receptor. Redundant action allows multiple cytokines to perform the same action, like recruitment of macrophages. Synergic action allows for compounded effect of multiple cytokines to act on a single outcome. Antagonistic action as it implies allows an inhibitory effect on protein release or cell recruitment and proliferation, or negative feedback type response on cytokine release, like that of anti-inflammatory responses. Thus, a cytokine here could exhibit a number of these actions, and for example be both pleiotropic and antagonistic having proinflammatory effects on some cells whilst inhibitory on others. Lastly, we have cascade induction, which infers a metered stepwise release of cytokines toward an amplified response like that of the clotting cascade.

Cytokines are specialized into various families. Interferon family, which acts as antiviral proteins. Chemokine family which serve to activate cells, facilitate cell migration and and adhesion. Tumor necrosis factor family, which regulate inflammation and immune response. Interleukin family, which are pleiotropic, with varying actions dependent on target cell type. Haematoproteins, which promote cell differentiation and proliferation. Transforming growth factor family, which regulate immune cell activation and recruitment.

Action of cytokines are tightly regulated and their production is transient, with short lives. There are examples like that of HIV infection and other autoimmune diseases which result in dysregulation of these cytokines resulting in long term exposure to the cytokines which can have detrimental and pathological effects, from prolonged inflammation.

The chemokine family of cytokines are a powerful chemoattractant, allowing recruitment and migration of immune cells to an affected area. These molecules are generally smaller and more soluble, and thus capable of recruiting cells from other tissues and through blood vessel walls. The release of cytokine from differing locations forms a concentration gradient from the site of release. This forms a concentration derived positioning system informing directionality to migration of cells. Thus, dependent on cell receptors encoding for multiple types of cytokines, on the surface of target cells, migration of these immune cells can be coordinated to a specific location that exhibits a specific concentration of cytokine unique to that cell/cell type. In converse to this it is also possible to have some cell locations which release inhibitory cytokines to repel certain cells.

2.6 Cytokines in HIV

Even with ART there is still an initial period of infection with elevated proinflammatory markers, which often persists even after viral suppression(McMichael et al. 2010). Cytokine markers linked to primary and long term HIV-1 infection have been well studied over the years (Chevalier et al. 2016; Gloster et al. 2004; McMichael et al. 2010; Okafor et al. 2020; Rao, Ruiz & Prasad 2014; Thurman et al. 2020).

Cytokines that have been implicated during HIV-1 infection include IL-10 (Kedzierska & Crowe 2001), IP-10, interferon-α, interferon-γ, Interleukin-6, Interleukin-10, and Interleukin-15 (Gloster et al. 2004), MIP-1 alpha, MIP-1 beta and RANTES (Cocchi et al. 1995), CCL2, sCD14, and TNF-α (Rosenberg et al. 1997). Cytokines often act as part of a multiple step-wise release and interplay between cytokines and cell-types, thus further study is always welcome to define the exact interplay of cytokines. The pleiotropic nature of cytokines also pose a problem when considering different cell-types and tissues, not all effects may be similar, especially when dealing with the specialized cell-types and environment within the CNS. In the case of neopretin, which in systemic tissues is observed as a predictor of clinical severity, whilst within the CNS is a marker of cell activation. Neopretin has also shown association with neurocognitive decline when in higher concentrations(Hagberg et al. 2010; Molero-Luis et al. 2020). Additionally specific to the CNS, we have neutrophic factor (NT3), this cytokine plays an important role in neuronal differentiation and stimulation of neuronal growth and maintaining neuron cues for survival. NT3 has been shown to associate with neurocognitive

impairments with lower concentrations observed in the CSF of individuals living with HIV-1 (Babu et al. 2019). Observed systemic, or otherwise blood sample derived, measurements of cytokines differ from that within the CSF (Babu et al. 2019). Additionally, plasma concentrations of sCD30 was lower in individuals who had viral suppression, yet sCD30 levels were elevated within the CNS despite systemic viral suppression.

The collection of CSF is painful, invasive, and includes the possibility of complication during a lumbar-puncture procedure. As a result, acquiring CSF samples is not always ethically feasible. Ethics committees often only allow the collection of CSF when clinical manifestations of neurologic disease or inflammation is present. The collection of CSF is possibly confounding and biasing results with indications of elevated concentrations of cytokine markers, in an already possibly advanced state of inflammation. This is where MRI techniques excel as they are non-invasive and allow for study and comparison of healthy controls.

Some studies have observed associations of blood sample derived inflammatory markers with that of disturbance to CNS structure. Higher concentrations of RANTES, MCP-1 and IL-6 have been associated with larger cortical white and gray matter, implying proinflammatory response to HIV-1 infection within the CNS (Ruhanya et al. 2021b). While IL-9, VEGF and PDGF-BB also associated with larger structures at higher levels they imply a attempt at protection against inflammatory processes (Ruhanya et al. 2021b). IL-6 and sCD14 also shown association with white matter injury and cognitive impairment (Blokhuis et al. 2019).

Observations relating to subcortical structural volumes derived through automated techniques, included larger putamen, amygdala and globus pallidus were associated with higher concentrations of IFN-γ, MCP-1, and TNF-α (Gongvatana et al. 2014). Additionally smaller putamen, thalamus, globus pallidus, amygdala and total GM and WM were all associated with higher concentrations of IL-1β, IL-6, IL-16, IL-18, IP-10, MIP-1β, and SDF-1α (Gongvatana et al. 2014).

2.7 Neuropathogenesis of HIV-1 Infection

The pathway that HIV-1 leverages to enter the CNS is not well understood, however, it is known that HIV-1 invades the CNS as early as 10 days post-infection (Ivey, MacLean & Lackner 2009).

Infection of the CNS generally occurs through invasion of infected monocytes, macrophages and other CD4+ T lymphocytes (Ivey, MacLean & Lackner 2009; van Rie et al. 2007). CNS infection has also been found to be favoured by macrophage tropic mutations of HIV-1 (Aquaro et al. 2002; van Rie et al. 2007). Autopsy studies have observed higher concentrations of HIV-1 in astrocytes, perivascular macrophages and microglia which are heavily associated with CD4 and chemokine coreceptors (Blumberg, Gelbard & Epstein 1994; Medders & Kaul 2011; van Rie et al. 2007; Schnell et al. 2011; Tornatore et al. 1994; Wiley et al. 1986).

Findings showing few infected CD4+ T cells in the brain post-mortem suggest once activated and recruited in the CNS, CD4+ T cells are fairly short lived (Richards et al. 2016). With this in mind, there are a group of CD8+ T cells, which are not short-lived, which express CD4 on their surface termed '$CD4^{dim}CD8^{bright}$' (Richards et al. 2016; Wahl & Al-Harthi 2023). Higher CD8 T-cell count in children living with HIV has been associated with more notable disease progression (Paul et al. 2005). This perhaps informs a more plausible method of entry of HIV into the CNS in children via CD8 cell carriers, due to their relative abundance as well as extended duration for infiltration.

Within the CNS there may be two additional mechanisms of infection involved, cell-to-cell transfer (Lehmann, Nikolic & Piguet 2011) and endocytosis (Freed 2015). Both pathways have been indicated in the infection of astrocytes (Dubois-Dalcq et al. 1995; Gray et al. 2013; Kramer-Hämmerle et al. 2005; Tornatore et al. 1994; Wahl & Al-Harthi 2023). Astrocytes form an integral component of the BBB, are the most common glial cell within the CNS, and send star-like processes/projections from its centre linking multiple endothelial capillary cells and neurons (Kandel, Schwartz & Jessell 2000). Infection of these astrocytes, ultimately disrupt their function and can cause neuronal dysfunction, inhibition of the reuptake of neurotransmitters, localised neurotoxicity relating to lack of waste and neurotransmitter clearance and impairment of the BBB (Blumberg, Gelbard & Epstein 1994). Inflammatory

responses initiated by recruited immune cells are amplified through cell-cell astrocyte interactions (Blumberg, Gelbard & Epstein 1994). The release of such inflammatory cytokines lead to further immune activation and recruitment, of macrophage, microglia and astrocytes (Blumberg, Gelbard & Epstein 1994). Thus, when compartmentalized with the BBB a relatively small invasion of HIV-1 can result in a compounding cascade of proinflammatory effects causing widespread tissue pathology. Although, it is unclear whether HIV-1 is capable of infecting neurons throughout the CNS, some evidence has indicated marginal infection of neurons (Cantó-nogués et al. 2005). Spectroscopy has further indicated glial recruitment and reactive gliosis prior to neuronal cell loss (Chang et al. 2002; Ernst, Chang & Arnold 2003).

Although the neuropathogenesis may not be particularly localized to infecting neurons the impact of infection is capable of affecting their function. The increased concentrations of neurotoxins through uncleared cellular debris, neurotransmitters, viral proteins, cytokines form a hostile environment for glial and neuronal function (Lu et al. 2011). This environment would ultimately lead to damage and disruption to neural networks and a slew of HIV-associated neurocognitive disorders (HAND) (Lindsey et al. 2007; Lu et al. 2011; McGuire et al. 2015). The ability of ARVs to be effective against CNS-based infection are inhibited by their ability to traverse the BBB, which could result in unique drug resistant strains within the CNS (Letendre et al. 2004; Yazdanian 1999). As discussed, the CNS is compartmentalized from the blood via the BBB. As such, viral load observed in the blood may not be representative of viral reservoirs within the CNS (Pillai et al. 2006; Strain et al. 2005). Calcifications within the basal ganglia appear to be a common finding in HIV-1 infected children (Chiriboga et al. 2005; Epstein et al. 1986; Johann-Liang et al. 1998; Mitchell, Wendy 2001; Nozyce et al. 2006; Rosenfeldt, Valerius & Paerregaard 2000; Shah et al. 1996) and adults (Berger & Arendt 2000; Mcarthur, Brew & Nath 2005; Walot et al. 1996).

Neurodegeneration is a common finding relating to HIV-1 infection in adults (Berger & Arendt 2000). ART tends to reverse the neurodegeneration to a degree and slows its progression (Tamula et al. 2003). Individuals living with HIV are at risk of developing a spectrum of neurological problems, such as cognitive, motor or emotional disturbances. The relative impact or severity has been compartmentalized into specific diagnosis stages. These include: Asymptomatic Neurocognitive Impairment (ANI), the earliest stage of infection; Mild Neurocognitive Disorder (MND), which occurs as infection progresses; and HIV-Associated

Dementia (HAD), which involves impaired memory and loss of concentration. Much like Alzheimer's disease, HAD is linked with AIDS dementia complex or sub-acute encephalitis and markedly linked to neuronal cell loss leading to global white and gray matter volume loss (Ances et al. 2012; Becker et al. 2011; Thompson et al. 2006).

In children, however, the brain is immature and still developing. Similar findings of white and gray matter loss have been observed in children (Andronikou et al. 2015; Lewis-de Los Angeles et al. 2016; Sarma et al. 2014). The paediatric brain may experience impaired growth and disturbances to cognitive development due to the effects of HIV infection. Children living with HIV are at risk of progressive HIV-encephalopathy, which is characterised by developmental delay and failure to reach developmental milestones in thought, language, motor and behavioural (Mitchell, Wendy 2001; Shanbhag et al. 2016; Tardieu et al. 2000). Accelerated ageing has been shown in perinatally infected children between ages 9 and 12 years, based upon discrepancies in epigentetic and chronological age in a cohort from Cape Town(Horvath et al. 2018). Such differences between chronological and epigenetic ages can indicate accelerated tissue ageing. Accelerated epigenetic ageing in these children was associated with decreased attention, executive function, working memory, and processing speed which were more prevalent(Horvath et al. 2018). Following-up after 36months the workgroup observed that accelerated epigentetic ageing persists and is increased ampngs those with PHIV (Heany et al. 2020).

Neuropathogenesis of HIV-1 infection in children and adults share similarities, such as potential for neurologic complications, however, there are some distinct differences. These differences may be due to developmental factors, timing and mode of infection, disease progression, as well as the initial immune system response.

Unlike adults, children are typically vertically infected with HIV at birth or early infancy. The infant immune system is less mature than in adults, and the less efficient immune response may lead to faster and more rapid onset of pathology (Johansson et al. 2008; Saunders, Liddelow & Dziegielewska 2012). Penetration of HIV into the CNS is also easier in children compared to adults as the BBB is still developing. Compared to adults, infants have a higher plasma viral load (PVL) in their first month post infection(Mariani et al. 2012; Tornatore et al. 1994). The time needed for the effects of treatment to lower PVL is slower in

infants (Cavarelli & Scarlatti 2011; Mariani et al. 2012). As a result, infants may experience longer periods of HIV exposure at higher levels in the CNS.

Both children and adults can develop a range of neurological complications, including HIV-associated neurocognitive disorders (HAND) and peripheral neuropathy(Govender et al. 2011). In adults, HIV-1 infection has been observed to associate with neurocognitive impairment, particularly in faculties involved with spatial working memory, intellectual and learning development, language and verbal learning, psychomotor, information processing, and executive functioning (Epstein et al. 1986; Kolson 2017; Mcarthur, Brew & Nath 2005; Sacktor et al. 1996). In children, similar disturbances have been observed to psychomotor, language and behavioural faculties (von Giesen et al. 2003; Govender et al. 2011; Langerak et al. 2014; Laughton et al. 2012)s. Neuropsychologically, differences in behaviour have been indicated relating to impaired social skills, apathy and difficulty processing emotions, withdrawal syndrome, irritability, depression, and personality changes (Le Doaré, Bland & Newell 2012; Epstein et al. 1986; Mitchell, Wendy 2001; van Rie et al. 2007). Recently a workgroup from Zambia provided a much welcome link with cognitive impairment and neuroimaging findings in a group of children (9 to 17 years) (Dean et al. 2020). Total brain volume, and GM volume were smaller amongst individuals with cognitive impairment (lower global deficit score)(Dean et al. 2020).

Extensive systematic review has already been compiled by a few publications pertaining to the impact of HIV-1 infection (Hoare et al. 2014; Van Den Hof et al. 2019; Musielak & Fine 2016), as well as more recently an emphasis on the impact of HIV-1 and ARV exposure in uninfected infants and children (Martín-Bejarano et al. 2021; Wedderburn et al. 2022). There is an increasing concern about the development of children that are uninfected yet exposed to both HIV and ARVs as this population grows due to increased access to treatment (Boivin et al. 2019; Wedderburn et al. 2019; Williams et al. 2021) A common observation amongst the systematic review studies is the lack of longitudinal cohorts followed through multiple time points. A further limitation across most investigative studies are lack of sufficient sample size and methodological limitations (Van Den Hof et al. 2019). Evidence is still too sparse to imply concrete interpretations of findings.

To date, to our knowledge, four studies have used automated segmentation methods to examine longitudinal structural brain changes in children vertically infected with HIV-1 and

stable on ART (Hoare et al. 2014; Van Den Hof et al. 2019; Musielak & Fine 2016; Nwosu et al. 2023; van Rie, Mupuala & Dow 2008). Longitudinal analysis often have 2 time points, implying a linear trend to growth and development (Van den Hof et al. 2021; Wade et al. 2019). The most recent study to introduce growth trajectory analysis across 3 time points, involving the same cohort as the present study from ages 5 through 9 years, where no difference in cortical thinning nor gyrification development trajectories was observed between PHIV and uninfected children following multiple comparison correction (Nwosu et al. 2023). Prior to correction 6 cortical GM regions were identified to be consistently larger amongst PHIV compared to uninfected controls across the age range (Nwosu et al. 2023). Additionally, although there have been recent inquiry related to the impact of inflammatory markers relating to HIV-1 infection (Thurman et al. 2020), none have included immunological biomarkers, collected at birth capturing the time of initial primary infection with subcortical structures volumes in children at a later age.

Objective biomarkers that diagnose and predict disease progression of HIV-related neuropathology are needed. These biomarkers would aid guideline development for targeted individual treatment plans, drug trials and possible vaccine targets.

Anatomical and structural development of the CNS in healthy children are well documented (Bendersky et al. 2006; Dowker 2006; Fan et al. 2011; Giedd, Jay N et al. 1999; Rapoport et al. 2001).

Oster et al. (1993) were conducting stereological studies on individuals infected with HIV-1 to assess relative volume, and morphological changes which the CNS undergoes during HIV-1 infection. The study comprised of a formalin fixed cadaver sample, perhaps giving more insight into the effects of HIV-1 on the brain than imaging studies. Oster observed a 55% increase in ventricular size for patients with HIV-1 compared to the controls. Further autopsy study of 13 HIV-infected individuals, in McClernon et al.'s (2001) study, showed significant localized differences of HIV-1 vRNA between subcortical regions. The caudate was particularly observed to have higher concentrations of viral RNA (McClernon et al. 2001). Apart from loss of global tissue mass Oster and colleagues also observed significant atrophy in central brain nuclei, mainly that of the striatum and thalamus (Oster et al. 1993). Pre-Blood-Brain-Barrier manifestations of HIV-1 infection in children by use of MR images, CT scans, as well as autopsy findings found certain cerebrovascular abnormalities in HIV-1

infected children (Shah et al. 1996). The abnormalities included subacute infarction, fusiform dilation in major vessels of the Circle of Willis, ischaemic lesions and arteriopathy (Shah et al. 1996).

Automated MRI volumetric analysis, found that there was a significant decrease in the volumes of basal ganglia in HIV-1 infected males with dementia as compared to those without dementia and controls (Aylward et al. 1993). Additionally, hypermetabolism has been reported within the basal ganglia(von Giesen et al. 2000)¶. The result may be due to reactive gliosis and recruitment of glial cells to the localized inflammatory response. (McClernon et al. 2001; Sacktor et al. 2004; Silverstein & Kumar 2013)

Important to consider is that HIV-1 infection may not solely be the cause of possible CNS disturbances. Certain drug therapies have also been indicated to have adverse effects within the CNS. Prenatal exposure to Zidovudine in exposed but uninfected children born to seropositive mothers, exposed that 22 of 49 children in the cohort had clinically relevant mitochondrial dysfunction, whilst an additional 14 children had idiopathic neurological symptoms (Tardieu et al. 2005). More recently, it has been suggested the use of nevirapine may have an effect on cognitive development in children living with HIV (Fairlie et al. 2022). Children living with HIV aged 5 to 11 years old who initiated ART before 3 years of age were part of the IMPAACT multisite study. The study reported children randomized to receive nevirapine as well as those that switched to nevirapine showed poorer global performance scores than those who received lopinavir/ritonavir (Fairlie et al. 2022). With that said, the use of long-term ART has still been shown to have beneficial effects to cognition, Brahmbhatt et al. showed that children below six years of age who had been on ART for 24 to 60 months had decreased impairments in fine motor, receptive language, expressive language and overall neurodevelopment compared to those receiving ART for less than 12 months (Brahmbhatt et al. 2014). Further study of these children at later ages (7 to 14 years of age) revealed that sustained therapy accompanied decreased risk of impairment to working memory (Brahmbhatt et al. 2017).

Boivin and colleagues, have also addressed multiple other factors which may contribute to poorer cognitive performance adding to bias between children living with HIV and uninfected children (Boivin et al. 2018, 2019). Factors such as sex, number of years attending

school, weight for age, height for age, Home environment score, and socioeconomic status have been observed to impact cognitive performance (Bangirana et al. 2017).

In addition to global atrophy seen in many HIV-1 infected children, many of the manifestations experienced in the subcortical brain structures in adults may also be present in children (Safriel et al. 2000). Neuropsychological impairment may follow the accompanied atrophy of regions, exhibiting specific functional deficits. Atrophy has also been associated with the depletion of CD4+ T-lymphocytes (Chiang et al. 2007; Rosca et al. 2011).

2.8 Normal Brain Development

Apart from the novel research into longitudinal analysis of the pathological effects of HIV-1 and ART on brain development, this is also one of the few studies to actively document volume changes within selected structures of healthy children via manual segmentation (Casey et al. 2005). It is also pertinent to understand normal developmental changes in the South African context, if we wish to analyse *any* negative effects related to pathology.

A longitudinal study conducted by Giedd and colleagues (Giedd, Jay N et al. 1999) involving 145 healthy subjects with age range 4.2 to 21.6 years (where at least 65 subjects were scanned twice) observed grey matter volume increases during childhood followed by a decrease before adulthood. This was postulated to be as a result of neuronal establishment and accompanied pruning (Giedd, Jay N. et al. 1999). The basal ganglia typically decrease in volume with age (Berger & Arendt 2000; Berridge 2007; Berridge & Robinson 1998; Giedd, Jay N et al. 1999; Moberg et al. 1998). Thompson et al. (Thompson et al. 2000) suggest that in the case of the caudate, most of the tissue loss takes place in the head of this structure; thus, segmentation of the tail is of little importance. In contrast to the basal ganglia, the temporal lobe structures (amygdala and hippocampus) appear to increase in volume with age. In healthy children the caudate, putamen and globus pallidus have all been indicated to decrease in size with age across numerous studies, with children spanning 4 to 18 years of age (Giedd et al. 1996; Jernigan et al. 1991; Thompson et al. 2000).

The process of myelination is extremely active before birth through the first 2 years of life, however is ongoing throughout life (Durston et al. 2001; Reiss et al. 1996). As such, the corpus callosum continues to increase in size as a result of the ongoing myelination. Contrary to the typical pattern of caudal to rostral development, as set forth by Yakovlev and Lecours in 1967, anterior regions mature earlier than posterior areas of the corpus callosum, which do not mature until adolescence (Giedd, Jay N. et al. 1999). It is also known that in adults a global decrease in white matter is not expected (Good et al. 2001). Albeit, grey matter volume in adults decreases linearly with age. The point at which this gradual decline is initiated is still to be determined (Good et al. 2001). This is exclusive of the major atrophy we expect in the later years of individuals 60+ years old, where gyral grey matter thinning and dilation of sulcal spaces is greatly pronounced (Kochunov et al. 2008).

2.9 Standardising Terminology

It is important to standardize terminology when referring to different regions of interest. Study of dopaminergic pathways is a massive field of research in neurophysiology, however these often include animal models. The terminology and regions may not necessarily be interchangeable with that of human anatomical norms. In some texts the striatum is defined as including only the caudate and putamen (Netter 2002), whether inclusion of nucleus accumbens is inferred is up to debate.

The term corpus striatum is often mentioned interchangeably with dorsal striatum, however the term 'dorsal striatum' does not include the nucleus accumbens which is part of the ventral striatum (Netter 2002). There is often overlap of anatomical and neurophysiological terms, as well as incongruencies between texts. Thus, definitions and terms used within this dissertation are standardized according to the following texts:

Barr's The Human Nervous System: An Anatomical Viewpoint By John Kiernan, Raj Rajakumar, 10th edition (Kiernan & Rajakumar 2013);

Principles of Neural Science By Eric Kandel, James H. Schwartz, and Thomas Jessell: Chapter 43: The Basal Ganglia (DeLong 2000).

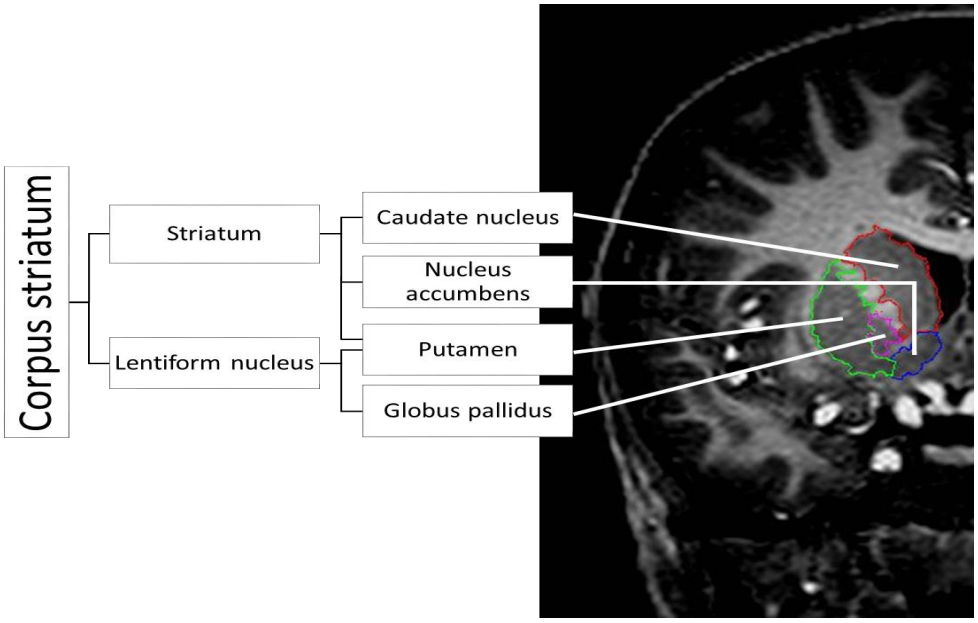

Figure 2.1 Hierarchical structure of the corpus striatum

The basal ganglia consists of four subcortical gray matter nuclei, the striatum, globus pallidus, substantia nigra, the subthalamic nucleus (DeLong 2000). These grey matter nuclei are highly connected to the cortex and subcortical motor areas forming complex pathways involved with movement, cognition, affect, motivation and procedural learning (DeLong 2000).

The striatum comprises that of two main bodies, the caudate nucleus and putamen (Pu) (Fig2.1). The ventral striatum is comprised of the nucleus accumbens (NA) and olfactory tubercle. The putamen together with the globus pallidus is termed the lentiform nucleus. Finally, the addition of the globus pallidus to the striatum is termed the corpus striatum or striated body. The addition of the globus pallidus to the striatum amends the terminology to corpus striatum (Fig 2.1). The Caudate Nucleus, Pu, and GP function in planning and modulation of movement pathways. Locomotor deficits have been observed in children living with perinatal HIV-1 (Bagenda et al. 2006; von Giesen et al. 2003; Govender et al. 2011; Laughton et al. 2012, 2013) The NA forms part of the mesolimbic dopamine pathway. In presence of a reward stimulus the NA projects signals to the cortex; a pleasurable sensation is achieved via subsequent activations. This area is paramount to goal-directed learning, and addiction (Bernier, Whitaker & Morikawa 2011; Berridge 2007; Doya 2000).

The corpus callosum (CC) consists of white matter, formed by neuronal axons and myelinated by oligodendrocytes, it facilitates interhemispheric connection and communication, via callosal fibres.

2.10 Magnetic Resonance Imaging Summary

Magnetic Resonance Imaging (MRI) is a non-invasive imaging technology. The technology can be leveraged to measure a multitude of different variable outcomes. For the scope of the current work we specifically use structural MRI, which produces three dimensional detailed anatomical images.

The sophisticated technology involves exciting protons (Hydrogen atoms) in a strong magnetic field, these protons begin to precess in the direction of the given field(B0). A secondary perpendicular radiofrequency and resulting magnetic field is transmitted at the same resonant frequency (B1) (Mark Hammer 2014). This applied field causes the precession to realign to the applied field. When the B1 field is removed, relaxation occurs, where the proton spins return to the B0 equilibrium (Mark Hammer 2014). The spin of protons themselves create subtle magnetic fields. The spin relaxation back to equilibrium releases signal which is capable of being collected. The time taken to return to equilibrium B0 is measured, this is T1 relaxation(Mark Hammer 2014). Additionally T2 involves spin-spin interactions and is a measure of time taken for relaxation to occur in the presence of interaction with other magnetic fields created by other precessing protons (Mark Hammer 2014). T2* considers the additional effects of magnetic inhomogeneities and inclusion of iron deposits and air and represents the process of dephasing.

T1 characteristics are determined by the ability of protons to exchange energy with their environment. When not as easily constrained by surrounding molecules, like protons in water rich areas, it takes a relatively longer times for these protons to relax to equilibrium. Protein and fatty acids are large in comparison, when water molecules and associated protons interact with these large molecules it slows the return to equilibrium. As stated, the time to equilibrium is measured, this leads to longer exposure time in water rich areas compared to protein and fat rich areas. Therefore, signal and thus tissue contrast is developed via comparisons resultant of density and size of surrounding molecules within areas.

There are various parameters one is able to tweak for desired effects to vary contrast in MRI scans. Repetition time (TR) being the time between successive B1 pulses, and echo time (TE) being the time between introduction of B1 and the peak of echo signal. Each of which

leverages a different contrast profile, TR affects T1 contrast, whilst TE affects T2 contrast in MR signal. Weighting these specific parameters results in different types of images.

T1-weighted contrast images, maximizes contrast between tissues, and involves short TR and TE. T1 is appropriate for observing density differences between tissue types within particular structures, like that of the brain. T2-weighted contrast employs T2 relaxation time, using long TR and TE. T2-weighted contrast is more apt at measuring tissue-specific characteristics and fluids.

As T1 weighted images allows for maximal contrast between tissues within structures, it is most suited for study of the structure differences within the CNS.

2.11 MRI Scanner Variability

Attempts at making MRI more sensitive, more powerful and able to scan larger objects has been the mode of the day. Technological advances include higher static fields, faster gradients, stronger RF transmitters and antenna design(Knake et al. 2005; Liu, Zhao & Crozier 2003; Schick 2005). The rapid adoption of such advances has increased the potential for unwanted side effects.

With time, especially in research settings with a high throughput of subjects being scanned, the wear and tear MRI scanners are subjected to are high. This is cause for concern for longitudinal studies using a single scanner(Biberacher et al. 2016; Huppertz et al. 2010). Once an MRI scanner is obsolete and/or loses function, it needs be replaced by a new scanner. Larger or global cohort studies often need a multicentre approach. In these cases interscanner variability would be an issue (Biberacher et al. 2016; Droby et al. 2015; Huppertz et al. 2010). In our setting, our cohort study involved a 3T Allegra Siemens scanner to image 106 children at 5, 7 and 9 years of age. The imaging centre has since been moved and a new scanner installed, a 3T Skyra Siemens scanner, which has been used to scan the cohort at 9 and 11 years of age. As a result, inter-scanner variability is of concern for any longitudinal analysis and needs to be assessed.

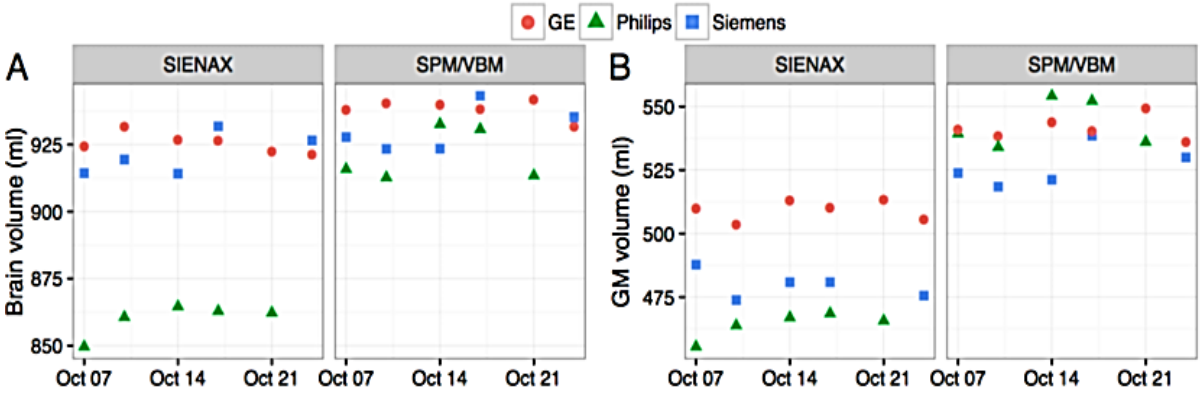

Figure 2.2 Volume measures between scanners over time for patient 1, as captured from Biberacher et al. 2016

Biberacher et. al. (2016) compared data from three different 3T scanners (Philips Achieva; Siemens Verio; GE Signa MR750). The two patients diagnosed with relapsing remitting multiple sclerosis were both scanned 6 times per scanner in 3 weeks. Volumes from T1-weighted images of whole brain, global white matter and grey matter, and cortical thickness were derived using automated segmentation techniques. Global tissue volume and cortical

thickness was observed to differ between scanners. Another finding included differences in similar volumetric tests between repeated scans on the same scanner, even when using multiple automated segmentation tools (Biberacher et al. 2016). The study reported high inter-scanner variability, however, they only included two subjects with multiple sclerosis and didn't consider many possible treatment confounders. In addition, intra-scanner variability was less pronounced and the results more consistent compared to multicentre comparisons.

A retrospective study of 11 healthy volunteers (10 males, age range 22 – 51 years) scanned twice on five 3T scanners using FAST segmentation suite, observed significant differences between scanners. Intra-scanner reliability of GM and WM volume were above 72%, where there were two consecutive visits at the same 3T scanner. However, inter-scanner reliabilities for the 3T scanners were only above 41% (Shokouhi et al. 2011).

Delineation of deep GM structures as well as boundaries between GM and WM tissues is the least reproducible when conducting multicentre studies. Usage of a post-mortem brain phantom, a standardised calibration tool transferred between sites, may aid in correcting these issues (Droby et al. 2015). Due to obvious constraints here an appropriate human phantom analogue would be necessary.

As observed in Figure 2.2, there exists large disparity even between automated segmentation tools when conducting such research. This may be as a result of their voxel-based algorithm approach to measuring volumes. It is possible that manual segmentation, being more subjective in nature, may alleviate incongruences of unclear boundary identification which automated tools may not be sufficiently sensitive to discern.

Some scanners are head only, whilst others full body; the human head itself is symmetrical, however this symmetry is not maintained internally within the rest of the body. Therefore inhomogeneities of the RF field may be more pronounced in the abdominal and pelvic areas, when using a 3T scanner(Schick 2005). These RF inhomogeneities could lead to signal void of tissue structures being scanned (Schick 2005). However, these effects occur when scanning those specific areas. These dielectric effects, and additional biological influences, are variable and unpredictable (Kangarlu et al. 2000; Liu, Zhao & Crozier 2003; Schick 2005). Even shape of the body surface and the conductivity of the underlying tissues play a role in determining these disturbances.

2.12 Manual and Automated segmentation

Segmentation involves the delineation of specific structures within the brain, in order to quantify their shape or overall volume. Manual segmentation is done by a trained neuroanatomist. It involves the physical outlining of each structure of interest based on knowledge of the surrounding anatomy and comparative contrast between tissue types which is visually evident. As such, manual segmentation is subjective. As the size of datasets increase the toll and labour requirements on the research team, manual segmentation is no longer feasible. Reliability of the technique is also placed under scrutiny as Inter-rater variability decreases as emphasis on turn-around time is amplified in large datasets requiring more individuals to segment (Mulder et al. 2014; Powell et al. 2008).

Automated segmentation tools were thus developed to provide an alternative to manual segmentation. As a result, manual segmentation has now become a tool to aid in testing accuracy of automated techniques. Automated segmentation allows for more objective, less time consuming, less costly as well as provide fairly consistent repeatable results (Morey et al. 2009). Updates to segmentation algorithms and atlases are easily deployed and accommodated (Han & Fischl 2007; Morey et al. 2009).

Automatic segmentation (aseg) involves the use of an atlas containing probabilistic information on the location of structures (Fischl et al. 2002). The atlas is derived from a training set of manually derived segmentations (particularly that of Western adults) (Fischl et al. 2002). Manual segmentation, albeit cumbersome, remains the gold standard of the two techniques (Barnes et al. 2008; Boccardi et al. 2011; Dewey et al. 2010; Hasan & Pedraza 2009; Morey et al. 2009; Sánchez-Benavides et al. 2010; Tae et al. 2008).

Although automated segmentation strives to be more objective, discrepancies in the outputs have been observed (Gronenschild et al. 2012). These discrepancies were observed between FreeSurfer versions, as well as between type and version of operating system as well as workstation specifications (Gronenschild et al. 2012). Accuracy of segmentation techniques may also be affected by a different MR scanner or acquisition protocol (Han & Fischl 2007). This could include scanners of different make or model, or the same scanner following substantial hardware and software upgrades. This is of concern within the current

study, should we wish to assimilate and compare longitudinal findings using the replacement 3 T Siemens Skyra scanner.

MRI in conjunction with manual segmentation would be preferred in estimating the volumes of brain regions (Barnes et al. 2008; Boccardi et al. 2011; Dewey et al. 2010; Hasan & Pedraza 2009; Morey et al. 2009; Sánchez-Benavides et al. 2010; Tae et al. 2008). With exception of our previous work, Dewey and colleagues (Dewey et al. 2010), are the only workgroup to assess reliability and accuracy of segmentation techniques within a sample of individuals living with HIV-1 (n=120; mean age 47.3±7.2 yrs). Three segmentation methods were assessed FreeSurfer and Individual Brain Atlases using Statistical Parametric Mapping (IBASPM), as well as auto-assisted manual segmentation (AAM). The AAM method was performed via a customization of FreeSurfer, with manual correction of already auto generated delineations (Dewey et al. 2010). Although the use of AAM provides considerable advantage to time saving, the method may introduce bias. Association with FreeSurfer derived outputs would naturally be higher. Dewey and colleagues addressed the possible bias by resegmenting a subset of the sample manually and assessing their congruence with AAM results. Strong association was observed between AAM and manual segmentation in all regions of interest (Cronbach's $\alpha>0.90$) (Dewey et al. 2010).

CHAPTER 3 COHORT BACKGROUND

The Children with HIV-1 early antiretroviral therapy (CHER) trial is supported under the umbrella of the Comprehensive International Program for Research on AIDS in South Africa (CIPRA-SA). The trial was initially established to compare three treatment strategies in infants with perinatally acquired HIV-1 infection, diagnosed between 6 and 12 weeks of age (Cotton et al. 2013; Violari et al. 2008). (First and second line ART drugs are listed in Appendix A). The CHER study was an open-label randomised controlled trial comprising 377 HIV-1 infected asymptomatic infants, 6 to 12 weeks of age, born to seropositive mothers (Cotton et al. 2013). Infants were prenatally identified from the public prevention of mother-to-child transmission programmes in the Western Cape and Gauteng provinces.

A prevention of mother-to-child transmission (PMTCT) regimen was administered to all participants, prenatally, with a single-dose of nevirapine. The cohort of mothers in the Western Cape received zidovudine from 34weeks gestation to parturition and to neonates for a further 7 days (Cotton et al. 2013). The timing of administration of PMTCT treatment is vital as it reduces the risk of vertical transmission and takes into consideration the known complications caused from treatment of zidovudine at an early gestational age. Treatment of zidovudine at an early gestational age increases risk of mitochondrial dysfunction and neurological disorders in neonates (Tardieu et al. 2005). As per protocol infants were formula fed, against current guidelines, as MTCT was not fully understood at the time.

Sub-studies have been aimed to follow and document the development of a third of these subjects through their childhood (Cotton et al. 2013). The continued monitoring of these subjects with the incorporation of additional uninfected controls has resulted in the CIPRA Neurodevelopmental sub study. The subjects have undergone regular follow-up appointments that have included regular neurodevelopmental testing at the Family Clinical Research Unit (FAM-CRU). The aim of the follow-ups in this sub study was to compare the neurocognitive outcomes of the various treatment regimens that resulted from the original CHER study (Laughton et al. 2012). The children returned to FAM-CRU at 5 years of age for neurodevelopmental assessments, additionally a subset children went on to receive high-resolution neuroimaging. They have since received further clinic follow-ups every 6 months and MRI scanning at ages 5, 7, 9, 10 and 11 years. Data related to socioeconomics was not

consistently acquired throughout the study. The children included as a control group were from an interlinking vaccine trial in the same community. In brief summary, the control children in the cohort come from a low socioeconomic community where parents are highly dependent on social grants, and less likely to complete high school (Holmes et al. 2017). The majority of housing in the community includes electricity and an indoor toilet (Holmes et al. 2017). A summary of the limited sociodemographic data related to the control children has been published (Holmes et al. 2017) and is representative of the sample and community affected.

3.1 Summary of neuroimaging outcomes in the CHER cohort

Different imaging modalities were used to evaluate the impact of HIV-1 and ART on the cohort. These studies demonstrate HIV-related alterations across modalities, brain region and ages. Although the changes reported are less severe than findings reported in the pre-ART era, taken together these studies point to atypical neurodevelopment despite early ART. Across ages and modalities, the basal ganglia are consistently reported among HIV-related changes in the cohort. Lastly, associations between immune health in early infancy and imaging outcomes at later ages were observed.

3.1.1) Magnetic Resonance Spectroscopy (MRS)

At ages 5 and 7 years, cross sectional analysis reported no HIV-related differences in metabolite levels in the basal ganglia with the exception of higher NAA in children living with HIV-1 at age 5 (Mbugua et al. 2016; Robertson et al. 2018). At age 5, positive associations between CD4/CD8 in infancy and NAA as well as choline levels were observed. At 9 years of age lower levels of NAA, creatine and glutamate were observed in children living with HIV-1 in the basal ganglia. At 11 years of age higher choline in grey matter and reduced creatine in white matter were observed in infected children (Graham et al. 2020). A longitudinal analysis from 5 to 11 years across three regions (basal ganglia, grey and white matter) found significantly higher choline levels. In addition, they also reported elevated myo-inositol in the basal ganglia and grey matter regions. Observed together, elevated choline and myo-inositol are markers of neuroinflammation (van Biljon et al. 2021).

3.1.2) Diffusion Tensor Imaging (DTI)

Continued observation of lower fractional anisotropy (FA) and higher mean diffusivity (MD) in children living with HIV-1 is indicative of compounding damage to white matter. This was observed across ages 5, 7 and 9 years to the corticospinal tracts inferring progressive WM disruption in HIV-1 positive children (Ackermann et al. 2014, 2016; Jankiewicz et al. 2017; Mberi et al. 2018). A recent study further investigated white matter integrity at 7 years using tractography to examine tracts between anatomical seeds in functional networks (Madzime et al. 2021). Children living with HIV-1 had lower FA/higher MD in tracts within the somatosensory, salience, default mode, and motor networks. Seeds in the superior temporal cortex, superior frontal cortex, and putamen were implicated in all four networks.

3.1.3) Functional MRI (fMRI)

Resting state fMRI through seed-based correlation analysis revealed altered functional connectivity between several resting state networks in children living with HIV-1 compared to controls (Toich et al. 2018). Implicated networks include the default mode, executive, visual, auditory and somatosensory networks. In addition, immune health in infancy was associated with connectivity in the basal ganglia, salience and somatosensory networks.

3.1.4) Structural MRI

Via a modified MRI segmentation technique, the various regions of the CC were observed to be smaller in children living with HIV-1 at 32 months of age (Andronikou et al. 2015). Study of cortical structures revealed thicker cortex in bilateral frontal and left temporo-insular regions amongst children living with HIV-1(Nwosu et al. 2021). Additionally, lower local gyrification indices were observed in left superior and bilateral medial orbitofrontal cortex extending into rostral anterior cingulate(Nwosu et al. 2021). Reduced cortical gyrification and thickness was observed bilaterally at 7 years of age (Nwosu et al. 2018). However, longitudinal analysis at ages 5, 7 and 9 years showed no HIV-related differences in growth trajectory for both cortical thickness and gyrification(Nwosu et al. 2023). Morphometric analysis of scans, through manual segmentation have revealed larger NA, and Pu bilaterally, and smaller CC at 5 years of age using manual segmentation [APPENDIX B] (Randall et al. 2017). Clinically, we observe children living with HIV-1 – with poorer immune health (low CD4/CD8 ratio) exhibit larger bilateral caudate [APPENDIX B] (Randall et al. 2017).

3.1.5) Multimodal MR analysis

Khobo and colleagues (2022) used the embedded feature selection of logistic elastic-net regularization to select neuroimaging measures (proton MRS, DTI, structural MRI, fMRI) that best distinguished PHIV from uninfected controls, at 7 years of age (72PHIV, 55controls), and measure their classification performance via the area under the receiver operating characteristic curve using repeated cross validation. They compared single versus multiple modality fits. The best single modality in predicting differences was structural MRI. The best multimodal MRI set consisted of 22 DTI and structural MRI volume features. The specific features included reduced volumes of the bilateral globus pallidus and amygdala, as well as increased mean diffusivity and radial diffusivity in the right corticospinal tract in PHIV. Consistent with previous studies of CPHIV, select subcortical volumes obtained from structural MRI provide reasonable discrimination between PHIV and controls therefore volumetric changes were the most predictive imaging outcome across modalities.

3.1.6) Neurocognitive outcomes in the CHER cohort

Possible neurocognitive effects were observed at early ages (11months) (Laughton et al. 2012). Children living with HIV-1 had lower performance on Griffiths Mental Developmental Scales (GMDS) in both general and locomotor tests. Earlier treatment groups performed better than late treatment groups (Laughton et al. 2012). Locomotor test scores were lower irrespective of treatment in children living with HIV-1. At 5 years of age locomotor scores appeared to improve whilst disruption to performance of visuospatial and perception scores were still evident (Laughton et al. 2018).

3.1.7) Regions of study

Locomotor deficits may infer functional disturbance to the basal ganglia. All imaging modalities report the basal ganglia, or tracts to/from the basal ganglia, as affected by perinatal HIV-1. Several measures of the basal ganglia – volumes, metabolite levels and functional connectivity – were associated with clinical immune health markers in infancy. Taken together, previous studies in the cohort support further analysis focused on basal ganglia development as well as the influence of the early immune system.

As a result, we propose additional study of the structures basal ganglia (Caudate head, Putamen, Nucleus Accumbens and Globus Pallidus) and the corpus callosum in this cohort.

CHAPTER 4 RESEARCH AIMS AND OBJECTIVES

4.1 Aims

- Conduct a longitudinal assessment of developmental changes and long-term consequences that occur in HIV-1 infected and healthy developing brains of children between 5 to 10 years of age using high-resolution structural MRI and manual segmentation.
- Further investigate HIV-1 volume changes at age 5, specifically by identifying the possible contributions of early life immunological biomarkers on subcortical volumes in PHIV

4.2 Objectives

- Perform manual segmentation of selected subcortical structures on of 125 AC-PC transformed MRI scans.
- Assess overall reproducibility and reliability of MRI scanner data at 10 years of age.
- Gauge the level of agreement between manual and automated segmentation at 10 years of age.
- Amalgamate 10 year old data with 5, 7 and 9 year data.
- Assess growth trajectories of diagnostic groups via mixed effect modelling.
- Associate and model volumetric data at 5 years of age with perinatal immunological biomarkers from blood samples.

4.3 Motivation and Research Outline

While there are an increasing number of imaging studies identifying disruptions to brain development in PHIV on treatment using imaging techniques; the majority of studies are cross sectional and in adolescents. While neuroimaging provides insight into neurodevelopment, most imaging outcomes do not provide functional information or knowledge about the mechanisms driving the observed changes. Within the field of PHIV neuroimaging, there is a growing need for longitudinal studies starting in early childhood to understand if cross sectional findings represent developmental delay or damage. Further, there is a need to combine cross sectional findings with clinical and cognitive data. Together, these approaches would give context to cross-sectional neuroimaging outcomes in PHIV populations.

The work presented in this thesis seeks to address these gaps in the literature. We explore the possible long term effects of HIV-related anatomical abnormalities observed at 5 years of age in our cohort. Using the same segmentation method as at 5 years, we used longitudinal analysis to identify differences in volumetric trajectories from ages 5 to 10 years. We aimed to determine if the changes observed at 5 years represented a regional delay in brain growth, or persistent damage.

To perform longitudinal analysis, we first needed to assess the potential bias in the segmented data due to a scanner change. As such, chapter 5 addresses inter-scanner reproducibility at 9 – 10 years of age of segmented data.

The longitudinal trajectories in chapter 6 suggest the volumetric 5-year-old HIV related abnormalities resolve by age 7 years. In order to better understand the volume changes at 5 years, Chapter 7 presents an exploratory analysis assessing the possible link between blood sample derived immunological biomarkers obtained at birth to subcortical volume outcomes in a small selection of PHIV.

Chapter 8 provides a discussion of the results in the context of the literature and possible future work based on the findings presented.

CHAPTER 5 INTER-SCANNER REPRODUCIBILITY USING MANUAL AND AUTOMATED SEGMENTATION OF SUBCORTICAL STRUCTURES IN 9- 10-YEAR-OLD CHILDREN

5.1 Abstract

While attention has been given to inter-scanner variability among automated segmentation outputs, no work has examined manually segmented brain volumes across different scanners. In addition, within the literature little attention has been given to variability in subcortical volumes as well as pediatric populations between scanners. Given the increase in multi-site and longitudinal studies, a better understanding of reproducibility among segmentation methods and populations is needed.

We manually (MultiTracer) and automatically (FreeSurfer V6) segmented select subcortical regions in both hemispheres (Caudate, nucleus accumbens(NA), Putamen(Pu), Globus pallidus(GP) and corpus callosum(CC)) in a group of 27 children(9years) scanned within 11months on two different 3 T scanners, from the same manufacturer, with similar acquisition protocols. Measures of reproducibility and variability were assessed for segmentation methods between and within scanners.

Time between scans had no significant impact on volumes. High reproducibility in both consistency and absolute agreement was observed for manually segmented volumes between scanners. Volumes from both scanners were strongly associated (Pearson correlation: $r>0.80$, $p<0.001$), with exception to weaker association in CC and bilateral NA ($r>0.49$, $p<0.001$). Automated segmentation demonstrated lower variability and overall better consistency between scanners. Systematic differences were evident in certain regions. Scanner differences were observed between 2.9 - 7.4% in the bilateral caudate, CC, and both the right GP and NA. Automated volumes were strongly associated between scanners ($r>0.80$, $p<0.001$), with marginally weaker associations ($r>0.70$, $p<0.001$) for left NA, left GP and CC. Automated segmentation achieved higher consistency than manual segmentation in R NA ($r=0.82$ vs 0.68) and CC ($r=0.76$ vs 0.49). Both segmentation techniques derived highly reproducible volumes in the select structures across two Siemens scanners within a pediatric sample. Automated segmentation should employ a covariate in future analyse.

5.2 Introduction

An increasing number of neuroimaging studies involve large cohorts or longitudinal data derived from multiple sites. As such, there has been much interest in reproducibility of measurements between sites and strategies to combine data across different scanners (Biberacher et al. 2016; Droby et al. 2015; Huppertz et al. 2010; Lee et al. 2019). Inter-scanner variability may result from changes in the protocol or scanner hardware differences, or a combination of these. Even at the same field strength, differing numbers of receive coil channels, differing sensitivity profiles of radiofrequency coils and differences in shim gradients cause differences in signal to noise ratio (SNR) (De Guio et al. 2016; Kruggel et al. 2010; Preboske et al. 2006). Variability of tissue contrast (CNR) has been observed to significantly influence volumetry measures (De Guio et al. 2016; Kruggel et al. 2010; Schnack et al. 2004).

Over time, MRI scanners are also subjected to wear and tear, including electronic component degradation, and both hardware and software maintenance upgrades (Lee et al. 2019). These factors may introduce intra-scanner variability, which is of concern in longitudinal studies even when using a single scanner (Biberacher et al. 2016; Huppertz et al. 2010). Additionally, on occasion updated sequences may not always be backward compatible resulting in possible outdated firmware, as well as no longer being eligible for service by the manufacturer. Once a machine becomes obsolete and needs to be replaced, inter-scanner variability again becomes an issue.

To minimize systematic inter-scanner differences (Biberacher et al. 2016; Reig et al. 2009; Shokouhi et al. 2011), longitudinal multi-site studies use strategies such as standardization of imaging protocol, scanner vendor and voxel resolution (De Guio et al. 2016; Iscan et al. 2015; Jack et al. 2008); imaging of water, gel, human or post-mortem brain phantoms (Droby et al., 2015) across sites; and performing both T1 and T2 weighted tissue segmentation as opposed to solely T1 weighted (Reig et al. 2009). Additionally, quantitative T1 mapping may be employed in an attempt to remove scanner related differences and variability associated with acquisition parameters (Fischl et al. 2004; Tsialios et al. 2017). Post-processing strategies include employing the same pipelines for data acquired on different scanners (Iscan et al.

2015), use of longitudinal processing pipelines (Reuter et al. 2012), calibration of histogram analysis (Schnack et al. 2004), visual checks and manual correction (Iscan et al. 2015; Reig et al. 2009; Schnack et al. 2004), artefact control (De Guio et al. 2016) and the inclusion of a covariate to capture the inter-scanner variance.

Numerous studies have reported differences in brain morphometry from data acquired in adults on different scanners when using automated segmentation techniques (Biberacher et al. 2016; Gracien et al. 2020; De Guio et al. 2016; Liu et al. 2020; Reig et al. 2009; Schnack et al. 2004; Shokouhi et al. 2011). One study, for example, in a comparison of morphometry data from 3 T scanners of 3 different vendors (Philips, Siemens and GE) revealed global tissue volume and cortical thickness differences between scanners independent of the brain imaging software tool used (SPM7/VBM8; SIENAX of FSL; FreeSurfer) (Biberacher et al. 2016). Further, deep gray matter (GM) structures, brainstem and GM/white matter (WM) tissue boundaries demonstrated substantial intra-scanner variability on repeated scans conducted at each participating site. In a different study, retrospective analyses of imaging data acquired in 11 healthy males scanned twice on 3 T scanners at each of 5 centres, demonstrated significant effects of centre and visit on GM, WM and cerebrospinal fluid (CSF) volumes obtained using Brainvisa and FSL FAST (Shokouhi et al. 2011). These studies highlight the need to include scanner-related variability in statistical models, and that inter- and intra-scanner variability may limit our ability to detect pathology-related differences.

Although manual segmentation is the gold standard for volumetry (Biffen et al. 2020; Jovicich et al. 2013; Morey et al. 2009; Narayanan et al. 2016; Randall et al. 2017), few studies use it due to its labor-intensiveness (Akudjedu et al. 2018; Jovicich et al. 2013). The use of manual segmentation is perhaps best suited for quality control and validation(Pulli et al. 2022). However, manual segmentation may be better suited to accommodate variability related to different scanners, as a trained anatomist may be able to identify anatomical boundaries regardless of fluctuating contrast. Although there has been much work assessing inter-scanner variability using automated segmentation, to the best of our knowledge, no previous study has examined and compared manually segmented brain volumes across different scanners. Moreover, the majority of existing studies only examine scanner-related effects on global or total GM and cortical GM, and there is little literature regarding variability in measured subcortical volumes between scanners.

Further, while studies have compared outcomes from manual and automated segmentation (Akudjedu et al. 2018; Dewey et al. 2010; Morey et al. 2009; Sánchez-Benavides et al. 2010), and manual correction of automated outcomes (Iscan et al. 2015; Schnack et al. 2004), none have looked at the reliability of both methods on data acquired on different scanners. Since atlases used in automated segmentation software packages are based on adult brains (Fischl et al. 2002), they may not be optimal when examining subtle volumetric alterations in pediatric populations, particularly non-European populations. This may affect automated segmentation differently on different scanners.

In this work, we present subcortical volumetric data using both manual and automatic segmented methods in a small group of children scanned within 11 months on two different 3 T scanners with similar protocols. We present measures of reproducibility and variability and discuss the strengths and weaknesses of the two segmentation approaches. Based on the statistical outcomes, we aimed to determine whether the data acquired could be used for future analysis without controlling for scanner type.

5.3 Materials and Methods

As part of an ongoing longitudinal neurodevelopmental study, we scanned 27 children on a 3 T Siemens Allegra (Erlangen, Germany) at the Cape Universities Body Imaging Centre (CUBIC) in Cape Town, South Africa. Scanning was performed according to protocols approved by the Human Research Ethics Committees of the Universities of Cape Town and Stellenbosch. The children were rescanned after a mean period of 10.7±3.1 months on a 3 T Siemens Skyra. As the ongoing study is focused on the effects of HIV-1 infection on the developing brain, participants scanned included both children with and without perinatal HIV-1 infection (PHIV). The protocol included a high-resolution T1-weighted 3D echo planar imaging (EPI) navigated multi-echo magnetization prepared gradient echo (MEMPRAGE)acquisition (van der Kouwe et al. 2008; Tisdall et al. 2012) (FOV 224x224 mm2, TR=2530 ms, TI=1160 ms, TE's=1.53/3.19/4.86/6.53 ms, bandwidth 650 Hz/px, 144 sagittal slices, 1.0x1.0x1.3 mm3; the 3T Skyra differed in 176 sagittal slices, and 1.0x1.0x1.0 mm3).

Manual segmentation was performed by a single neuroanatomist (SRR) using MultiTracer (Woods 2003) for select structures within the basal ganglia. These included the caudate head, nucleus accumbens (NA), putamen (Pu), globus pallidus (GP) and corpus callosum (CC). The CC was traced across 3 sagittal slices spanning the midpoint between hemispheres. The volumes of the 3 slices were averaged to obtain an estimate for the center most slice. As each slice is 1 mm thick, it is still interpreted as a volume rather than a surface area. The condensed protocol is referred to in a previous publication (Randall et al. 2017). The neuroanatomist was blinded to all participant data during segmentation. Intra-rater reliabilities were assessed by re-tracing a random subset of 10 brains. For all regions, Cronbach's α exceeded 0.83 (Cronbach 1951).

FreeSurfer v6 (http://www.freesurfer.net) was used to perform automated segmentation of the same structures and to determine intracranial volume (ICV), utilising the longitudinal pipeline, albeit not originally designed for pediatric population manual correction was performed. In the case of the CC, volumes of the CC sub-regions determined by FreeSurfer were summed. The total CC volume was then divided by the number of sagittal slices, so as to obtain an average volume per slice. ICV was not controlled for in our analyses as the scope of the research is to assess gross volume differences between scanners using manual

segmentation and comparing that to inter-scanner volume differences obtained when using FreeSurfer. Since the labor-intensive practice of manual segmentation did not allow for gross ICV measurement, ICV measurements were gathered only from FreeSurfer. Seeing as FreeSurfer and manual segmentation outputs are being viewed alongside each other on the same participant, controlling for a FreeSurfer derived ICV in manual outcomes may introduce bias.

Statistical analyses were performed in IBM SPSS28.

For both manual and FreeSurfer derived volumes, we report regional absolute (ΔVol=Skyra-Allegra) and percentage (ΔVol%$=\frac{(Skyra-Allegra)}{Allegra}$ %) inter-scanner volume differences. Consistency between Allegra and Skyra regional volumes was assessed separately for manual and automatically derived volumes using Pearson correlation, and absolute agreement using one-sample two-tailed t-tests to test the null hypothesis that ΔVol=0. We also computed coefficient of variation (CV) to assess inter-scanner variability in brain volumetry.

Time between scans, HIV-1 diagnosis (due to possible pathological progression) and sex (due to possible peripubertal hormone alterations which may affect rate of brain maturation during the time period between scans (Biro et al. 2013, 2014)) were investigated as possible confounders of inter-scanner volume differences. ANCOVA analyses were used to examine whether regional inter-scanner volume differences remained significant after adjustment for any variable showing weak association (at $p < 0.10$) with ΔVol of that region. In addition, for both manual and automated segmentation, we plotted the mean and 95% confidence intervals (CIs) of regional inter-scanner volume differences (ΔVol and ΔVol%).

Additionally, among images from each scanner, we compared consistency and absolute agreement between regional volumes from manual and automated segmentation. These outcomes quantify reproducibility and variability of segmentation techniques. Bland-Altman plots were generated in cases where there were significant difference between manual and automated segmentation to visualize biases between techniques.

5.4 Results

We excluded one child from our analysis due to an unsuccessful acquisition, resulting in a final sample size of 26 children. The demographics of this sample are summarized in Table 5.1. Although Skyra data yielded smaller ICVs on FreeSurfer analyses than Allegra data, the difference between Allegra and Skyra ICVs was not associated with time between scans ($r(25) = -0.03$, $p = 0.854$).

Table 5.1 Biographical data of pediatric participants

Demographic Data		Paired Totals (N=26)	Allegra (n=26)	Skyra (n=26)	*t*	*p*
Sex: Male	n(%)	17 (65%)				
Diagnosis: PHIV	n(%)	8 (31%)				
Age: Scan [Yrs]	Mean(SD) [Range]		9.2 (0.2) [8.4- 9.4]	10 (0.3) [9.2 - 10.4]	15.08	<0.001
Time between scans [Months]	Mean(SD)	10.7(3.1)				
ICV [mm3]	Mean(SD)		$1.45x10^6$ ($0.13x10^6$)	$1.43x10^6$ ($0.13x10^6$)	2.38	0.026
Values are Mean (SD), number(%)						
ICV=Intracranial Volume. Yrs=Years. mm=millimeters. SD=Standard deviation.						

5.4.1) Inter-scanner Volume Comparisons

Except for FreeSurfer segmented volumes of the right (R) caudate, left (L) NA and L Pu, we found no association (all p's > 0.13) of regional inter-scanner volume differences (on manual or automated segmentation) with HIV-1 diagnosis, sex, nor time between scans. In the R caudate and L NA, increasing time between scans was associated with larger differences between Allegra and Skyra volumes obtained with automated segmentation (R caudate: $r = 0.43$, $p = 0.03$; L NA: $r = 0.46$, $p = 0.02$). Moreover, differences between Allegra and Skyra volumes from automated segmentation tended to be smaller in children with HIV-1 than in controls in the R caudate ($p=0.071$) and L Pu ($p=0.056$).

Table 5.2 Consistency and absolute agreement between Allegra and Skyra volumes obtained using either manual or automated segmentation.

Allegra vs Skyra																			
	Manual Segmentation									Automated FreeSurfer								
	Pearson correlation			t-test		ΔVol		ΔVol%		arson correlati			t-test		ΔVol		ΔVol%	
ROI	*r*	*p*	CV	*t*	*p*	Mean	(SD)	Mean	(SD)	*r*	*p*	CV	*t*	*p*	Mean	(SD)	Mean	(SD)
L Caudate	**0.81**	**<0.001**	4.5	-1.120	0.300	-55	(249.00)	-1.80%	(0.07%)	**0.97**	**<0.001**	0.6	**7.787**	**<0.001**	167	(107.00)	4.40%	(0.03%)
R Caudate	**0.89**	**<0.001**	10.8	-0.480	0.600	-25	(270.00)	-0.40%	(0.08%)	**0.95**	**<0.001**	1.0	**5.068**	**<0.001**	168	(166.00)	4.10%	(0.04%)
L NA	**0.75**	**<0.001**	9.0	-0.540	0.600	10	(90.00)	-1.40%	(0.20%)	**0.7**	**<0.001**	21.2	-0.236	0.820	-4	(89.00)	-2.00%	(0.13%)
R NA	**0.68**	**<0.001**	9.2	-0.570	0.600	10	(92.00)	-1.10%	(0.22%)	**0.82**	**<0.001**	2.4	**-2.085**	**0.048**	-26	(62.00)	-4.40%	(0.10%)
CC	**0.49**	**<0.001**	4.8	-1.080	0.300	-11	(53.00)	-4.50%	(0.13%)	**0.76**	**<0.001**	1.2	**4.269**	**<0.001**	27	(31.00)	7.40%	(0.08%)
L Pu	**0.93**	**<0.001**	16.0	-0.320	0.800	15	(240.00)	0.40%	(0.05%)	**0.95**	**<0.001**	14.2	0.351	0.730	15	(218.00)	0.10%	(0.04%)
R Pu	**0.93**	**<0.001**	4.8	-1.040	0.300	-50	(242.00)	-1.10%	(0.05%)	**0.95**	**<0.001**	4.0	1.259	0.220	52	(206.00)	0.90%	(0.04%)
L GP	**0.82**	**<0.001**	6.5	-0.760	0.500	-23	(150.00)	-1.70%	(0.10%)	**0.77**	**<0.001**	3.9	1.281	0.210	42	(162.00)	2.00%	(0.08%)
R GP	**0.85**	**<0.001**	23.9	0.190	0.900	6	(144.00)	0.00%	(0.10%)	**0.88**	**<0.001**	2.4	**2.066**	**0.050**	56	(134.00)	2.90%	(0.07%)

CV - Coefficient of Variation, SD - standard deviation, L & R represent Left & right, NA -nucleus accumbens, CC-corpus callosum, Pu-putamen, GP-globus pallidus

ΔVol - Volume Difference = Skyra - Allegra

ΔVol%- Percentage Volume Difference=(Skyra - Allegra)/(Skyra)%

Bolded values are significant at p<0.05

5.4.2) Manual segmentation

Across regions, we found strong associations between manually traced volumes from Allegra and Skyra images (Pearson correlation: $r>0.80$, $p<0.001$), with weaker association in bilateral NA and CC ($r\geq0.49$, $p<0.001$). Coefficients of variation (CVs) of manually derived Allegra and Skyra volumes ranged from 4.5% in the left caudate to 23.9% in the R GP. In no regions did manually segmented volumes obtained from Allegra and Skyra images differ (Table 5.2, Figure 5.1).

5.4.3) Automated segmentation

In most regions, Allegra and Skyra automated volumes were strongly associated ($r>0.80$, $p<0.001$), with marginally weaker associations ($r\geq0.70$, $p<0.001$) for left NA, left GP and CC (Table 5.2). Automated segmentation achieved substantially better consistency than manual segmentation in R NA ($r=0.82$ vs 0.68) and CC ($r=0.76$ vs 0.49). Although CVs of automated Allegra and Skyra volumes were smaller than CVs of manually derived volumes in all regions except the left NA, significant inter-scanner differences were evident in 5 of the 10 regions examined. Volumes on Skyra images were between 2.9 to 7.4% smaller than those on Allegra images in the bilateral caudate, CC and right GP, and larger by 4.4% in the right NA (Table 5.2; Fig 5.1B & 5.11D). Differences in the R caudate remained significant after adjustment for potential confounding by time between scans and HIV-1 status ($F(23) = 4.014$, $p=0.05$).

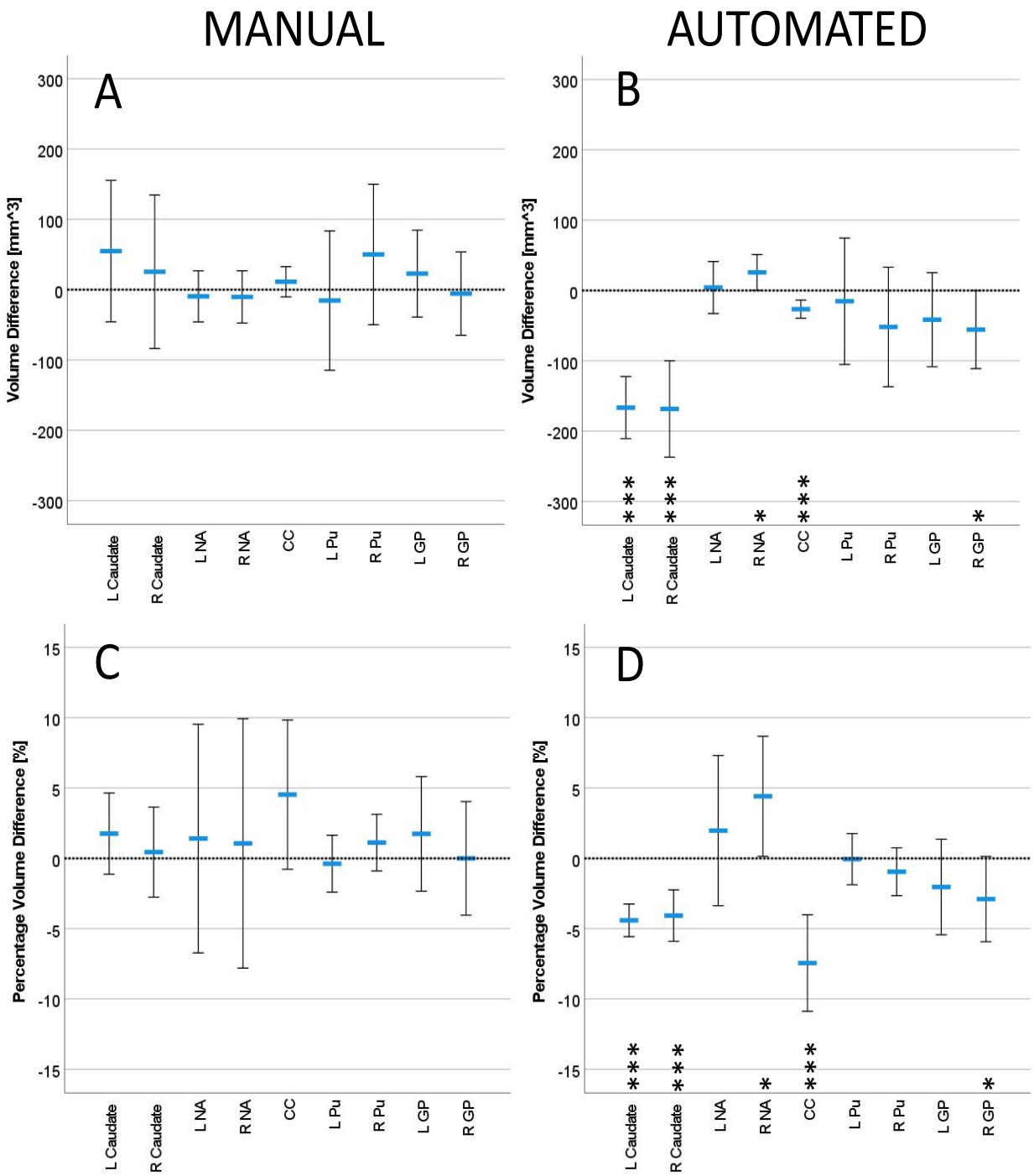

*Figure 5.1. Mean and 95% confidence intervals of regional (top row) absolute and (bottom row) relative (%) inter-scanner volume differences for (left column) manual and (right column) FreeSurfer segmented volumes, respectively. These results reflect how volumes on Skyra images differ from those on Allegra images. *p<0.05; **p<0.01; ***p<0.001. NA nucleus accumbens; CC corpus callosum; Pu putamen; GP globus pallidus; L left; R right.*

5.4.4) Within scanner comparisons of Manual vs Automated Segmentation

Table 5.3 Consistency and absolute agreement between manual and automated segmented volumes for images acquired on different MRI scanners

ROI	Allegra Manual vs Automated				Skyra Manual vs Automated			
	r	*p*	*t*	*p*	*r*	*p*	*t*	*p*
L Caudate	**0.67**	**<0.001**	**-4.22**	**<0.001**	**0.71**	**<0.001**	-0.89	0.38
R Caudate	**0.71**	**<0.001**	**-3.08**	**0.005**	**0.72**	**<0.001**	-0.46	0.65
L NA	**0.52**	**0.007**	**-6.68**	**<0.001**	**0.6**	**0.002**	**-9.79**	**<0.001**
R NA	**0.51**	**0.009**	**-5.07**	**<0.001**	**0.57**	**0.003**	**-7.59**	**<0.001**
CC	**0.57**	**0.003**	-0.17	0.9	**0.71**	**<0.001**	**4.76**	**<0.001**
L Pu	**0.95**	**<0.001**	**-4.96**	**<0.001**	**0.95**	**<0.001**	**-5.34**	**<0.001**
R Pu	**0.94**	**<0.001**	**-8.38**	**<0.001**	**0.93**	**<0.001**	**-5.75**	**<0.001**
L GP	**0.54**	**0.005**	**-6.82**	**<0.001**	**0.66**	**<0.001**	**-5.44**	**<0.001**
R GP	**0.68**	**<0.001**	**-5.19**	**<0.001**	**0.82**	**<0.001**	**-5.47**	**<0.001**

L & R represent Left & right, NA -nucleus accumbens, CC-corpus callosum, Pu-putamen, GP-globus pallidus
Bolded values indicate significance at p<0.05

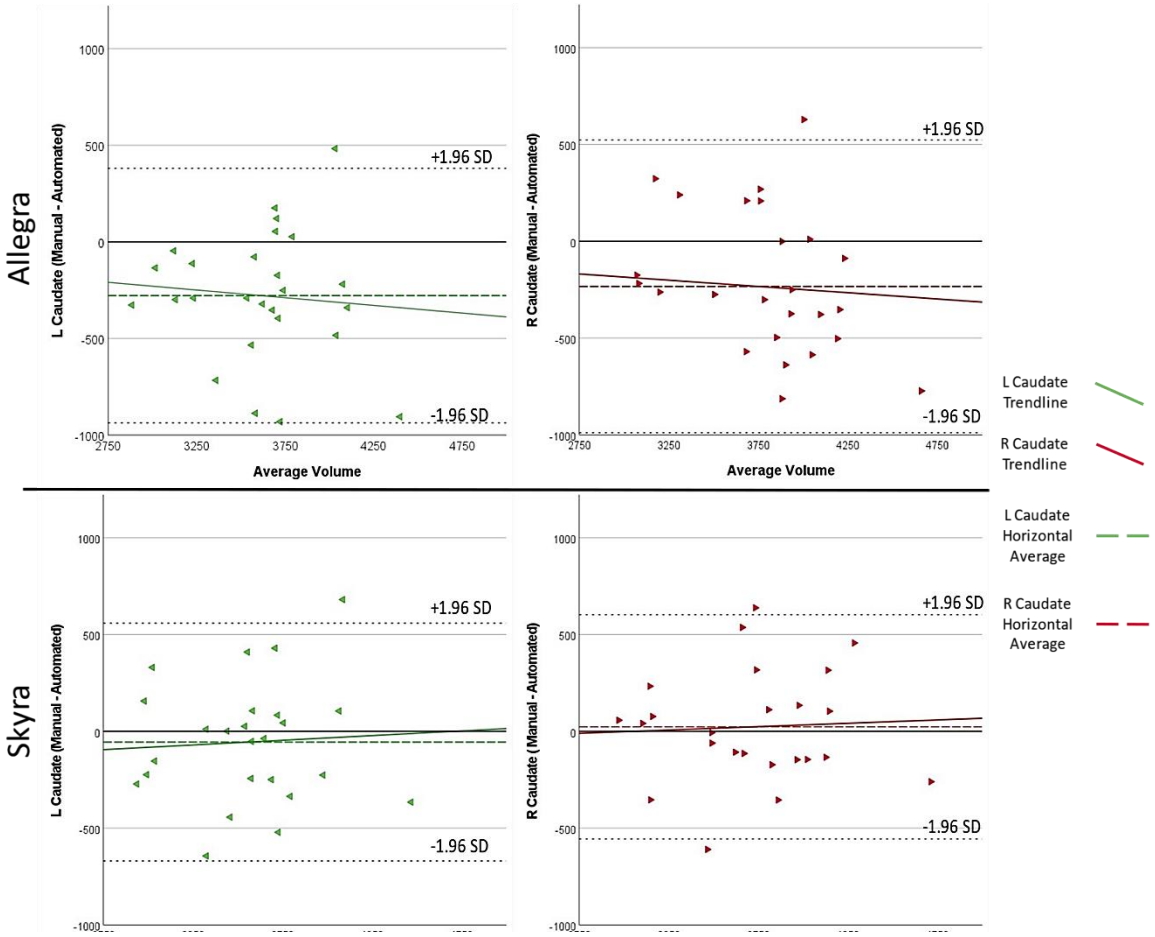

Figure 5.2 Bland-Altman plots comparing manual and automated segmented volumes of the caudate nuclei on Allegra (top) and Skyra (bottom) images, respectively.

In the regions examined here, consistency between manual and automated volumes were generally similar on both Skyra and Allegra data (Table 5.3). Only the NA and CC demonstrated somewhat poorer consistency on Allegra than Skyra data. Automated volumes were significantly larger than manual volumes in all GM regions, except the bilateral caudate on Skyra images where manual and automated volumes were similar. In contrast to GM, manual and automated CC volumes were similar on Allegra images, while automated CC volumes were smaller than manual volumes on Skyra images. Bland-Altman plots of bilateral caudate volumes demonstrate better agreement between manual and automated segmentation of this region on Skyra than Allegra images (Fig 5. 2).

5.5 Discussion

5.5.1) Inter-scanner Volume Comparisons

The goal of our study was to assess reproducibility of select volumes between two MRI scanners using different segmentation methods in a small pediatric population. Within the regions assessed, both manual and automatic segmentation yielded high consistency and absolute agreement between Allegra and Skyra volumes pointing to high reproducibility. Automated segmentation demonstrated higher consistency between Allegra and Skyra volumes, but systematic differences were evident in 5 of 10 regions. Specifically, automatically segmented Skyra volumes were smaller than those from the Allegra in the bilateral caudate, CC and right GP, and larger in the right NA. Statistical models based on automatically segmented data across scanners in this cohort would benefit from the inclusion of a scanner variable to capture systematic differences.

The absence of inter-scanner differences for manually segmented volumes within these regions in this small sample suggests that there are no gross volume alterations or calibrative issues when conducting structural studies using the two different scanners. In contrast, this is not the case for automated FreeSurfer derived volumes. Of the automated volumes that significantly differed between scanners, there was a minimum difference of 2.9% (56mm3) in the left GP and maximum of 7.4% (27mm3) in the CC.

Although manually segmented volumes did not differ between scanners, the CVs of manually derived Allegra and Skyra volumes were considerably larger than for automated segmentation in all but one region. Liu and colleagues (2020) reported CVs for FreeSurfer derived volumes in 15 healthy adults scanned on GE, Siemens and Philips scanners that ranged from 6.9% for global gray matter to 12.3% in the left GP. In our data, CVs for FreeSurfer derived volumes from Skyra and Allegra scans similarly ranged from 0.6% in the left caudate to 14.2% in the left Pu, except for left NA where it was 21.2%. Similarly, CVs for manually derived volumes ranged from 4.5% in the left caudate to 16% in the left Pu, except for right GP where it was 23.9%. Notably, left caudate yields the lowest CVs for both our FreeSurfer and manually derived volumes. Moreover, the GP where we observe the largest variance in our manually derived volumes is the same region where Liu et al. (2020) observed substantial variance between scanners using FreeSurfer. Although Liu et al. (2020) did not perform

manual segmentation as one of the three segmentation techniques evaluated (FreeSurfer, FSL-FIRST, and AccuBrain), they noted significantly smaller inter-scanner CV values using AccuBrain than FreeSurfer for all regions examined, except the bilateral hippocampus where CV values were similar. CV values of FreeSurfer and FSL-FIRST were generally similar, except in the bilateral amygdala and right NA where FreeSurfer performed better, and left GP where FSL-FIRST performed better (Liu et al. 2020).

Subjective visual inspection by the primary manual tracer (SR) revealed that the newer Skyra scanner has more observable definition in structural images compared to the Allegra. This was particularly noticeable in terms of distinguishing the anterior cerebral artery from the CC. The increase in definition and quality of images might be a result of the slightly higher resolution of our Skyra acquisitions (1.0x1.0x1.0 mm3 vs. 1.0x1.0x1.3 mm3). As manual segmentation is subjective, and the ability of the tracer to distinguish features in context of their surrounds, whilst also allowing for variation to shape and vessel branching pattern, manually traced volumes may not be as influenced by these resolution differences as automated segmentation.

In high-field MRI, undesired inhomogeneities of the radiofrequency (RF) and static field (Hoult & Phil 2000) can lead to signal loss (Schick 2005). Since such field distortions may lead to false volumetric data in both automated segmentation, as well as with subjective contouring during manual segmentation, these may contribute to inter-scanner discrepancies (Gracien et al. 2020). Image contrast is also affected by the homogeneity profile of the receive coil. Notably, the Allegra images were collected using a single-channel transmit-receive head coil and the Skyra images using a 32-channel receive head coil. Despite poorer SNR, the simpler design of the single-channel birdcage coil results in a more uniform RF receive profile, albeit more prone to gradient distortion. In multi-channel coils, where images from different coils are combined, substantial brightening occurs closer to the coil elements where sensitivity is greatest. Although a prescan normalize function within the protocol attempts to correct for these non-uniformities, slight residual brightening may remain in the center of the head due to uncorrected RF transmission inhomogeneities.

Moreover, the Allegra transmit-receive head coil, which exhibits a uniform yet localized transmit field, only excites spins within the head, while the Skyra body coil excites spins far into the neck and below. The main consequence of the Allegra's localized transmit field is that

inflowing blood appear bright on the images due to not being excited by the inversion pulse of the MPRAGE sequence. As a result, the anterior cerebral artery adjacent to the corpus callosum appears bright on Allegra images and is often incorrectly included with the corpus callosum during automated segmentation. This may explain why automated segmentation yielded CC volumes on Allegra images that were substantially larger than on Skyra images.

Since the Allegra is a head-only scanner, it was designed with faster-switching gradients than would be safe in a whole-body scanner. These gradients, however, produce non-linear fields, resulting in more geometrically distorted images. Since not even an experienced neuroanatomist would be able to correct for such distortions, this cannot, however, explain the differences between Allegra and Skyra volumes observed with automated segmentation only.

Despite significant differences between FreeSurfer derived volumes in 5 of 10 regions, Allegra and Skyra volumes showed strong association in most regions. This suggests that statistical tests related to specific research questions (e.g., differences between diagnostic groups) performed on data from each scanner separately would yield similar results. However, when combining data from different scanners within a single analysis, such as when performing multi-center or longitudinal studies, scanner effects would need to be accounted or controlled for. Jovicich et al. (2013) reported better across-session test–retest reproducibility when using the fully automated longitudinal FreeSurfer segmentation analysis (Reuter et al. 2012) pipeline compared to the cross-sectional analysis. They suggest that this method may be effective in lessening the impact in longitudinal cohort studies of inter-scanner differences resultant from major upgrade or device replacement (Jovicich et al. 2013).

5.5.2) Within scanner comparisons of Manual vs Automated Segmentation

When comparing manual and FreeSurfer segmented volumes, we observe marginally stronger associations for Skyra than Allegra data, specifically in the GP and CC (Table 5.3). Therefore, it is likely that FreeSurfer is more apt at segmenting Skyra images, with less variability, than Allegra images. Nonetheless, even our Skyra results demonstrate significant differences between manual and automatically segmented volumes in every structure examined, except bilateral caudate. This may be due to well distinguishable boundaries of the caudate head, with the ventricle medially and white matter laterally.

Except for Skyra caudate volumes, our results (Table 5.3 and Fig. 5.2) reveal that automated segmentation consistently overestimates the volumes of the subcortical GM regions examined here compared to manual segmentation. Improved performance of automated segmentation in the caudates on Skyra data may, in part, be due to the fact that the training dataset from which the FreeSurfer segmentation atlas was derived used data from a scanner and acquisition protocol with similar specifications to that of the Skyra scanner. The idea of biases involving segmentation software is not a new concept (Biberacher et al. 2016; Gronenschild et al. 2012; Lee et al. 2019; Liu et al. 2020). Gronenschild et al. (2012) showed it was possible to have differing outputs from FreeSurfer analyses depending on FreeSurfer version, operating system or workstation. Although the Allegra scanner has fairly non-linear gradients, which may introduce a marginal volume bias particularly in structures further from the isocenter, this is likely not the cause for discrepancies between automated and manually segmented volumes as even a seasoned neuroanatomist would not be able to control for this through mere delineation. This may, however, have contributed to the larger ICV found in the Allegra than Skyra images (Table 5.1).

In the case of the CC, both the definition and protocol for deriving volume differs between manual and automated segmentation. Anatomically the CC only exists in the mid-sagittal line, and all projections laterally from this area are merely white matter projections toward GM areas. Manual segmentation of the CC involves averaging the area of the CC on 3 mid-sagittal slices, each of thickness 1mm. This yields an estimate for the CC volume on the center most slice. In the case of FreeSurfer segmentation, we obtain a CC volume by summing the volumes of the various corpus callosal sub-regions that FreeSurfer outputs. However, FreeSurfer assigns the CC a relatively arbitrary thickness spanning 8 to 10 slices. To facilitate comparison between manual and automated CC volumes, we divided the total CC volume by the number of slices to obtain an average CC volume per slice. Since the area of the CC will decrease on slices further from the midline, thereby decreasing the average CC volume per slice, it is not surprising that our automated CC volume is smaller than the manually traced CC volume on Skyra images. On Allegra data, the automated CC volume is erroneously enlarged due to incorrect inclusion of the bright anterior cerebral artery into the corpus callosum segmentation as discussed previously. This may also accounts for the poorer consistency between manual and automated CC volumes on Allegra data.

5.5.3) Conclusion

We find both manual and automated derived volumes to be highly reproducible in the select structures across two Siemens scanners within a pediatric sample. Automated segmentation in FreeSurfer V6 yielded greater consistency across scanners and less inter-scanner variability but was more susceptible to scanner related bias. As a result, longitudinal studies using automated segmentation methods in this cohort may need a covariate to account for systematic inter-scanner variability.

CHAPTER 6 ALTERED BASAL GANGLIA GROWTH TRAJECTORIES FROM AGE 5-10 YEARS IN CHILDREN LIVING WITH HIV

6.1 Abstract

340 000 children live with HIV-1 in South Africa (SA). Ongoing neurological pathology may lead to impaired CNS maturation and poorer cognitive outcomes. Previous cross-sectional study in this group of children, who were perinatally infected with HIV-1 (PHIV), showed larger subcortical gray matter and smaller white matter in children with PHIV as compared to controls, at 5 years of age. The current work serves as a longitudinal follow-up to assess whether these morphometric differences persisted into later childhood.

Participants were forty children (20 PHIV, 20 uninfected controls) in long-term follow-up at the Family Centre for Research with Ubuntu in Cape Town, SA. Children with perinatal HIV-1 (PHIV) were from the Children with HIV Early antiRetroviral (CHER) trial (Cotton et al. 2013; Violari et al. 2008) and controls from an interlinking vaccine trial (Madhi et al. 2010).

High-resolution T1-weighted images were acquired at ages 5, 7, 9 years at the Cape Universities Brain Imaging Centre (CUBIC) on a 3 T Allegra (Siemens, Erlangen, Germany) and at 9/10 years on a 3 T Skyra (Siemens, Erlangen, Germany) using the same sequences and similar imaging parameters (125 total scans). Images were manually traced to determine volumes of basal ganglia structures and corpus callosum using MultiTracer.

Volumetric growth curves were fit using mixed effects models with subject-specific random effects, with adjustment for possible two-way interactions between age and diagnosis. We investigated linear, quadratic, cubic and logarithmic fits for each volume. Logarithmic models had the lowest Bayesian information criteria (BIC) scores. HIV-related alterations to growth trajectories were observed in the right NA and bilateral Pu. Volumes were relatively constant from 5-10 years in uninfected children, whilst children with PHIV demonstrated substantial volume reductions over this period. Gray matter volume reductions with age were evident among all children in the caudate and globus pallidus. HIV-related corpus callosum reductions previously reported at age 5 did not alter the growth trajectories from 5 to 10 years. Our results show that HIV-related volume differences observed at 5 years do not persist and become less apparent with age.

6.2 Introduction

The rate of new human immunodeficiency virus (HIV-1) infections in children have decreased by 10 000 every year from 2015 (190 000 new cases) to 2019 (150 000 new cases) (Communications and Global Advocacy UNAIDS 2020). While more than 95% of pregnant women living with HIV-1 receive combination antiretroviral therapy (ART) to prevent vertical HIV-1 transmission, only 47% of children living with HIV-1 receive ART in South Africa (WHO-UNAIDS 2019). Despite suboptimal coverage of ART amongst children, successful treatment has led to many perinatally infected children entering adolescence and early adulthood. Nonetheless, ongoing neurological disease resultant from HIV reservoirs in the brain may lead to impaired CNS maturation and poorer outcomes (Lewis-de los Angeles et al. 2020; van Rie, Mupuala & Dow 2008). Additionally, ART or other factors (lack of adherence, low socioeconomic status (SES), nutrition and environmental stressors) may cause neurodevelopmental impairment despite systemic virologic suppression (van Rie et al. 2007).

Normal brain development is characterised by gray matter (GM) volume increases across childhood due to neuronal establishment, followed by pruning-related volume reductions commencing during late childhood or early adolescence(Giedd, Jay N et al. 1999; Giedd & Rapoport 2010; Lenroot et al. 2007). To date, the effects of HIV infection on the developing brain in the presence of long-term ART is not well understood (Van den Hof et al. 2020; Van Den Hof et al. 2019; Musielak & Fine 2016; Phillips et al. 2016). Although neuroimaging allows this question to be examined directly and non-invasively, studies using neuroimaging have typically been performed in low prevalence regions (Lewis-de los Angeles et al. 2017; Nagarajan et al. 2012) and are predominantly cross-sectional spanning wide age ranges (Paul et al. 2018; Sarma et al. 2014; Wade et al. 2019). Studies of brain morphometry have provided evidence of HIV-related brain changes despite viral suppression, including cortical thickness, gyrification and volume alterations (Cohen et al. 2016; Lewis-de los Angeles et al. 2017, 2020; Nwosu et al. 2023; Paul et al. 2018; Sarma et al. 2014; Wade et al. 2019; Yadav et al. 2017), and altered cortical maturation (Lewis-de los Angeles et al. 2020; Paul et al. 2018; Yu et al. 2019). There is a need for longitudinal pediatric studies with multiple time-points to model the trajectory of brain integrity in the context of sustained viral suppression on ART (Paul et al. 2018). Recently, Nwosu et al. through use of automated segmentation techniques, observed no difference in growth trajectory of cortical thickness nor gyrification between

PHIV and uninfected children (Nwosu et al. 2023). Both PHIV and uninfected children followed from 5 to 9 years of age showed similar trend of generalized cortical thinning, albeit 6 cortical regions were identified to be thicker in the PHIV group (Nwosu et al. 2023).

The Children with HIV Early antiRetroviral (CHER) trial performed in South Africa investigated ART initiation strategies in infants with perinatally-acquired HIV (PHIV), diagnosed between 6 and 12 weeks of age (Violari et al. 2008). In an ongoing neurodevelopmental follow-on study, we are repeatedly imaging children with PHIV from the CHER trial who are resident in Cape Town, together with age- and community-matched uninfected children. The goal of the study is to examine the long-term consequences of PHIV on the developing brain in children who initiated ART in infancy and have been virally suppressed from a young age. Previously we reported subcortical volume alterations in these children at ages 5 (Randall et al. 2017) and 7 years (Nwosu et al., 2018), albeit in different directions and using different methodologies. Since not all subcortical structures mature at the same rate (Giedd, Jay N et al. 1999; Giedd & Rapoport 2010), a snapshot over a narrow age range cannot provide a clear picture of the impact of pathology on brain development, highlighting the need for longitudinal analyses.

Here we present growth trajectories for a sub-group of children from our ongoing neuroimaging study for whom we have manually traced the basal ganglia structures and corpus callosum (CC) on magnetic resonance (MR) images acquired from ages 5 to 10 years. We hypothesize that all children will demonstrate age-related basal ganglia volume reductions that will be steeper in the nucleus accumbens and putamen in PHIV than uninfected controls. Since we previously found that CC areas were smaller in PHIV at age 5 years (Randall et al., 2017) and equal at 7 years (Nwosu et al., 2018), we hypothesize steeper volumetric increases over this age range in PHIV than controls.

6.3 Methods

6.3.1) Participants

Participants were 40 children (20 PHIV, 20 uninfected controls) from our ongoing longitudinal neuroimaging study in Cape Town, South Africa. Children with PHIV were recruited from the CHER trial (Cotton et al. 2013; Violari et al. 2008) and uninfected controls from an interlinking vaccine trial (Madhi et al. 2010). Uninfected children were demographically matched according to age, sex, location, SES and population group. Children were scanned at ages 5, 7, 9 and 10 years without sedation in accordance with protocols approved by the Human Research Ethics Committees of the Faculties of Health Sciences at the Universities of Cape Town and Stellenbosch. Parents/guardians provided written informed consent. Children provided assent.

6.3.2) Image acquisition

Children were scanned at 5, 7 and 9 years of age at the Cape Universities Brain Imaging Centre (CUBIC) on a 3 T Allegra (Siemens, Erlangen, Germany) using a volumetric echo-planar imaging (EPI) navigated (Tisdall et al. 2012) multi echo magnetization prepared rapid gradient echo (MEMPRAGE) sequence (van der Kouwe et al. 2008). Imaging parameters were: FOV 224 x 224 mm2; 144 sagittal slices, TR 2530 ms; TE 1.53/3.19/4.86/6.53 ms; TI 1160 ms; flip angle 7°; voxel size 1.3 x 1.0 x 1.0 mm3, scan time 5:20 min. At age 9/10 years, children were scanned on a 3 T Skyra (Siemens, Erlangen, Germany) using the same sequence and similar imaging parameters, except for 176 sagittal slices, TE 1.69/3.54/5.39/7.24 ms; TI 1100 ms; and voxel size 1.0 mm3.

6.3.3) Image processing and analysis

Each participant's MR image volume was transformed into the AC-PC plane and rotated for hemispherical symmetry using BrainVoyager QX software (Brain Innovation, Maastricht).

On each participant's MR images, the caudate head, nucleus accumbens (NA), globus pallidus (GP) and putamen (Pu) were manually outlined in both hemispheres using MultiTracer software (Woods 2005). Contours were traced slice by slice on the coronal plane. Sagittal and transverse views were used to identify landmarks to assist with tracings. Based on these tracings, MultiTracer provides frust volumes for each structure. "Frust" volumes

assume that a contour applies to the centre of the slice on which it is drawn and that the square root of the cross-sectional area changes linearly across the slice thickness (Woods 2003). The CC was traced on 3 mid-sagittal slices, and the areas averaged as a measure of CC size. Screen settings were standardized across all tracings to ensure consistent screen brightness and contrast. A single expert neuroanatomist (SR) who was blind to participant demographics and clinical data performed all tracings. Intra-rater reliabilities were assessed by re-tracing a random subset of 10 brains. For all ROIs Cronbach's α exceeded 0.83 (Cronbach 1951).

6.3.4) Statistical analyses

IBM SPSS 28 was used for descriptive statistics. Associations between outcome variables (regional volumes) and demographic data were investigated for model building. Two demographic variables, sex and birthweight, were investigated as covariates. Only sex showed weak association (at $p<0.10$) with regional volumes and was included as a covariate in our models. Moreover, sex has been shown to affect peripubertal hormone levels across the age range studied here, which may affect rate of brain maturation during the time period between scans (Biro et al. 2013, 2014). Since we have previously shown no effect of scanner on regional volumes obtained with manual segmentation at 9- to 10-years [chapter 5](Randall et al. 2021) we did not control for scanner in our analyses.

Volumetric growth curves were fit using mixed effects models with subject-specific random effects, with a term included to adjust for possible two-way interactions between age and diagnosis. Each model was run twice altering the reference categories within diagnosis. The R Software Package (lme4) was used for modelling and visualizing of data. We investigated linear and non-linear fits (linear, quadratic, cubic and logarithmic) for each volume. The Bayesian information criteria (BIC) were used to identify the best fit model.

6.4 Results

We present volumes for 4 subcortical regions (both left and right) and the corpus callosum from 125 MR images acquired in 40 children (20 PHIV; 20 uninfected controls) between 5 and 10 years of age. Of these children, 11 were scanned twice, 13 three times and 16 were scanned 4 times. Table 6.1 provides participant demographics for each time point and clinical measures for the PHIV. The distribution of the sample on diagnosis and sex did not differ across time points (all p's > 0.4). At enrolment (age < 12 weeks), 5 of the infants with PHIV had CD4% < 25%, 9 had CD4/CD8 ratios below 1, and only 2 were virally suppressed (plasma viral load<400 copies/mm3). PHIV infants initiated ART at a mean age of 0.3 ± 0.3 years (range 0.12 – 1.2 years).

Table 6.1. Sample characteristics at each scanning time point.

Sample Descriptives	Total Individuals	3 T Allegra MRI			3 T Skyra MRI
		5 yrs	7 yrs	9 yrs	10 yrs
N	40	30	29	32	34
Sex: number of males (%)	22 (52%)	15 (50%)	15 (52%)	15 (47%)	22 (65%)
Age (yrs)	--	5.5 ± 0.3 [5.1-6.3]	7.2 ± 0.1 [7.1-7.4]	9.2 ± 0.2 [8.3-9.4]	9.9 ± 0.4 [9.1-10.4]
PHIV: n (%)	20 (50%)	16 (53%)	15 (52%)	12 (38%)	16 (47%)
PHIV: number of males (%)	11 (52%)	7 (44%)	7 (47%)	7 (58%)	10 (63%)

	Age				
Clinical Measures for Children with PHIV	At Enrolment onto CHER Trial (<12 weeks)	5 yrs	7 yrs	9 yrs	10 yrs
N	20	16	15	12	16
PVL - Suppressed (<400 copies/mL): n (%)	2 (10%)	16 (100%)$_1$	14 (93%)$_1$	11 (92%)$_1$	16 (100%)$_1$
CD4 Count (cells/mm3)	1499 ± 820 [294-4272]	1131 ± 421 [487-2101]$_1$	1105 ± 284 [609-1598]$_1$	1008 ± 490 [568-2129]$_1$	1155 ± 441 [742-2562]$_1$
CD8 Count (cells/mm3)	1549 ± 975 [565-4337]	978 ± 403 [358-1571]$_1$	819 ± 429 [303-1726]$_3$	809 ± 277 [513-1177]$_4$	908 ± 6 [351-1515]$_1$
CD4/CD8 Ratio	1.1 ± 0.8 [0.2-2.7]	1.3 ± 0.7 [0.6-3.4]$_1$	1.8 ± 1.0 [0.6-3.6]$_3$	1.2 ± 0.2 [0.9-1.5]$_4$	1.4 ± 0.5 [0.7-2.8]$_1$
CD4%	30.5 ± 10.5 [9.9-50]	36.8 ± 7.3 [24.4-55.2]$_1$	38.4 ± 6.0 [28-51]$_1$	38.4 ± 6.1 [27-47]$_1$	39.9 ± 6.6 [31-56]$_1$

PVL - Plasma Viral Load, yrs - years
Values are Number(Percentage) and Mean±Standard Deviation [Range]
Subscript values indicate number of missing clinical sample cases

The logarithmic model had the lowest BIC scores for all models (Appendix C). The model demonstrated HIV-related alterations of growth trajectories in the right NA and bilateral Pu. While volumes in these regions were relatively constant over this age range in uninfected children, children with PHIV demonstrated substantial volume reductions over this period (Table 6.2).

Table 6.2. Logarithmic mixed-effects model of growth trajectories from 5 to 10 years for basal ganglia structures and corpus callosum (CC) in children living with HIV and uninfected control children.

Logarithmic Model		Log(Age at scan) + Age at scan + Diagnosis + Sex + Log(Age at scan):Diagnosis + Age at scan:Diagnosis						
		Controls			**PHIV**			**Interaction Term**
		β_1	**SE**	*p*	β_1	**SE**	*p*	*p*
L Caudate	Log(Age at scan)	**-12170.58**	**3170.03**	**<0.001**	**-20783.19**	**4339.11**	**<0.001**	0.113
	Age at scan	**629.13**	**182.80**	**<0.001**	**1093.19**	**257.25**	**<0.001**	0.145
R Caudate	Log(Age at scan)	**-9489.13**	**2924.68**	**0.002**	**-18330.58**	**4029.82**	**<0.001**	0.080
	Age at scan	**472.83**	**168.63**	**0.006**	**945.82**	**239.11**	**<0.001**	0.110
L NA	Log(Age at scan)	-83.56	881.12	0.925	-1659.95	1199.15	0.170	0.293
	Age at scan	1.21	50.79	0.981	91.47	71.03	0.202	0.304
R NA	Log(Age at scan)	68.24	1036.14	0.948	**-3477.71**	**1411.95**	**0.016**	**0.046**
	Age at scan	-14.11	59.66	0.814	**186.86**	**83.59**	**0.028**	0.054
CC	Log(Age at scan)	**-2673.57**	**592.25**	**<0.001**	**-1844.80**	**799.64**	**0.024**	0.407
	Age at scan	**139.71**	**34.12**	**<0.001**	**99.51**	**47.31**	**0.039**	0.493
L Pu	Log(Age at scan)	902.37	2718.81	0.741	**-13694.30**	**3534.09**	**<0.001**	**0.001**
	Age at scan	-47.45	156.73	0.796	**703.55**	**209.67**	**0.001**	**0.005**
R Pu	Log(Age at scan)	-1140.89	2689.44	0.673	**-15855.21**	**3497.34**	**<0.001**	**0.001**
	Age at scan	53.34	155.04	0.732	**813.65**	**207.21**	**<0.001**	**0.004**
L GP	Log(Age at scan)	**-6247.21**	**2192.48**	**0.006**	**-9505.12**	**2827.39**	**0.001**	0.365
	Age at scan	**329.92**	**126.37**	**0.011**	**494.09**	**167.38**	**0.004**	0.436
R GP	Log(Age at scan)	**-8604.64**	**2087.79**	**<0.001**	**-8489.11**	**2695.32**	**0.002**	0.973
	Age at scan	**447.35**	**120.34**	**<0.001**	**415.19**	**159.61**	**0.011**	0.873

Values are unstandardised Betas and standard errors (SE); Bold indicates significance at $p < 0.05$

NA nucleus accumbens; CC corpus callosum; Pu putamen; GP globus pallidus; L left; R right

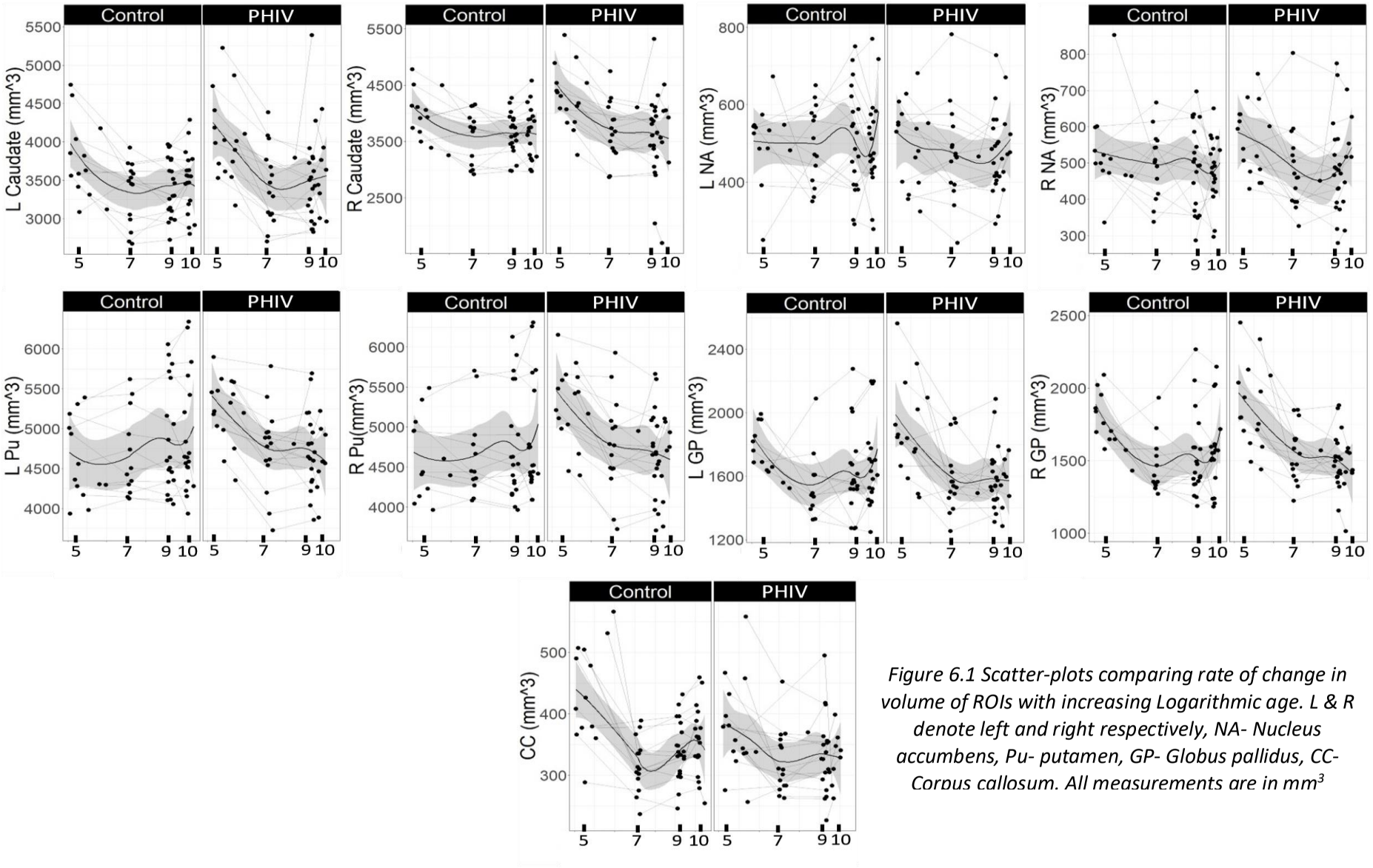

Figure 6.1 Scatter-plots comparing rate of change in volume of ROIs with increasing Logarithmic age. L & R denote left and right respectively, NA- Nucleus accumbens, Pu- putamen, GP- Globus pallidus, CC- Corpus callosum. All measurements are in mm³

Table 6.3 Cross- sectional Univariate Analysis of Variance at each age grouping

	5 Year Data					7 Year Data					9 Year Data					10 Year Data				
	Control n=14		PHIV n=16			Control n=14		PHIV n=15			Control n=20		PHIV n=12			Control n=18		PHIV n=16		
ROI [mm^3]	Mean	(SD)	Mean	(SD)	*p*	Mean	(SD)	Mean	(SD)	*p*	Mean	(SD)	Mean	(SD)	*p*	Mean	(SD)	Mean	(SD)	*p*
L Caudate	3764	(518)	4046	(440)	0.166	3336	(409)	3417	(501)	0.575	3413	(379)	3578	(331)	0.204	3515	(387)	3478	(699)	0.774
R Caudate	3961	(457)	4285	(527)	0.092	3592	(459)	3693	(518)	0.700	3626	(366)	3712	(597)	0.691	3698	(454)	3568	(811)	0.902
L NA	507	(100)	500	(106)	0.874	498	(474)	474	(126)	0.562	509	(134)	469	(110)	0.295	489	(112)	480	(112)	0.680
R NA	525	(118)	564	(97)	0.347	498	(94)	484	(118)	0.635	494	(117)	482	(120)	0.804	478	(89)	499	(128)	0.226
CC	**437**	**(82)**	**373**	**(76)**	**0.039**	318	(43)	321	(51)	0.493	340	(48)	331	(65)	0.656	361	(50)	335	(51)	0.642
L Pu	**4592**	**(508)**	**5231**	**(411)**	**<.001**	4673	(532)	4744	(524)	0.531	4844	(679)	4817	(427)	0.854	4910	(716)	4619	(472)	0.885
R Pu	**4615**	**(498)**	**5258**	**(484)**	**0.002**	4644	(538)	4763	(593)	0.422	4772	(685)	4704	(516)	0.678	4844	(712)	4634	(515)	0.882
L GP	1748	(156)	1887	(295)	0.138	1547	(212)	1585	(211)	0.587	1612	(260)	1598	(189)	0.829	1668	(280)	1562	(185)	0.853
R GP	1753	(191)	1865	(289)	0.241	1465	(197)	1551	(192)	0.316	1524	(284)	1515	(184)	0.809	1556	(275)	1458	(179)	0.674

ROI volumes are Mean(SD) mm^3, SD - Standard Deviation
L and R denotes left and right respectively, NA - nucleus accumbens, CC - corpus callosum, Pu - putamen, GP - globus pallidus

Cross-sectional analysis for each time point showed larger bilateral putamen, and smaller CC at the 5 year time of scanning. At the same age we observe a similar, although not significant finding for the bilateral caudate and GP. No differences were observed at other time points.

6.5 Discussion

Cross-sectional studies within this and other cohorts have reported HIV-related alterations in regional and global brain volumes in pediatric populations. However, due to the study designs, it is difficult to determine whether reported differences represent persistent or ongoing damage, or developmental delay. Previously we reported larger basal ganglia (NA and Pu) volumes and smaller corpora callosa in children with PHIV from the CHER cohort compared to controls at age 5 (Randall et al. 2017). To explore the long-term consequences of these findings, we followed a subset of these children longitudinally to age 10. Across all children and ROIs, we find that logarithmic mixed effects models best capture the regional volume growth trajectories. Bilaterally, the caudate and globus pallidus, and the corpus callosum, demonstrated similar age-related volume reductions over this period in controls and PHIV. As hypothesized, growth curves in the NA and Pu were altered in PHIV. While NA and Pu volumes remained relatively constant from 5 to 10 years in controls, volumes of the right NA and bilateral Pu decreased with increasing age in PHIV. Contrary to our hypothesis, neither controls nor PHIV demonstrated age-related size increases in the CC. Taken together, our volumetric findings at age 5 years and the longitudinal results presented here suggest a delay in NA and Pu development in PHIV. In contrast, the smaller CC volumes we observed in children with PHIV at 5 years does not appear to significantly influence its development across this age range. Cross-sectional analysis of this sample confirms the volumetric disturbance is only at 5 years of age, with PHIV exhibiting larger bilateral Pu and smaller CC, with no differences observed between groups at any other age.

6.5.1) Typical subcortical development from 5 to 10 years

Studies of typical brain development from birth to adulthood find subcortical GM volumes follow an inverted U-shaped trajectory, consisting of non-linear preadolescent volume increases followed by post-adolescent decreases likely related to accelerated neuronal pruning (Giedd, Jay N et al. 1999; Lenroot et al. 2007; Paul et al. 2018; Sowell et al. 2003). Age-related growth varies regionally, with peak volumes occurring at different ages across the brain (Giedd, Jay N et al. 1999; Lenroot et al. 2009). As a result, studies with smaller age ranges report varying age-related changes across structures. Some studies have reported logarithmic fits for these structures in childhood (Croteau-Chonka et al. 2016; Deoni et al.

2015; Remer et al. 2017). Mid-sagittal CC area increases throughout childhood and adolescence (Jahanshad & Thompson 2017; Lenroot et al. 2007; Luders, Thompson & Toga 2010; Westerhausen et al. 2011).

We observed age-related reductions in the bilateral caudate and GP across all children. In uninfected children, volumes of bilateral NA and Pu remained relatively constant with age. While the basal ganglia and global GM are said to typically decrease in volume with age throughout adulthood (Berger & Arendt 2000; Berridge 2007; Berridge & Robinson 1998; Giedd, Jay N et al. 1999; Moberg et al. 1998), developmental brain changes in healthy children are ongoing. The maturation of subcortical structures is therefore nuanced and blanket statements suggesting a linear and continual decrease in size with increasing age do not account for regional differences within the basal ganglia. Different regions within the basal ganglia mature at different rates (Lenroot et al. 2007), as well as growth being non-linear with differing trajectories (Deoni et al. 2015; Lenroot et al. 2007). Some studies of typically developing children across ages 3 to 18 years find linear and non-linear age-related decreases of the caudate, putamen and globus pallidus (Giedd et al. 1996; Jernigan et al. 1991; Sowell et al. 2002; Thompson et al. 2000; Tyborowska et al. 2018). Although studies observe age-related decreases, the slopes reported are often of small magnitude reflecting little change each year.

The process of myelination is active before birth through the first 2 years and continuous throughout life (Durston et al. 2001; Reiss et al. 1996). Lenroot et al. (2007) describes an increase in CC volume, at varying rates, with no peak within their age range from 7 to 20 years. A 2017 study looked at regional CC maturation between birth and 18 years in small age intervals revealing periods of growth punctuated by periods of growth plateau(Vannucci, Barron & Vannucci 2017). While our results point to a decrease in CC volume from 5 to 7 years instead of remaining constant as reported by Vannucci (2017), there is evidence of increasing size from 7 to 10 years. Observing changes across narrow age intervals, even if the observations are linear across a wide age range, may provide additional insight into age-related alterations.

Within the sample of uninfected children, we find growth trajectories consistent with the literature. The volumetric differences previously observed in children with PHIV at age 5 in

the CC and GP do not interrupt subsequent maturation in this age range. Within the PHIV, we observe similar growth patterns in all structures except the NA and Pu.

6.5.2) Atypical subcortical development from 5 to 10 years

Children with PHIV demonstrated different trajectories in the right NA and bilateral Pu. Our prior work with a larger sample of 79 children (Randall et al. 2017) showed larger bilateral Pu, left GP, right NA and smaller CC volumes in PHIV cross-sectionally at 5 years. These results are consistent in the current sub-sample where we observe larger bilateral Pu and similar trends in other GM structures (Table 6.3). We suggested increased basal ganglia volumes may indicate inflammation as a neuroprotective mechanism to the viral infection. This finding is congruent with other literature in pediatric populations (Paul et al. 2018; Sarma et al. 2014; Sowell et al. 2004). In support, HIV reservoirs persist predominantly in brain macrophages/microglia rather than astrocytes (Ko et al. 2019) during suppressive ART. Visual inspection of trajectories suggests slope differences occur due to the changes before 5 years, as volume ranges appear similar at later ages. Visually, as well as cross-sectionally, we do not observe major volume differences between diagnostic groups at 7, 9 and 10 years. Our findings may suggest HIV-1 and ART influence developmental pruning mechanisms in early childhood, which relaxes when approaching preadolescence. Or that are otherwise attenuated in later childhood. Similarly, controls appear to match the smaller CC in the 5-year PHIV group at around 7 years of age, this perhaps indicates a period of high metabolic demand in the CC driving hyper-pruning early in development before 5 years of age.

6.5.3) Limitations

The population presented are a subset of a larger cohort with limited statistical power. Additionally, the current study lacked sufficient sample to analyse subgroups nested within groupings, such as treatment interruption. We also were not able to include potential confounding variables, such as SES and maternal education, due to a lack of data. The work doesn't include any functional outcomes, such as cognitive scores, as they are part of another thesis project. Lastly, we did not include any variables related to PHIV health due to a lack of data across time points.

6.5.4) Conclusion

Subcortical age-related changes in this cohort between ages 5-10 years are best modelled by logarithmic growth models. GM volume reduction is ongoing among all children in the caudate, GP and CC from age 5-10 years. Children with PHIV show volume reductions in the right NA and Pu, which is primarily due to increased volumes previously reported at age 5. Accelerated pruning in children with PHIV potentially compensates for early neurodevelopmental delay, resultant from the degree of initial infection onslaught capable of passing the BBB. Unexpectedly, the corpus callosum reductions reported at age 5 did not alter the growth trajectories from 5 to 10 years. Overall, volume differences at 5 years are not persistent and become less apparent with age.

CHAPTER 7 PERINATAL PROINFLAMMATORY BIOMARKERS ARE PREDICTORS OF BASAL GANGLIA VOLUMETRIC DISTURBANCE AT 5 YEARS OF AGE.

7.1 Abstract

The severity of initial systemic infection has been linked to the severity of CNS neuropathogenesis of HIV-1 infection. Earlier age of infection coupled with high systemic viral loads places children at increased risk of HIV encephalopathy (Mitchell, Wendy 2001). Thus, systemic samples obtained at the time of initial infection, before ART initiation, are an ideal time-point to examine immune biomarkers predicting later neuropathological disease progression.

This study includes 27 children living with HIV-1 (5.3±0.2years, 11 Male) from the Children with HIV Early Antiretroviral (CHER) cohort. Blood samples were collected in infancy at study enrolment for isolation of peripheral blood mononuclear cells (PBMC). MRI protocol included a high-resolution T1-weighted 3D EPI-navigated MEMPRAGE acquisition (van der Kouwe et al. 2008; Tisdall et al. 2012) (FOV 224x224 mm2, TR=2530 ms, TI=1160 ms, TE's=1.53/3.19/4.86/6.53 ms, bandwidth 650 Hz/px, 144 sagittal slices, 1.0x1.0x1.3 mm3. Manual segmentation was performed by a single neuroanatomist (SR) using MultiTracer™ Software (Woods 2003). Subcortical structures included caudate head, nucleus accumbens, putamen, globus pallidus and corpus callosum. Cytokine levels were Z-Score transformed, principle component analysis performed to derive component variables that associate with volumetric outcomes. Cytokine coefficient loadings above 0.4 were considered plausible toward interpretation.

Within the associated component variable, 6 cytokines had coefficient loadings above 0.45 (IL-10, IP-10, LBP, IL-17F, IFNα, CD40L) and 4 loaded poorly (GCSF, PDGF-BB, TGFβ1 and TGFβ2). Results suggests an increase of IL-10, IP-10, LBP and IFN-α, and accompanying decrease in IL-17F and CD40L contribute to smaller basal ganglia volumes at 5 years. No association was observed for the CC. This exploratory work suggests the severity of initial infection and subsequent immunological response in early perinatal infection influences later development of basal ganglia components.

7.2 Introduction

As the developing brain is vulnerable, perinatally infected children with HIV-1 (PHIV) are at an increased risk of central nervous system (CNS) disturbance. The specific mechanisms of ongoing CNS pathology in virally suppressed children receiving treatment are unknown. HIV-1 can pass the blood brain barrier (BBB) and infect cells within the CNS, forming a viral reservoir. This initial invasion of HIV-1 into the CNS can occur as early as 10 days after infection (Ivey, MacLean & Lackner 2009). The severity of initial systemic infection has been linked to the severity of CNS neuropathogenesis of HIV-1 infection(Andronikou et al. 2014; Becker et al. 2011). Earlier age of infection coupled with high systemic viral loads places children at increased risk of HIV encephalopathy (Mitchell, Wendy 2001). Additionally, plasma levels of inflammatory markers have also been associated with poorer cognitive performance in youth (8-26 years of age), despite virologic suppression (Eckard et al. 2017). Thus, systemic samples obtained at the time of initial infection, where plasma viral load (PVL) is high and before ART initiation, is an ideal time to examine immune biomarkers predicting later disease progression.

HIV-1 is primarily found in supporting cells in the brain, particularly microglia and CNS-derived macrophages, rather than neurons (Takahashi et al. 1996). The body initiates a complex response that involves an interplaying cascade of multiple insult specific immunological cytokines regulated by both proinflammatory and mediatory anti-inflammatory markers. Often these large immunological response cascades cause damage and scarring to surrounding tissue (Martin & Leibovich 2005).

In children living with HIV, development and maturation of the immune system, BBB and CNS occurs around the time of initial infection (Bilbo & Schwarz 2012). As a result, the impact of HIV-related immune activation and CNS pathology may be more severe than described in adult studies, as they haven't fully developed their course of adaptive immunity. There is a need to study the impact or mitigation of disease progression following the release of immunological biomarkers during initial infection of HIV-1 and the developing brain.

The BBB pertains to a specialized set of properties compartmentalizing the CNS from the systemic blood supply. Its purpose is to protect the CNS by tight regulation of the movement of molecules, ions, and cells (Daneman & Prat 2015). The barrier allows strict regulation of

homeostasis needed for normal neuronal function, as well as compartmentalizing the CNS from toxins, pathogens, inflammation, injury and disease (Daneman & Prat 2015). However, some diseases are capable of impeding or causing dysfunction to the BBB (Zlokovic 2008), whilst others – like HIV-1 – infect monocyte-macrophages which can traverse the BBB (Strazza et al. 2011). Infected cells can infect neighbouring support cells such as astrocytes and microglia (Strazza et al. 2011). The release of viral toxins in combination with inflammatory mediators further disrupts the BBB, this results in the recruitment and invasion of immune cells into the CNS, further complicating the effects of inflammation (Lane et al. 2000). There is a lower turnover of cerebrospinal fluid (CSF) in the developing brain as compared to adults, which leads to higher concentrations and accumulation of proteins (Johansson et al. 2008; Saunders, Liddelow & Dziegielewska 2012). These could include accumulations of immunological cytokines as well as viral proteins and associated metabolic waste products. The BBB impedes drug delivery to the CNS, where penetration by ART is limited (Ene et al. 2011). As a result, the CNS becomes a viral reservoir in which few drugs are available to impact (van Rie et al. 2007). In addition, systemic blood viral loads may not reflect what is occurring in the CSF (Blokhuis et al. 2019; Ene et al. 2011; McCoig et al. 2002). Once traversing the BBB the resultant infection of HIV-1is less impacted by ARVs, due to lack of penetration through the BBB. Mutations within the compartmentalised viral reservoir may result in unique genetic differences between plasma and CSF strains (Ene et al. 2011; Strain et al. 2005). This limited antiretroviral action is further complicated by the preference of HIV-1 to infect specific CD4+ cell types (astrocytes, microglia and macrophages) and thus create unique genetic variants within the CNS (Ene et al. 2011; Lanier et al. 2001; Ritola et al. 2005; Schnell et al. 2011).

In our data at 5 years of age, we observed larger basal ganglia and reduced corpus callosum volumes in PHIV children compared to controls. Our results were unexpected as the majority of imaging studies observed localized (Ances et al. 2012; Aylward et al. 1993; Becker et al. 2011; Chiang et al. 2007) as well as global atrophy or smaller gray matter in individuals with HIV compared to uninfected controls (Chiang et al. 2007; Johann-Liang et al. 1998; Lewis-de los Angeles et al. 2017; Mitchell, W 2001; Sarma et al. 2014; Thompson et al. 2006). However, some studies have reported larger GM amongst PHIV (Blokhuis et al. 2017; Nwosu et al. 2023; Paul et al. 2018). While the outcomes reported may be related to methodology or study design, it may also be due to ongoing biological processes.

While we didn't find volume differences in caudate volumes, we reported a positive relationship between immune health outcomes (CD4/CD8 ratio) in infancy and 5-year-old caudate volumes. Similar findings were reported in the cohort from MRS findings, with NAA and Cho levels in the basal ganglia at 5 years related to CD4/CD8 ratios in infancy (Mbugua et al. 2016). Both results suggest a potential link between an early immune response and basal ganglia development in early childhood. We also presented cross sectional and longitudinal analyses indicating the enlargements observed at 5 years diminish with age, driving differences in growth trajectories (Chapter 6). We speculated that the biological reasons for the observed abnormalities at 5 years were possibly indicative of hyper-pruning in the presence of possible ongoing stress and inflammation at earlier ages. In order to better understand the link between the infant immune system and the brain at 5 years, we present an exploratory and retrospective analysis between subcortical volumes at 5 years of age in a subgroup of PHIV children from the cohort and available cytokine data from available stored blood samples collected at enrolment.

There are few studies of cytokine levels in relation to brain volumes in individuals living with HIV. One study in adults observed the concentration of interferon induced protein 10 (IP-10) to associate negatively with the size of the putamen, globus pallidus, thalamus, hippocampus, amygdala and global WM and GM (Gongvatana et al. 2014). There are similar findings of association of MCP-1 with decreasing global GM (Ragin et al. 2010). The studies to date examine plasma derived cytokine biomarkers and brain imaging outcomes at the same time point, linking volume abnormalities with current immune health. (Cao et al. 2015; Gongvatana et al. 2014; Ragin et al. 2010).

Our group has studied the ongoing influence of HIV-1 in a cohort of children with perinatal HIV-1 that initiated ART in infancy. Previous work identified HIV-related disparities in subcortical volumes at age 5 years (Mbugua et al. 2016; Randall et al. 2017). We hypothesize that volumetric abnormalities observed at age 5 years are related to the body's immune response in early infancy before treatment. The exploratory work presented in this chapter addresses potential relationships between biomarkers from the participant's initial immune response to brain imaging outcomes at 5 years in perinatally infected infants. As such, this work may represent different biological processes as compared to previous studies.

7.3 Materials and Methods

This study includes children from the Children with HIV Early Antiretroviral (CHER) cohort who participated in an ongoing longitudinal neurodevelopmental study. Blood samples were collected in infancy at study enrolment for isolation of peripheral blood mononuclear cells (PBMC) (stored in cryovials and placed in liquid nitrogen) and plasma (stored in polypropylene Eppendorf's at -80°C) storage. Early collected samples (PBMCs and plasma) were retrieved from Clinical Laboratory Services (CLS)™ in Cape Town, South Africa, storage repository. Due to parent study design involving the CHER cohort and community matched controls, no samples were available from uninfected children at infancy or at 5 years for comparison.

First line ART comprised of lopinavir-ritonavir, zidovudine and lamivudine at ART initiation. Second line ART comprised didanosine, abacavir, nevirapine.

7.3.1) Brain Imaging

At age 5 years, PHIV children from the CHER cohort In Cape Town underwent brain imaging using a 3 T Siemens™ Allegra (Erlangen, Germany) at the Cape Universities Brain Imaging Centre (CUBIC) in Cape Town, South Africa. Scanning was performed according to protocols approved by the Human Research Ethics Committees of the Universities of Cape Town and Stellenbosch.

The protocol included a high-resolution T1-weighted 3D EPI-navigated MEMPRAGE acquisition (van der Kouwe et al. 2008; Tisdall et al. 2012) (FOV 224x224 mm2, TR=2530 ms, TI=1160 ms, TE's=1.53/3.19/4.86/6.53 ms, bandwidth 650 Hz/px, 144 sagittal slices, 1.0x1.0x1.3 mm^3.

Manual segmentation was performed by a single neuroanatomist (SR) using MultiTracer™ Software (Woods 2003) for select structures within the basal ganglia, these included the caudate head, nucleus accumbens (NA), putamen (Pu), globus pallidus (GP) and corpus callosum (CC). The condensed protocol is referred to in a previous publication (Randall et al. 2017). The rater was blinded to all participant data during segmentation.

7.3.2) HIV-1 Plasma Viral Load Quantification

Viral loads were quantified by an accredited routine diagnostic laboratory, the National Health Laboratory Services (NHLS), Tygerberg Cape Town, South Africa. HIV-1 plasma RNA levels were first measured using the Roche Amplicor HIV monitoring assay (version 1.0) with a lower limit of detection (LOD) of 400 copies/mm^3 and upper limit of 750000 copies/mm^3

7.3.3) Blood Plasma Immune Biomarker Measurements

An extensive panel of 44 soluble biomarkers were assessed. We chose a broad range of immune biomarkers to cover both innate and adaptive immune pathways, as well as biomarkers which were previously indicated in the literature involved in immune health and populations infected with HIV-1. Biomarkers assessed included: IL-17F, IL-1β, IL-1Ra, IL-1α, IL-2, IL-3, IL-4, IL-5, IL-6, IL-7, IL-8 (CXCL8), IL-9, IL-10, IL-12, IL-13, IL-15, IL-17A, IP-10 (CXCL10), IFN-γ, macrophage chemoattractant protein 1 (MCP-1 or CCL2), MIP-1α (CCL3), MIP-1β (CCL4), TNF-α, TNF-β, GCSF, GMCSF, CD40L, VEGF, INF-α, fibroblast growth factor (FGF), RANTES, (CCL5) PDGF-BB, TGFβ1,2 and 3, sCD14, sCD163, IL-18, hsCRP, LBP, I-FABP, MAdCAM-1 and s100A8/A9), which were measured using (a) validated Hycult® Biotech Enzyme Linked ImmunoSorbent Assays (ELISA) [for hsCRP, LBP and I-FABP measurements]; and (b). Luminex® Multiplex assays from R&D Systems [for sCD14, sCD163, IL-18, MAdCAM-1 and s100A8/A9] and Milliplex®MAP (Merck) [for all remaining markers]. A classical Sandwich ELISA method was applied to samples for measurement of hsCRP, LBP and I-FABP. Standards were prepared in duplicate. Due to retrospective nature of study with limited available sample volumes, single measures were taken. Depending on the number of analytes measured in each kit, standard curves for each analyte were generated using known concentration standards of the cytokine/chemokine levels evaluated and provided in the selected kits. Plasma cytokine levels were determined using a multiplex array reader from Luminex® Instrumentation System (Bio-Plex II Workstation from Bio-Rad®, California, USA). Plasma cytokine/chemokine concentrations were calculated as the average of two independent measures using Bioplex® Manager Software (California, USA). Study participants with values out of range were assumed to have a biomarker value of half the detection limit. Standard curves were configured as a five-parameter logistic curve via computer software during plate reading.

7.3.4) Statistical Analysis

Statistical analyses were performed in SPSS28.

Age and sex (due to possible peripubertal hormone alterations which may affect rate of brain maturation during the time period between scans (Biro et al. 2013, 2014)), were investigated as possible confounders.

All immunological variables were Z-score transformed to account for varying differences of scale between concentration values, as well as outlier identification. This served to make the data more normal. Principle component analysis (PCA) was performed using all cytokines. Pearson correlation was used to assess association of generated component variables with subcortical region volumes. Component variables showing the highest association with volumetric variables were identified. As the present study is purely exploratory with a limited sample size we are not capable of assessing inference, however we aim to identify immunological markers with possible long term effects for future study. Conservatively coefficient loading values above 0.4 were considered to be plausible and relevant for interpretation as per Stevens (1992), when dealing with coefficients irrespective of sample size. Additionally, for interpretation of strength of loading we applied binned terminology aligning with that of Tabachnik and Fidell (2018) and Comrey and Lee (2013), indicating values above 0.32 (poor), 0.45 (fair), 0.55 (good), 0.63 (very good) or 0.71 (excellent).

7.4 Results

We present sample characteristic information from 27 children with PHIV (11 Male). Clinical data is presented for enrolment and at time of scanning. All 27 children had active HIV-1 infection at the time of enrolment, while 23 of 25 children were virally suppressed at the time of scanning.

Table 7.1. Description of sample with clinical measures at time of enrolment and at scan.

Sample Descriptives	**Enrolment**		**Scan**	
N	27			
Sex: number of males (%)	11 (41%)			
Age	8.0 ± 1.6 [6.0-11.9] Wks		5.3 ± 0.2 [5.0-5.9] Yrs	
Clinical Measures for Children with PHIV	**Enrolment**		**Scan**	
PVL - Suppressed (<400 copies/mL): n (%)	0 (0%)		23 (92%)$_2$	
Age at ART Initiation (Wks)	4.6 ± 3.7 [2 - 15]			
Time to Suppression (Wks)	47 ± 47 [1 - 200.6]$_1$			
CD4 Count (cells/mm3)	1802 ± 938 [294 - 3828]$_1$		1250 ± 765 [438 - 3220]$_2$	
CD8 Count (cells/mm3)	1597 ± 866 [422 - 4119]$_1$		1014 ± 533 [332 - 2660]$_2$	
CD4/CD8 Ratio	1.4 ± 0.9 [0.3-3.5]$_1$	12(46%)<1.0	1.3 ± 0.5 [0.5 - 2.4]$_2$	9(36%)<1.0
CD4%	34.3 ± 11.1 [12.9-53.9]$_1$	3(12%)<25%	36.3 ± 8.3 [18.9 - 51.3]$_2$	1(4%)<25%

PVL - Plasma Viral Load, Yrs - years, Wks - weeks
Values are Number(Percentage) and Mean±Standard Deviation [Range]
$_1$ - 1 Child with missing Clinical data
$_2$ - 2 Children with missing Clinical data

7.4.1) Covariate Analysis Of Sample Characteristics

Univariate analysis of variance assessing possible volumetric difference within biological sex (Table 7.2) revealed larger right caudates and CC in male children, and a similar trend level difference in left putamen and right GP.

Table 7.2. Univariate ANOVA – Sex difference in subcortical gray matter volumes

	Female Mean(SD)	Male Mean(SD)	*F*	*p*
L Caudate	4006 (297)	4227 (394)	2.753	0.110
R Caudate	**4154 (307)**	**4440 (377)**	**4.709**	**0.040**
L NA	603 (122)	641 (97)	0.735	0.399
R NA	650 (85)	645 (151)	0.012	0.913
CC	**319 (45)**	**367 (53)**	**6.478**	**0.017**
L Pu	5118 (477)	5514 (719)	2.978	0.097
R Pu	5161 (534)	5512 (684)	2.245	0.147
L GP	1805 (301)	1971 (178)	2.669	0.115
R GP	1761 (281)	1935 (180)	3.247	0.084

Pearson correlation analysis of continuous sample characteristic variables (Table 7.3) revealed that increasing age resulted in decreasing size of the CC and similar trend level decline of the L NA with increasing age.

Table 7.3. Pearson association of age with subcortical gray matter volumes

	Age at Scan	
	r	*p*
L Caudate	-0.226	0.258
R Caudate	-0.242	0.224
L NA	-0.362	0.064
R NA	-0.036	0.860
CC	**-0.437**	**0.023**
L Pu	-0.071	0.727
R Pu	-0.048	0.813
L GP	-0.266	0.181
R GP	-0.222	0.265

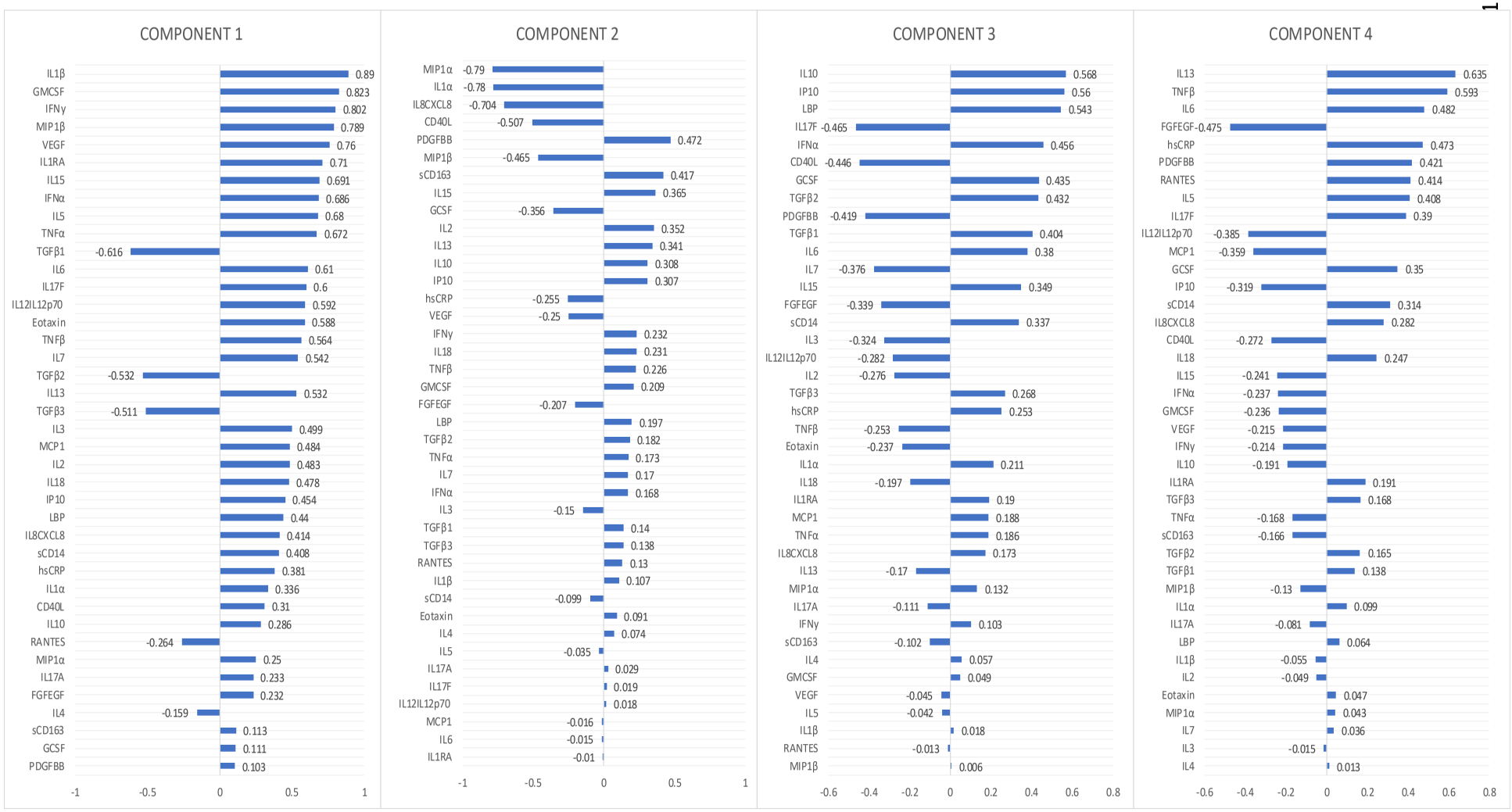

Figure 7.1 Four Component Variable Loadings From Principle Component Analysis Of Immunological Biomarkers

PCA revealed 7 unique components, of which four met the chosen criteria for a good fit, shown in figure 7.1. Only the 3rd component variable showed any association with subcortical structures. All relevant associations were observed to be negative with r>-0.380, these associations were not strengthened when controlling for confounders in affected structures.

Table 7.4 Pearson correlation of Component 3 association with subcortical volumes.

	PCA Component 3	
	r	*p*
L Caudate	-0.180	0.379
R Caudate	**-0.430**	**0.025**
L NA	**-0.384**	**0.048**
R NA	-0.323	0.101
CC	-0.137	0.497
L Pu	**-0.436**	**0.023**
R Pu	**-0.389**	**0.045**
L GP	**-0.478**	**0.012**
R GP	**-0.402**	**0.037**

In table 7.3 we observe a list of cytokines from the 3rd component variable which was identified to associate with subcortical volumes. We present their respective coefficient loadings for cytokines above 0.32, however for interpretation purposes we will only include those above 0.4 as per (Stevens 1992). We observe 3 cytokines experiencing good loadings (IL-10, IP-10, LBP), similarly 3 at the fair level (IL-17F, IFNα, CD40L) and 4 had poor loading (GCSF, TGF-β1, TGF-β2, PDGF-BB).

Table 7.5 Component 3 Principal Component Analysis Coefficient Loadings

Biomarker	Loading Coefficient	Loading Boundaries
IL-10	0.57	Good [> 0.55]
IP-10	0.56	
LBP	0.54	
IL-17F	-0.47	Fair [0.45-0.55]
IFNα	0.46	
CD40L	-0.45	
GCSF	0.44	Poor [< 0.45]
TGF-β2	0.43	
PDGF-BB	-0.42	
TGF-β1	0.40	
IL-6	0.38	
IL-7	-0.38	
IL-15	0.35	
FGFEGF	-0.34	
sCD14	0.34	
IL-3	-0.32	

Coloured bars are a visual representation of loading coefficients. Red indicates negative, whilst green indicates a positive loading.

7.5 Discussion

Our analysis of the potential relationship between volumes and immunological markers in PHIV shows areas of the basal ganglia at 5 years of age are associated with immune activity in infancy. Specifically, we find a loading array of infant immunological biomarkers that associates negatively with basal ganglia – right caudate, bilateral nucleus accumbens, putamen and globus pallidus – volumetric outcomes at 5 years of age. The aim of this analysis was to explore the potential involvement of specific immune biomarkers in infancy in HIV-related volume alterations at 5 years. While this is a subset of the PHIV cohort, it is interesting that we identified one set of cytokines related to subcortical volumes, many of which were larger in volume than their uninfected peers. The markers identified represent proinflammatory cytokines involved in innate immunity as well as cytokines related to maintaining and sustaining latent HIV-1 reservoirs. In PHIV, our exploratory analysis suggests immunological activity in early infection may contribute to disruptions in basal ganglia development in childhood.

We identified 10 of 44 possible immunological markers related to volumes at 5 years. The biomarkers with loading coefficients considered fair or good predictors included IL-10, IP-10, LBP, IL-17F, IFNα, CD40L, and those loading poorly include GCSF, PDGF-BB, TGFβ1 and TGFβ2. The results suggests that in infancy an increase of IL-10, IP-10, LBP and IFN-α, and accompanying decrease in IL-17F and CD40L contribute to smaller basal ganglia volumes at 5 years. The structures implicated in this analysis overlap with increased volumes – bilateral nucleus accumbens, putamen and left globus pallidus – reported earlier (Randall et al. 2017), as well as in the previous chapter.

The highest loading cytokine within the 3rd PCA component was IL-10, a potent anti-inflammatory cytokine. HIV-1 infection is associated with an increased production of IL-10 from T-helper cells (Harper et al. 2022). The function of IL-10 is to inhibit T-cell proliferation, predominantly by suppressing synthesis of Th1 cytokines, inhibit macrophage activation and decrease secretion of proinflammatory cytokines. The negative association with structure size may indicate a neuroprotective effect in which higher concentrations inhibit proinflammatory responses. This is supported by findings showing IL-10 being produced by resident microglial cells functioning to balance and mediate the immune response within the CNS (Lobo-Silva et

al. 2016). Up-regulation of IL-10 has also been found to inhibit viral replication in immune cells (Brockman et al. 2009; Gongvatana et al. 2014). In contrast, IL-10 may also contribute to the establishment of viral latency, where the virus remains dormant and hidden within host cells, evading immune surveillance and antiretroviral therapy (Harper et al. 2022).

While IL-10 is a potent anti-inflammatory, it is also involved in a pro-inflammatory response when accompanied with interferon alpha IFN-α (Gongvatana et al. 2014). IFNα presented with a positive loading in the 3rd PCA component, and is an antiviral capable of suppressing HIV-1 replication (Sugawara, Thomas & Balagopal 2019). Interferon responses are upregulated after the acute phase of HIV-1 infection (Hardy et al. 2013; Huang et al. 2016). Multiple studies have observed after HIV infection an initial rapid increase of IFN-α in plasma, accompanied shortly afterwards by tumor necrosis factor (TNF)-α, Interferon induced protein (IP-10), IL-18, IL-10 and IFN-γ production (Huang et al. 2016; Jiao et al. 2012; Norris et al. 2006). Initially, IFN-alpha is part of the innate immune response against viral infections and can help restrict HIV replication. However, prolonged exposure to IFN-alpha, as seen in treated HIV infection, can induce an antiviral state in infected cells that promotes HIV latency (Sugawara, Thomas & Balagopal 2019). IFN-alpha activates intracellular antiviral defense mechanisms, such as the expression of restriction factors, which can inhibit HIV transcription and maintain the virus in a latent state.

Interferon induced protein 10 (IP-10) was the second highest loading variable in our analysis. IP-10 levels in the blood have been associated with rapid disease progression in early HIV-1 infection (Jiao et al. 2012; Wang et al. 2021). IP-10 is known to be involved in the trafficking of immune cells in response to interferon (Joshi 2021). In HIV infection, there is an early and sustained production of type I interferons, including IFN-α, as part of the antiviral response (Huang et al. 2016). IP-10, induced by interferons, plays a role in immune cell recruitment, and is elevated in HIV infection. IP-10 is actively produced in astrocytes and primarily induced by IFN in presence of other cytokines like TNFα (which loaded at below poor levels in our analysis) However, platelet-derived growth factor (PDGF-BB) augments IP-10 production even in absence of TNFα (Lei et al. 2019).

PDGF-BB is a powerful growth factor promoting cell proliferation and expression of stem cell markers. PDGF-BB is capable of passing the BBB, especially in compromised cases (Bethel-Brown et al. 2012). HIV-1 infection and specifically HIV-1 Tat has also been implicated in the

upregulation of PDGF-BB (Bethel-Brown et al. 2012). Importantly, the slow turnover of CSF in infants may allow for accumulation of these proteins (Johansson et al. 2008; Saunders, Liddelow & Dziegielewska 2012), which may exacerbate inflammatory activation in infants. Monocyte chemoattractant protein 1 (MCP-1) has been identified as a powerful factor in CNS disease progression and plays a neuroinflammatory role in recruitment of monocytes. PDGF-BB plays a role in mediating and regulating the release of MCP-1 (Bethel-Brown et al. 2012). In adults (0 to 4 months post-infection), MCP-1 is one of a few cytokines to associate with smaller global gray matter and lower fractional anisotropy (Cao et al. 2015). However, we did not observe associations with MCP-1 for any GM structure. It is possible the time frame of blood collection did not manage to capture the full immunological pathways at play.

LBP's primary function in monocyte and macrophage activation is responding to bacterial infections. It is possible that the cohort was exposed to bacterial or opportunistic infections, before therapy, that may not have been clinically monitored as part of the original cohort guidelines. The original protocol outlined formula feeding as opposed to breastfeeding(Cotton et al. 2013; Violari et al. 2008). As a result, primary acute immune response would be localized to exposure to possible pathogens in-utero, the initial HIV-1 infection, and exposure to environmental pathogens other than normal immune response to a mother's colostrum during breastfeeding (assuming parental adherence to guidelines). The Cape Town component of the CHER cohort (Violari et al. 2008) was at a higher risk of Tuberculosis bacteria (TB) infection (Den Boon et al. 2007) and the contribution of a TB coinfection cannot be excluded. We did not have access to data in relation to TB and could not control for this possible confounding effect.

Both IL-17F and CD40L loaded negatively within the component variable. The negative association of the overall component variable suggests that lower levels of these cytokines related to higher subcortical gray matter volumes. IL-17F is a proinflammatory signalling protein produced by T-helper cells, which are primary targets for HIV infection (Zayas & Mamede 2022) as well as play an important role in Mycobacterium tuberculosis responses (Devalraju et al. 2018). Chevalier and colleagues observed that within a group of individuals with acute HIV infection, averaging 42 days post-infection, those that exhibited high immune activation had lower IL-17 T-cell responses. They also confirmed that T-cell activation was primarily driven by HIV itself coupled to the consequent innate immune activation rather than

indirect CD4 T-cell responses (Chevalier et al. 2016). Additionally we consider the fact that HIV is capable of infecting certain CD8 cells (Richards et al. 2016; Wahl & Al-Harthi 2023). Higher CD8 T-cell count in children living with HIV has been associated with more notable disease progression (Paul et al. 2005). In healthy individuals activated CD8+ T-cells have a marked capacity to produce IL-17, however this is not the case in PHIV receiving ART (Perdomo-Celis et al. 2018). Perdomo-Celis et al. have shown the accompanying dysfunction of CD8 cells expressing IL-17 is associated with persistent immune activation (Perdomo-Celis et al. 2018). The findings of Chevalier et al. and Perdomo-Celis suggest that the severity of immune activation from the initial infection in infants in our cohort may lead to a spectrum of levels of IL-17F. Our findings link the lower levels of IL-7 – in combination with other cytokines – with larger basal ganglia volumes.

CD40 ligand (CD40L) is a transmembrane protein presented on B cells, dendritic cells and macrophages, the presentation and expression of which occurs shortly after T-cell activation (Kornbluth 2000). During the period of initial HIV infection, CD40L induces the release of HIV-suppressive chemokines as well as supports the production of anti-HIV antibodies and cytotoxic T-cells in attempt to hamper viral replication (Kornbluth 2000). However, activating certain antigen-presenting cells leads to increased CD4+ T-cells which promotes the replication of HIV. At later stages of severe infection it is observed that CD40L becomes depleted. This may be due to the gp-120-induced signal through CD4 which down-regulates CD40L expression(Zhang et al. 2004). Therefore the upregulation of CD40L expressing cells have been a primary focus of research toward treatment strategies in combatting opportunistic infections by promoting host immunity, through candidate HIV-1 vaccines targeting dendritic cells (Franco et al. 2011; Kornbluth 2000). Much like IL-17F we can postulate that individuals that experience more severe initial infection have higher immune activation, which may lead to lower levels of CD40L. These changes may weaken the immune system, leading to more severe disease progression and risk of opportunistic infection. Within our study we observe a depletion of CD40L forms a component of the factor associated with increased subcortical gray matter size.

The immunological predictors in the 3rd PCA involved proinflammatory pathways (IP-10, LBP, IL-17F, INF-α, CD40L). While IL-10 is normally anti-inflammatory, in the presence of IFN it can acquire proinflammatory action. The proinflammatory processes allow activation of

CD4+ T-lymphocytes in the CNS, which accelerates CNS inflammation and promote demyelination (Lane et al. 2000). T-lymphocytes from the blood to the brain may recruit microglia to affected areas (Cota et al. 2000). T-lymphocytes may also promote secretion of further proinflammatory cytokines, which can increase chemokine and viral production by infected astrocytes.

In our previous work the most significant finding reported were smaller CC amongst PHIV groups compared to their uninfected counterparts (Randall et al. 2017). In the current study we observed no association of CC volume with any cytokine PCA outcome, which may be related to otherwise uncaptured immunological processes in early infection, or due to chronic effects relating to HIV-1 infection. The association of decreasing size of the CC with age may have masked possible association with the component variable, or that the impact of HIV and the rapid decrease in size, in this cross-sectional analysis of the CC, is not captured by this particular set of cytokines outlined within the 3rd component. Associations with the basal ganglia are not unexpected since HIV-related abnormalities in the basal ganglia are well represented in the literature. This may be due to its proximity to the ventricles, as well as research linking the rate of initial infection to basal ganglia insult (Becker et al. 2011; Brouwers et al. 2000).

The study has various limitations. Our sample is small and does not include a matched control group as this was a retrospective analysis of available stored samples. The small sample also prevented further investigation of possible confounding variables such as treatment differences. The cross-sectional nature of this study coupled with the complexities in immunological pathways prevent interpretation of causal relationships. Lack of blood sample cytokine assays at 5 years of age in this group is specifically disadvantageous as it would paint a clearer picture of current progressive inflammatory processes, as well as the state of the adaptive immune response. A strength of the current study is the use of a multiplexed assay involving 44 biomarkers obtained at initial stages of infection in a group of vertically infected infants followed through 5 years of age. While cytokine analysis with cognitive outcomes is increasingly common (Cao et al. 2015; Gongvatana et al. 2014; Medders & Kaul 2011; Mulder et al. 2014; Ragin et al. 2010; Raskino et al. 1999; Ruhanya et al. 2021a) this adds to the few studies looking at associations between plasma cytokine levels and structural brain volumes. Whereas the previous studies studied adult populations, this

analysis examined associations in perinatally infected infants/young children, which likely involves different biological processes due to early brain and immune system development.

In conclusion, this exploratory work suggests the severity of initial infection and subsequent immunological response in early perinatal infection influences later development of basal ganglia components. In addition, we noted certain associated cytokines are involved in early immune recruitment, subsequent immune dysfunction, and maintenance of latent HIV-1 reservoirs. Based on our exploratory work. The cascading link and interplay between these cytokines and their involvement in monocyte recruitment requires special attention for further study in chronic HIV reservoir establishment and their accompanying association with volumetric outcomes throughout childhood.

CHAPTER 8 CUMULATIVE DISCUSSION AND CONCLUSION

8.1 Summary of Findings and Discussion

Previous work in this cohort reported HIV-related volume alterations in children living with PHIV at age 5 years, using manual segmentation. The findings of larger gray matter were not congruent with that of the consensus in the literature (Hoare et al. 2014; Van Den Hof et al. 2019; Martín-Bejarano et al. 2021; Phillips et al. 2016). The cross-sectional nature of our previous work made it difficult to determine whether the disturbances witnessed between PHIV and controls were due to earlier HIV related damage or ongoing developmental delays. The goal of this dissertation was to follow the existing cohort and investigate the longitudinal trajectory of possible volumetric disturbances to subcortical structure size. We continued with an exploratory analysis into the relationships of volumetric alterations observed at age 5 to early immune health markers.

To perform longitudinal analysis of volumes from 5 to 10 years, we needed to assess possible scanner biases, since data at age between 9 and 10 years were acquired with two different 3T scanners. Our analysis established that manual segmentation data collected from both scanners in this cohort could be combined reliably for longitudinal analysis.

There is a gap in the neuroimaging literature expressing the need for further study of longitudinal perinatally HIV-infected pediatric cohorts with specific reference to structural changes (Hoare et al. 2014; Van Den Hof et al. 2019; Martín-Bejarano et al. 2021; Musielak & Fine 2016). The effects of HIV in presence of ART provides diverse findings in that some studies would normally present smaller cortical and/or subcortical gray matter whilst others including ourselves have reported larger GM amongst PHIV groups (Martín-Bejarano et al. 2021). Within pediatric samples only very few have documented the presence of larger gray matter (Blokhuis et al. 2017; Paul et al. 2018; Randall et al. 2017; Yadav et al. 2017). Cross-sectionally results are not congruent with those involving the same cohort using automated segmentation, where, the right putamen was observed to be smaller in PHIV children at 7 years (Nwosu et al. 2018). Other prior works have been predominantly cross-sectional

spanning wide age ranges averaging into later childhood and early adolescence (Van Genderen et al. 2022; Martín-Bejarano et al. 2021; Musielak & Fine 2016; Paul et al. 2018; Sarma et al. 2014; Wade et al. 2019). has been postulated before, that these larger gray matter structures may be more apparent at younger years and attenuated approaching adolescence (Nwosu, Robertson & Meintjes 2019; Paul et al. 2018). We modelled age related changes of manually derived volumes of within the basal ganglia and of the CC. GM volume reduction was evident among all children in the caudate, GP and CC from age 5-10 years, supporting the proposal. We observe differences in growth trajectories between 5 to 10 years of age between PHIV and controls which varied in magnitude by region, this was congruent with our initial hypothesis. We do find congruence in a larger GM structure relating to larger cortical thickness(Nwosu et al. 2023), that was not considered for manual segmentation in this study. Longitudinal trajectories of cortical thickness and gyrification from 5 to 9 years were reported to be similar between PHIV and controls (Nwosu et al. 2023), unlike the present study where we observe difference in trajectories of the bilateral putamen. However, the longitudinal analysis did not include different growth functions such as logarithmic and quadratic. However, Nwosu et al. reported consistently thicker cortical GM in 6 regions, indicating larger GM across all ages.

In the right nucleus accumbens and bilateral putamen, increased volume size at 5 years of age drove the majority of altered age-related curves in children living with PHIV as compared to uninfected controls. Unexpectedly, the smaller CC size of PHIV reported at age 5 did not alter the growth trajectories from 5 to 10 years. With that said we do not find congruence with other studies of smaller GM at any of the later ages cross-sectionally (Hoare et al. 2014; Martín-Bejarano et al. 2021; Musielak & Fine 2016; Nwosu et al. 2018, 2023). However, there is some similarity in the literature where later ages showed no difference between PHIV and age matched controls at around 11 years of age (Van Genderen et al. 2022) .There is literature evidence of genetic and environmentally modulated differentiation of growth trajectories from early childhood to adolescence. (Boivin et al. 2018; Lenroot et al. 2009; Tyborowska et al. 2018). However, our sample was well matched and derived from the same population group with comparative SES, education level of parents, sex, age and environmental exposures (Holmes et al. 2017; Madhi et al. 2011; Violari et al. 2008). As such, the inflammation initially thought to be present within the CNS may begin to subside after 5

years of age. Our findings may also suggest HIV-1 in presence of ART influence developmental pruning mechanisms in early childhood, which relaxes when approaching preadolescence. This can only be tested with more extensive study of tissue blood sample data throughout later ages, with a larger sample size. Our findings, coupled to larger bilateral caudates associating with poorer immune health (Randall et al. 2017), and congruent with other literature in pediatric populations (Paul et al. 2018; Sarma et al. 2014; Sowell et al. 2004) motivated for an exploratory analysis of blood sample data obtained at early infancy. Specifically, an exploratory analysis as to whether biomarkers linked to early infection predict volumetric outcomes at the most affected time-point at 5 years of age. We explored if any inflammatory factors at the initial stages of infection predicted outcomes. The biomarkers with favourable loading coefficients included IL-10, IP-10, LBP, IL-17F, IFNα, CD40L, and those loading poorly include GCSF, PDGF-BB, TGFβ1 and TGFβ2. Association with the derived component variable suggest that during the period of initial infection, in infancy, an increase of IL-10, IP-10, LBP and IFN-α, and accompanying decrease in IL-17F and CD40L contribute to smaller basal ganglia volumes at 5 years. The structures implicated in this analysis overlap with larger volumes – bilateral nucleus accumbens, putamen and left globus pallidus – reported earlier (Randall et al. 2017), as well as in the previous chapter.

Without histological or CSF analysis exact mechanisms of action are unknown, we lack the ability to postulate upon existing reservoir target cells relating to latency and their change with time in this cohort. However, based on the existing literature we can provide speculative mechanisms which may be useful for future work.

Our results may indicate the presence of a biological cue which governs neuronal cell loss and pruning during early development. Such a mechanism may protect against hyperpruning beyond a certain critical level at a specific stage of development. The possibility of a biological cue can be observed by both groups normalising to a similar volume through later ages.

Contradictory to this, is the possibility of hyperpruning. Increased metabolic demand during inflammation and reactive gliosis (Epstein & Gelbard 1999; Walsh et al. 2004), coupled to possible hypoxia and ischaemia, due to possible cerebrovascular abnormalities and mitochondrial dysfunction observed in youths infected with HIV-1 (Crain et al. 2010; Patsalides et al. 2002; Shah et al. 1996; Takemoto et al. 2017; Tardieu et al. 2005). A cohort in Zambia have recently documented cerebrovascular abnormalities in 7 of 34 PHIV youths

between 9 and 17 years, whilst no abnormalities in controls (Dean et al. 2020). Due to conservation of energy and less available resources for cells, relative ischaemia and high metabolic demand may drive hyperpruning in the PHIV group. The resultant hyperpruning would lead to loss of actual neuronal cell bodies within gray matter structures, as well as associated loss of axons from these pruned cell bodies. The loss of these neurons is supported by our smaller WM findings, as well as supported by loss of cortical gyrification in PHIV (Nwosu et al. 2018). However, in GM the size reduction caused by neuronal loss may be entirely outweighed by previous scarring, or completely masked by support/glial and inflammatory cell proliferation and recruitment, further substantiating the idea of proinflammatory effects which result in larger GM structures. It is observed that proinflammatory cytokines, collected before ART initiation, are a valid biomarker toward determining the pathological effects of HIV-1 and CNS disease progression. Proinflammatory cytokines involved at initial stages of infection have lasting impact up to 5 years of age. Cytokine analysis from samples collected at 5 years of age would be advantageous here, the lack of just such blood samples in the cohort is a major limitation. It cannot be established, in the scope of this study, whether HIV and its neurotoxic products are the cause to volume disturbances or whether the impact of prolonged exposure to proinflammatory markers are causing the disturbances, or a combination of both. We must consider certain caveats in our immunological findings. Firstly, more study is required to identify the exact interplay of cytokines on the unique cells of the CNS. We also cannot assume cytokine activation or effect is linear with increasing concentration. We are unsure whether proinflammatory cytokines in systemic tissues act differently or are governed via different cascades within the CNS. For example, PDGF-BB is a potent proinflammatory cytokine – systemically, yet within the CNS has shown anti-inflammatory effects as well as neuroprotective qualities (Stampanoni Bassi et al. 2018). Within the CNS PDGF-BB has been shown to induce proliferation and differentiation of neuronal stem cells, as well as in development of glial cells (Kim et al. 2018). Elevated cytokines may not necessarily be causing decreased structure size - cytokines may be released as a neuroprotective mechanism against an additional disturbance which is actually causing the larger volumes. Given that blood samples were taken in infancy with an immature immune system, if we were to view the sample as a spectrum, and assume those with higher pro-inflammatory markers are able to mitigate the effects of the current infection long-term compared to those with lower pro-inflammatory markers we would somewhat expect healthy

uninfected children to exhibit similar characteristics to those with high inflammatory markers. This is perhaps evidenced when comparing healthy uninfected controls to PHIV children, where we observe smaller GM in uninfected children. The increased levels of these cytokines may be higher in attempt to also inhibit other cytokine actions. This was similarly described in another study where they postulated that elevated levels of some markers were neuroprotective, albeit associated with larger volumes (Ruhanya et al. 2021b).

8.2 Conclusion and Future work

8.2.1) Conclusion

Taken together, the results of this thesis have shown that increased putamen volumes in PHIV at 5 years were associated with component 3, a combination of cytokines related to HIV reservoir maintenance, Immune activation, and subsequent immune dysfunction related to early infection. Abnormal putamen volumes at age 5 led to altered growth trajectories in the putamen, which resolved by age 7 years. The reduced corpus callosum volume at age 5 years did not alter the longitudinal growth trajectory in PHIV and was not related to any combination of cytokines studied. Longitudinal analysis demonstrated that earlier volume alterations did not impact long term growth, suggesting HIV in the presence of ART may lead to age related growth differences or delays in childhood that do not persist, or are otherwise masked at later ages. Exploratory immunological work in this thesis suggests immune health in infancy may contribute to the altered growth trajectories of the putamen.

8.2.2) Future work

Based on the work presented in this thesis, longitudinal analysis including recently acquired imaging data into adolescence (at 11 and 15/16 years) would be particularly insightful to understanding the long-term consequences of volume abnormalities at 5 years on brain maturation. Longitudinal analysis using automated segmentation methods would also allow for a larger sample of children and structures to be studied in this cohort.

Once immunological data in later childhood – at 8 and 12 years – becomes available (it is currently unavailable due to PhD submission), analysis in combination with neuroimaging data would be insightful. The immunological data at later ages include a larger sample of the cohort, including control children, allowing for a better understanding of immunological factors that contribute to typical and atypical development. Association of these cytokines with structural volumes will be interesting as it may capture the adaptive immune response during periods of viral suppression, as well as allow comparison with that of healthy age and community matched controls.

To better understand the potential functional consequences of the volume abnormalities at 5 years, the inclusion of cognitive outcomes would be provide insightful. A difficulty for this work in the cohort would be the switching of cognitive tests between 5 and 7 years, which

complicates longitudinal analysis of neuropsychological domains. That said, cross sectional analysis would be feasible at each individual timepoint, once the data is available. The inclusion of cognitive outcomes would provide valuable insight into regions that, although volumetrically have matched the uninfected group at later ages of development, may still exist cognitive disparities.

As the study acquired imaging data from other modalities, future work looking at outcomes from MRS and DTI data with the 5-year-old volume abnormalities may provide additional insight. Ultimately, it would be most interesting to examine longitudinal growth trajectories across all modalities and time points to get a more complete picture of neurodevelopment in the cohort.

Although the primary focus of the studies using the CHER data is that of a pediatric cohort it would be advantageous to follow these individuals into early adulthood and in the long-term even late adulthood and assess the systemic, neurocognitive and neuroanatomical changes that occur in a well-documented perinatally HIV infected cohort receiving therapy from infancy.

Given the results and limitations observed within this study we suggest future studies follow a larger cohort from birth through adolescence. The study protocol would benefit from regular blood sample collection across all participants. This would allow for cytokine analysis during stages of initial infection in order to more accurately depict the immunological changes that occur in PHIV youths at earlier stages of infection. Additional avenues could involve assessing the impact of early treatment intervention, like those targeting CD40L pathways (Franco et al. 2011), in mitigating subcortical brain volume disturbances in childhood.

CHAPTER 9 BIBLIOGRAPHY

Ackermann, C, Andronikou, S, Laughton, B, Kidd, M, Dobbels, E, Innes, S, van Toorn, R & Cotton, M 2014, 'White matter signal abnormalities in children with suspected HIV-related neurologic disease on early combination antiretroviral therapy.', *The Pediatric infectious disease journal*, vol. 33, no. 8, pp. e207-12.

Ackermann, C, Andronikou, S, Saleh, MG, Laughton, B, Alhamud, AA, van der Kouwe, A, Kidd, M, Cotton, MF & Meintjes, EM 2016, 'Early Antiretroviral Therapy in HIV-Infected Children Is Associated with Diffuse White Matter Structural Abnormality and Corpus Callosum Sparing.', *AJNR. American journal of neuroradiology*, vol. 37, no. 12, pp. 2363–2369.

Akudjedu, TN, Nabulsi, L, Makelyte, M, Scanlon, C, Hehir, S, Casey, H, Ambati, S, Kenney, J, O'Donoghue, S, McDermott, E, Kilmartin, L, Dockery, P, McDonald, C, Hallahan, B & Cannon, DM 2018, 'A comparative study of segmentation techniques for the quantification of brain subcortical volume', *Brain Imaging and Behavior*, vol. 12, Springer US, no. 6, pp. 1678–1695.

Ances, BM, Ortega, M, Vaida, F, Heaps, J & Paul, R 2012, 'Independent effects of HIV, aging, and HAART on brain volumetric measures.', *Journal of acquired immune deficiency syndromes (1999)*, vol. 59, no. 5, pp. 469–77.

Andronikou, S, Ackermann, C, Laughton, B, Cotton, M, Tomazos, N, Spottiswoode, B, Mauff, K & Pettifor, JM 2014, 'Correlating brain volume and callosal thickness with clinical and laboratory indicators of disease severity in children with HIV-related brain disease.', *Child's nervous system : ChNS : official journal of the International Society for Pediatric Neurosurgery*, vol. 30, no. 9, pp. 1549–57.

Andronikou, S, Ackermann, C, Laughton, B, Cotton, M, Tomazos, N, Spottiswoode, B, Mauff, K & Pettifor, JM 2015, 'Corpus callosum thickness on mid-sagittal MRI as a marker of brain volume: a pilot study in children with HIV-related brain disease and controls.', *Pediatric radiology*, vol. 45, no. 7, pp. 1016–25.

Aquaro, S, Calio, R, Balzarini, J, Bellocchi, C, Garaci, E & Federico, C 2002, 'Macrophages and HIV infection : therapeutical approaches toward this strategic virus reservoir', vol. 55, pp. 209–225.

Aylward, EH, Henderer, JD, McArthur, JC, Brettschneider, PD, Harris, GJ, Barta, PE & Pearlson, GD 1993, 'Reduced basal ganglia volume in HIV-1-associated dementia: results from quantitative neuroimaging.', *Neurology*, vol. 43, no. 10, pp. 2099–104.

Babu, H, Ambikan, AT, Gabriel, EE, Akusjärvi, SS, Palaniappan, AN, Sundaraj, V, Mupanni, NR, Sperk, M, Cheedarla, N, Sridhar, R, Tripathy, SP, Nowak, P, Hanna, LE & Neogi, U 2019, 'Systemic inflammation and the increased risk of inflamm-aging and age-associated diseases in people living with HIV on long term suppressive antiretroviral therapy', *Frontiers in Immunology*, vol. 10, no. AUG, pp. 1–11.

Bagenda, D, Nassali, A, Kalyesubula, I, Sherman, B, Drotar, D, Boivin, MJ & Olness, K 2006, 'Health, neurologic, and cognitive status of HIV-infected, long-surviving, and antiretroviral-naive Ugandan children.', *Pediatrics*, vol. 117, no. 3, pp. 729–740.

Bangirana, P, Ruel, TD, Boivin, MJ, Pillai, SK, Giron, LB, Sikorskii, A, Banik, A & Achan, J 2017, 'Absence of neurocognitive disadvantage associated with paediatric HIV subtype A

infection in children on antiretroviral therapy', *Journal of the International AIDS Society*, vol. 20, no. 2, pp. 1–6.

Barnes, J, Foster, J, Boyes, RG, Pepple, T, Moore, EK, Schott, JM, Frost, C, Scahill, RI & Fox, NC 2008, 'A comparison of methods for the automated calculation of volumes and atrophy rates in the hippocampus.', *NeuroImage*, vol. 40, no. 4, pp. 1655–71.

Barron, P, Pillay, Y, Doherty, T, Sherman, G, Jackson, D, Bhardwaj, S, Robinson, P & Goga, A 2013, 'Cómo eliminar la transmisión del VIH de la madre al niño en Sudáfrica', *Bulletin of the World Health Organization*, vol. 91, no. 1, pp. 70–74.

Bazzoli, C, Jullien, V, Le Tiec, C, Rey, E, Mentr??, F, Taburet, A-MM, Mentré, F & Taburet, A-MM 2010, 'Intracellular pharmacokinetics of antiretroviral drugs in HIV-infected patients, and their correlation with drug action', *Clinical Pharmacokinetics*, vol. 49, no. 1, pp. 17–45.

Becker, JT, Sanders, J, Madsen, SK, Ragin, A, Kingsley, L, Maruca, V, Cohen, B, Goodkin, K, Martin, E, Miller, EN, Sacktor, N, Alger, JR, Barker, PB, Saharan, P, Carmichael, OT, Thompson, PM & Multicenter AIDS Cohort Study 2011, 'Subcortical brain atrophy persists even in HAART-regulated HIV disease.', *Brain imaging and behavior*, vol. 5, no. 2, pp. 77–85.

Bendersky, M, Musolino, PL, Rugilo, C, Schuster, G & Sica, REP 2006, 'Normal anatomy of the developing fetal brain. Ex vivo anatomical-magnetic resonance imaging correlation.', *Journal of the neurological sciences*, vol. 250, no. 1–2, pp. 20–6.

Berger, JR & Arendt, G 2000, 'HIV dementia: the role of the basal ganglia and dopaminergic systems.', *Journal of psychopharmacology (Oxford, England)*, vol. 14, no. 3, pp. 214–221.

Bernier, BE, Whitaker, LR & Morikawa, H 2011, 'Predictive Reward Signal of Dopamine Neurons Predictive Reward Signal of Dopamine Neurons', pp. 1–27.

Berridge, KC 2007, 'The debate over dopamine's role in reward: the case for incentive salience.', *Psychopharmacology*, vol. 191, no. 3, pp. 391–431.

Berridge, KC & Robinson, TE 1998, 'What is the role of dopamine in reward: Hedonic impact, reward learning, or incentive salience?', *Brain Research Reviews*, vol. 28, no. 3, pp. 309–369.

Bethel-Brown, C, Yao, H, Hu, G & Buch, S 2012, 'Platelet-derived growth factor (PDGF)-BB-mediated induction of monocyte chemoattractant protein 1 in human astrocytes: implications for HIV-associated neuroinflammation.', *Journal of neuroinflammation*, vol. 9, p. 262.

Biberacher, V, Schmidt, P, Keshavan, A, Boucard, CC, Righart, R, Sämann, P, Preibisch, C, Fröbel, D, Aly, L, Hemmer, B, Zimmer, C, Henry, RG & Mühlau, M 2016, 'Intra- and interscanner variability of magnetic resonance imaging based volumetry in multiple sclerosis.', *NeuroImage*, Elsevier B.V.

Biffen, SC, Warton, CMR, Dodge, NC, Molteno, CD, Jacobson, JL, Jacobson, SW & Meintjes, EM 2020, 'Validity of automated FreeSurfer segmentation compared to manual tracing in detecting prenatal alcohol exposure-related subcortical and corpus callosal alterations in 9- to 11-year-old children', *NeuroImage: Clinical*, vol. 28, Elsevier, no. July, p. 102368.

Bilbo, SD & Schwarz, JM 2012, 'The immune system and developmental programming of brain and behavior.', *Frontiers in neuroendocrinology*, vol. 33, no. 3, pp. 267–86.

van Biljon, N, Robertson, F, Holmes, M, Cotton, MF, Laughton, B, van der Kouwe, A, Meintjes, E & Little, F 2021, 'Multivariate approach for longitudinal analysis of brain metabolite levels from ages 5-11 years in children with perinatal HIV infection.', *NeuroImage*, vol. 237, p. 118101.

Biro, FM, Greenspan, LC, Galvez, MP, Pinney, SM, Teitelbaum, S, Windham, GC, Deardorff, J, Herrick, RL, Succop, PA, Hiatt, RA, Kushi, LH & Wolff, MS 2013, 'Onset of Breast Development in a Longitudinal Cohort', *PEDIATRICS*, vol. 132, no. 6, pp. 1019–1027.

Biro, FM, Pinney, SM, Huang, B, Baker, ER, Walt Chandler, D & Dorn, LD 2014, 'Hormone Changes in Peripubertal Girls', *The Journal of Clinical Endocrinology & Metabolism*, vol. 99, no. 10, pp. 3829–3835.

Blokhuis, C, Mutsaerts, HJMM, Cohen, S, Scherpbier, HJ, Caan, MWA, Majoie, CBLM, Kuijpers, TW, Reiss, P, Wit, FWNM & Pajkrt, D 2017, 'Higher subcortical and white matter cerebral blood flow in perinatally HIV-infected children.', *Medicine*, vol. 96, no. 7, p. e5891.

Blokhuis, C, Peeters, CFW, Cohen, S, Scherpbier, HJ, Kuijpers, TW, Reiss, P, Kootstra, NA, Teunissen, CE & Pajkrt, D 2019, 'Systemic and intrathecal immune activation in association with cerebral and cognitive outcomes in paediatric HIV', *Scientific Reports*, vol. 9, Springer US, no. 1, pp. 1–10.

Blumberg, BM, Gelbard, HA & Epstein, LG 1994, 'HIV-1 infection of the developing nervous system: central role of astrocytes in pathogenesis.', *Virus research*, vol. 32, no. 2, pp. 253–67.

Boccardi, M, Ganzola, R, Bocchetta, M, Pievani, M, Redolfi, A, Bartzokis, G, Camicioli, R, Csernansky, JG, de Leon, MJ, Detoledo-Morrell, L, Killiany, RJ, Lehéricy, S, Pantel, J, Pruessner, JC, Soininen, H, Watson, C, Duchesne, S, Jack, CR & Frisoni, GB 2011, 'Survey of protocols for the manual segmentation of the hippocampus: preparatory steps towards a joint EADC-ADNI harmonized protocol.', *Journal of Alzheimer's disease : JAD*, vol. 26 Suppl 3, no. 0 3, pp. 61–75.

Boivin, MJ, Barlow-Mosha, L, Chernoff, MC, Laughton, B, Zimmer, B, Joyce, C, Bwakura-Dangarembizi, M, Ratswana, M, Abrahams, N, Fairlie, L, Gous, H, Kamthunzi, P, McCarthy, K, Familiar-Lopez, I, Jean-Phillippe, P, Coetzee, J, Violari, A, Cotton, MC & Palumbo, PE 2018, 'Neuropsychological performance in African children with HIV enrolled in a multisite antiretroviral clinical trial', *Aids*, vol. 32, no. 2, pp. 189–204.

Boivin, MJ, Maliwichi-Senganimalunje, L, Ogwang, LW, Kawalazira, R, Sikorskii, A, Familiar-Lopez, I, Kuteesa, A, Nyakato, M, Mutebe, A, Namukooli, JL, Mallewa, M, Ruiseñor-Escudero, H, Aizire, J, Taha, TE & Fowler, MG 2019, 'Neurodevelopmental effects of ante-partum and post-partum antiretroviral exposure in HIV-exposed and uninfected children versus HIV-unexposed and uninfected children in Uganda and Malawi: a prospective cohort study.', *The lancet. HIV*, vol. 6, no. 8, pp. e518–e530.

Den Boon, S, Van Lill, SWP, Borgdorff, MW, Enarson, DA, Verver, S, Bateman, ED, Irusen, E, Lombard, CJ, White, NW, De Villiers, C & Beyers, N 2007, 'High prevalence of tuberculosis in previously treated patients, Cape Town, South Africa', *Emerging Infectious Diseases*, vol. 13, no. 8, pp. 1189–1194.

Brahmbhatt, H, Boivin, M, Ssempijja, V, Kagaayi, J, Kigozi, G, Serwadda, D, Violari, A & Gray, RH 2017, 'Impact of HIV and atiretroviral therapy on neurocognitive outcomes among

school-aged children', *Journal of Acquired Immune Deficiency Syndromes*, vol. 75, no. 1, pp. 1–8.

Brahmbhatt, H, Boivin, M, Ssempijja, V, Kigozi, G, Kagaayi, J, Serwadda, D & Gray, RH 2014, 'Neurodevelopmental benefits of antiretroviral therapy in ugandan children aged 0-6 years with HIV', *Journal of Acquired Immune Deficiency Syndromes*, vol. 67, no. 3, pp. 316–322.

Brik, A & Wong, C-H 2003, 'HIV-1 protease: mechanism and drug discovery.', *Organic & biomolecular chemistry*, vol. 1, no. 1, pp. 5–14.

Brockman, MA, Kwon, DS, Tighe, DP, Pavlik, DF, Rosato, PC, Sela, J, Porichis, F, Le Gall, S, Waring, MT, Moss, K, Jessen, H, Pereyra, F, Kavanagh, DG, Walker, BD & Kaufmann, DE 2009, 'IL-10 is up-regulated in multiple cell types during viremic HIV infection and reversibly inhibits virus-specific T cells.', *Blood*, vol. 114, no. 2, pp. 346–56.

Brouwers, P, Civitello, L, Decarli, C, Wolters, P & Sei, S 2000, 'Cerebrospinal ¯ uid viral load is related to cortical atrophy and not to intracerebral calci ® cations in children with symptomatic HIV disease', pp. 390–397.

Cantó-nogués, C, Sánchez-ramón, S, Álvarez, S, Lacruz, C & Muñóz-fernández, MÁ 2005, 'HIV-1 Infection of Neurons Might Account for Progressive HIV-1-Associated Encephalopathy in Children', vol. 27.

Cao, B, Kong, X, Kettering, C, Yu, P & Ragin, A 2015, 'Determinants of HIV-induced brain changes in three different periods of the early clinical course: A data mining analysis', *NeuroImage: Clinical*, vol. 9, Elsevier B.V., pp. 75–82.

Casey, BJ, Tottenham, N, Liston, C & Durston, S 2005, 'Imaging the developing brain: what have we learned about cognitive development?', *Trends in cognitive sciences*, vol. 9, no. 3, pp. 104–10.

Cavarelli, M & Scarlatti, G 2011, 'HIV-1 co-receptor usage: influence on mother-to-child transmission and pediatric infection.', *Journal of translational medicine*, vol. 9 Suppl 1, BioMed Central Ltd, no. Suppl 1, p. S10.

Chang, L, Ernst, T, Witt, MD, Ames, N, Gaiefsky, M & Miller, E 2002, 'Relationships among brain metabolites, cognitive function, and viral loads in antiretroviral-naïve HIV patients.', *NeuroImage*, vol. 17, no. 3, pp. 1638–48.

Chevalier, MF, Didier, C, Girard, PM, Manea, ME, Campa, P, Barré-Sinoussi, F, Scott-Algara, D & Weiss, L 2016, 'CD4 T-cell responses in primary HIV infection: Interrelationship with immune activation and virus burden', *Frontiers in Immunology*, vol. 7, no. SEP, pp. 1–7.

Chiang, M-C, Dutton, R a, Hayashi, KM, Lopez, OL, Aizenstein, HJ, Toga, AW, Becker, JT & Thompson, PM 2007, '3D pattern of brain atrophy in HIV/AIDS visualized using tensor-based morphometry.', *NeuroImage*, vol. 34, no. 1, pp. 44–60.

Chiriboga, CA, Fleishman, S, Champion, S, Gaye-Robinson, L & Abrams, EJ 2005, 'Incidence and prevalence of HIV encephalopathy in children with HIV infection receiving highly active anti-retroviral therapy (HAART).', *The Journal of pediatrics*, vol. 146, no. 3, pp. 402–407.

Cocchi, F, DeVico, AL, Garzino-Demo, A, Arya, SK, Gallo, RC & Lusso, P 1995, 'Identification of RANTES, MIP-1 alpha, and MIP-1 beta as the major HIV-suppressive factors produced by CD8+ T cells.', *Science (New York, N.Y.)*, vol. 270, no. 5243, pp. 1811–5.

Cohen, S, Caan, MWA, Mutsaerts, H-J, Scherpbier, HJ, Kuijpers, TW, Reiss, P, Majoie, CBLM & Pajkrt, D 2016, 'Cerebral injury in perinatally HIV-infected children compared to matched healthy controls.', *Neurology*, vol. 86, no. 1, pp. 19–27.

Communications and Global Advocacy UNAIDS 2020, 'UNAIDS FACT SHEET. Global HIV Statistics', *Ending the AIDS epidemic*, pp. 1–3.

Comrey, AL & Lee, HB 2013, *A First Course in Factor Analysis*, *A First Course in Factor Analysis*.

Cota, M, Kleinschmidt, A, Ceccherini-Silberstein, F, Aloisi, F, Mengozzi, M, Mantovani, A, Brack-Werner, R & Poli, G 2000, 'Upregulated expression of interleukin-8, RANTES and chemokine receptors in human astrocytic cells infected with HIV-1', *Journal of NeuroVirology*, vol. 6, no. 1, pp. 75–83.

Cotton, MF, Violari, A, Otwombe, K, Panchia, R, Dobbels, E, Rabie, H, Josipovic, D, Liberty, A, Lazarus, E, Innes, S, van Rensburg, AJ, Pelser, W, Truter, H, Madhi, S a, Handelsman, E, Jean-Philippe, P, McIntyre, J a, Gibb, DM, Babiker, AG & CHER Study Team 2013, 'Early time-limited antiretroviral therapy versus deferred therapy in South African infants infected with HIV: results from the children with HIV early antiretroviral (CHER) randomised trial.', *Lancet (London, England)*, vol. 382, Elsevier Ltd, no. 9904, pp. 1555–63.

Crain, MJ, Chernoff, MC, Oleske, JM, Brogly, SB, Malee, KM, Borum, PR, Meyer, WA, Mitchell, WG, Moye, JH, Ford-Chatterton, HM, Van Dyke, RB & Seage Iii, GR 2010, 'Possible mitochondrial dysfunction and its association with antiretroviral therapy use in children perinatally infected with HIV.', *The Journal of infectious diseases*, vol. 202, no. 2, pp. 291–301.

Cronbach, LJ 1951, 'Coefficient alpha and the internal structure of tests', *Psychometrika*, vol. 16, no. 3, pp. 297–334.

Croteau-Chonka, EC, Dean, DC, Remer, J, Dirks, H, O'Muircheartaigh, J & Deoni, SCL 2016, 'Examining the relationships between cortical maturation and white matter myelination throughout early childhood', *NeuroImage*, vol. 125, The Authors, pp. 413–421.

Cullen, BR 1991, 'Regulation of HIV-1 gene expression.', *The FASEB journal : official publication of the Federation of American Societies for Experimental Biology*, vol. 5, no. 10, pp. 2361–2368.

Cullen, BR 1992, 'Mechanism of action of regulatory proteins encoded by complex retroviruses.', *Microbiological reviews*, vol. 56, no. 3, pp. 375–394.

Daneman, R & Prat, A 2015, 'The blood-brain barrier.', *Cold Spring Harbor perspectives in biology*, vol. 7, no. 1, p. a020412.

Dean, O, Buda, A, Adams, HR, Mwanza-Kabaghe, S, Potchen, MJ, Mbewe, EG, Kabundula, PP, Moghaddam, SM, Birbeck, GL & Bearden, DR 2020, 'Brain Magnetic Resonance Imaging Findings Associated With Cognitive Impairment in Children and Adolescents With Human Immunodeficiency Virus in Zambia.', *Pediatric neurology*, vol. 102, no. 5, pp. 28–35.

DeLong, M 2000, 'The Basal Ganglia', in ER Kandel, JH Schwartz & TM Jessell (eds), *Principles of Neural Science*, 4th edn, McGraw-Hill Companies, Inc., New York, NY, pp. 730–741.

Deoni, SCL, Dean, DC, Remer, J, Dirks, H & O'Muircheartaigh, J 2015, 'Cortical maturation and myelination in healthy toddlers and young children', *NeuroImage*, vol. 115, Elsevier B.V.,

pp. 147–161.

Devalraju, KP, Neela, VSK, Ramaseri, SS, Chaudhury, A, Van, A, Krovvidi, SS, Vankayalapati, R & Valluri, VL 2018, 'IL-17 and IL-22 production in HIV+ individuals with latent and active tuberculosis', *BMC Infectious Diseases*, vol. 18, BMC Infectious Diseases, no. 1, pp. 1–10.

Dewey, J, Hana, G, Russell, T, Price, J, McCaffrey, D, Harezlak, J, Sem, E, Anyanwu, JC, Guttmann, CR, Navia, B, Cohen, R & Tate, DF 2010, 'Reliability and validity of MRI-based automated volumetry software relative to auto-assisted manual measurement of subcortical structures in HIV-infected patients from a multisite study.', *NeuroImage*, vol. 51, Elsevier Inc., no. 4, pp. 1334–44.

Le Doaré, K, Bland, R & Newell, M-L 2012, 'Neurodevelopment in children born to HIV-infected mothers by infection and treatment status.', *Pediatrics*, vol. 130, no. 5, pp. e1326-44.

Dowker, A 2006, 'What can functional brain imaging studies tell us about typical and atypical cognitive development in children?', *Journal of physiology, Paris*, vol. 99, no. 4–6, pp. 333–41.

Doya, K 2000, 'Complementary roles of basal ganglia and cerebellum in learning and motor control.', *Current opinion in neurobiology*, vol. 10, no. 6, pp. 732–9.

Droby, A, Lukas, C, Schänzer, A, Spiwoks-Becker, I, Giorgio, A, Gold, R, De Stefano, N, Kugel, H, Deppe, M, Wiendl, H, Meuth, SG, Acker, T, Zipp, F & Deichmann, R 2015, 'A human post-mortem brain model for the standardization of multi-centre MRI studies.', *NeuroImage*, vol. 110, Elsevier B.V., pp. 11–21.

Dubois-Dalcq, M, Altmeyer, R, Chiron, M & Wilt, S 1995, 'HIV interactions with cells of the nervous system.', *Current opinion in neurobiology*, vol. 5, no. 5, pp. 647–655.

Durston, S, Hulshoff Pol, HE, Casey, BJJ, GIEDD, JN, Buitelaar, JK & VAN ENGELAND, H 2001, 'Anatomical MRI of the developing human brain: what have we learned?', *Journal of the American Academy of Child and Adolescent Psychiatry*, vol. 40, no. 9, pp. 1012–20.

Eckard, AR, Rosebush, JC, O'Riordan, MA, Graves, CC, Alexander, A, Grover, AK, Thera Lee, S, Habib, JG, Ruff, JH, Chahroudi, A & McComsey, GA 2017, 'Neurocognitive dysfunction in HIV-infected youth: investigating the relationship with immune activation', *Antiviral Therapy*, vol. 22, no. 8, pp. 669–680.

Ene, L, Duiculescu, D, Ruta, SM, Sm, R & Ruta, SM 2011, 'How much do antiretroviral drugs penetrate into the central nervous system?', *Journal of medicine and life*, vol. 4, no. 4, pp. 432–9.

Epstein, LG & Gelbard, H a 1999, 'HIV-1-induced neuronal injury in the developing brain.', *Journal of leukocyte biology*, vol. 65, no. 4, pp. 453–7.

Epstein, LG, Sharer, LR, Oleske, JM, Connor, EM, Goudsmit, J, Bagdon, L, Robert-guroff, M & Koenigsberger, MR 1986, 'Neurologic Manifestations of Human Immunodeficiency Virus Infection in Children', *Pediatrics*, vol. 78.

Ernst, T, Chang, L & Arnold, S 2003, 'Increased glial metabolites predict increased working memory network activation in HIV brain injury', *NeuroImage*, vol. 19, no. 4, pp. 1686–1693.

Esposito, F, Corona, A & Tramontano, E 2012, 'HIV-1 Reverse Transcriptase Still Remains

a New Drug Target: Structure, Function, Classical Inhibitors, and New Inhibitors with Innovative Mechanisms of Actions.', *Molecular biology international*, vol. 2012, p. 586401.

Fairlie, L, Chernoff, M, Cotton, MF, Bwakura-Dangarembizi, M, Violari, A, Familiar-Lopez, I, Barlow-Mosha, L, Kamthunzi, P, McCarthy, K, Jean-Philippe, P, Laughton, B, Palumbo, PE & Boivin, MJ 2022, 'Antiretroviral choice and severe disease predict poorer neuropsychological outcomes in HIV+ children from Africa.', *Frontiers in pediatrics*, vol. 10, no. August, p. 899002.

Fan, Y, Shi, F, Smith, JK, Lin, W, Gilmore, JH & Shen, D 2011, 'Brain anatomical networks in early human brain development.', *NeuroImage*, vol. 54, Elsevier B.V., no. 3, pp. 1862–71.

Fischl, B, Salat, DH, Busa, E, Albert, M, Dieterich, M, Haselgrove, C, Van Der Kouwe, A, Killiany, R, Kennedy, D, Klaveness, S, Montillo, A, Makris, N, Rosen, B & Dale, AM 2002, 'Whole brain segmentation: automated labeling of neuroanatomical structures in the human brain.', *Neuron*, vol. 33, no. 3, pp. 341–55.

Fischl, B, Salat, DH, van der Kouwe, AJW, Makris, N, Ségonne, F, Quinn, BT & Dale, AM 2004, 'Sequence-independent segmentation of magnetic resonance images.', *NeuroImage*, vol. 23 Suppl 1, pp. S69-84.

Franco, D, Liu, W, Gardiner, DF, Hahn, BH & Ho, DD 2011, 'CD40L-containing virus-like particle as a candidate HIV-1 vaccine targeting dendritic cells', *Journal of Acquired Immune Deficiency Syndromes*, vol. 56, no. 5, pp. 393–400.

Freed, EO 2015, 'HIV-1 assembly, release and maturation', *Nature Reviews Microbiology*, vol. 13, no. 8, pp. 484–496.

Van Genderen, JG, Chia, C, Van Den Hof, M, Mutsaerts, HJMM, Reneman, L, Pajkrt, D & Schrantee, A 2022, 'Brain Differences in Adolescents Living with Perinatally Acquired HIV Compared with Adoption Status Matched Controls: A Cross-sectional Study', *Neurology*, vol. 99, no. 15, pp. E1676–E1684.

Ghodke, Y, Anderson, PL, Sangkuhl, K, Lamba, J, Altman, RB & Klein, TE 2012, 'PharmGKB summary: zidovudine pathway.', *Pharmacogenetics and genomics*, vol. 22, no. 12, pp. 891–4.

Giedd, Jay N, Blumenthal, J, Jeffries, NO, Castellanos, FX, Liu, H, Zijdenbos, A, Paus, T, Evans, AC & Rapoport, JL 1999, 'Brain development during childhood and adolescence: a longitudinal MRI study', *Nature Neuroscience*, vol. 2, no. 10, pp. 861–863.

Giedd, Jay N., Blumenthal, J, Jeffries, NO, Rajapakse, JC, Vaituzis, AC, Liu, H, Berry, YC, Tobin, M, Nelson, J & Castellanos, FX 1999, 'Development of the human corpus callosum during childhood and adolescence: A longitudinal MRI study', *Progress in Neuro-Psychopharmacology and Biological Psychiatry*, vol. 23, no. 4, pp. 571–588.

Giedd, JN & Rapoport, JL 2010, 'Structural MRI of pediatric brain development: what have we learned and where are we going?', *Neuron*, vol. 67, Elsevier Inc., no. 5, pp. 728–34.

Giedd, JN, Snell, JW, Lange, N, Rajapakse, JC, Casey, BJ, Kozuch, PL, Vaituzis, a C, Vauss, YC, Hamburger, SD, Kaysen, D & Rapoport, JL 1996, 'Quantitative magnetic resonance imaging of human brain development: ages 4-18.', *Cerebral cortex (New York, N.Y. : 1991)*, vol. 6, no. 4, pp. 551–60.

von Giesen, H-J, Antke, C, Hefter, H, Wenserski, F, Seitz, RJ & Arendt, G 2000, 'Potential Time Course of Human Immunodeficiency Virus Type 1–Associated Minor Motor Deficits', *Archives of Neurology*, vol. 57, no. 11, pp. 1601–1607.

von Giesen, HJ, Niehues, T, Reumel, J, Haslinger, B a, Ndagijimana, J & Arendt, G 2003, 'Delayed motor learning and psychomotor slowing in HIV-infected children.', *Neuropediatrics*, vol. 34, no. 4, pp. 177–81.

Gloster, SE, Newton, P, Cornforth, D, Lifson C, JD, Williams, I, Shaw, GM & Borrow, P 2004, 'Association of strong virus-specific CD4 T cell responses with efficient natural control of primary HIV-1 infection', *Aids*, vol. 18, no. 5, pp. 749–755.

Gongvatana, A, Correia, S, Dunsiger, S, Gauthier, L, Devlin, KN, Ross, S, Navia, B, Tashima, KT, DeLaMonte, S & Cohen, RA 2014, 'Plasma Cytokine Levels are Related to Brain Volumes in HIV-infected Individuals', *Journal of Neuroimmune Pharmacology*, vol. 9, no. 5, pp. 740–750.

Good, CD, Johnsrude, IS, Ashburner, J, Henson, RNAA, Friston, KJ & Frackowiak, RSJJ 2001, 'A voxel-based morphometric study of ageing in 465 normal adult human brains.', *NeuroImage*, vol. 14, no. 1 Pt 1, pp. 21–36.

Govender, R, Eley, B, Walker, K, Petersen, R & Wilmshurst, JM 2011, 'Neurologic and neurobehavioral sequelae in children with human immunodeficiency virus (HIV-1) infection.', *Journal of child neurology*, vol. 26, no. 11, pp. 1355–64.

Gracien, RM, Maiworm, M, Brüche, N, Shrestha, M, Nöth, U, Hattingen, E, Wagner, M & Deichmann, R 2020, 'How stable is quantitative MRI? – Assessment of intra- and inter-scanner-model reproducibility using identical acquisition sequences and data analysis programs', *NeuroImage*, vol. 207, no. November 2019, pp. 1–11.

Graham, AS, Holmes, MJ, Little, F, Dobbels, E, Cotton, MF, Laughton, B, van der Kouwe, A, Meintjes, EM & Robertson, FC 2020, 'MRS suggests multi-regional inflammation and white matter axonal damage at 11 years following perinatal HIV infection', *NeuroImage: Clinical*, vol. 28, Elsevier Inc., no. June, p. 102505.

Gray, LR, Tachedjian, G, Ellett, AM, Roche, MJ, Cheng, W-J, Guillemin, GJ, Brew, BJ, Turville, SG, Wesselingh, SL, Gorry, PR & Churchill, MJ 2013, 'The NRTIs lamivudine, stavudine and zidovudine have reduced HIV-1 inhibitory activity in astrocytes.', *PloS one*, vol. 8, no. 4, p. e62196.

Gronenschild, EHBM, Habets, P, Jacobs, HIL, Mengelers, R, Rozendaal, N, van Os, J & Marcelis, M 2012, 'The effects of FreeSurfer version, workstation type, and Macintosh operating system version on anatomical volume and cortical thickness measurements.', *PloS one*, vol. 7, no. 6, p. e38234.

De Guio, F, Jouvent, E, Biessels, GJ, Black, SE, Brayne, C, Chen, C, Cordonnier, C, De Leeuw, F-E, Dichgans, M, Doubal, F, Duering, M, Dufouil, C, Duzel, E, Fazekas, F, Hachinski, V, Ikram, MA, Linn, J, Matthews, PM, Mazoyer, B, Mok, V, Norrving, B, O'Brien, JT, Pantoni, L, Ropele, S, Sachdev, P, Schmidt, R, Seshadri, S, Smith, EE, Sposato, LA, Stephan, B, Swartz, RH, Tzourio, C, van Buchem, M, van der Lugt, A, van Oostenbrugge, R, Vernooij, MW, Viswanathan, A, Werring, D, Wollenweber, F, Wardlaw, JM & Chabriat, H 2016, 'Reproducibility and variability of quantitative magnetic resonance imaging markers in cerebral small vessel disease.', *Journal of cerebral blood flow and metabolism : official journal of the International Society of Cerebral Blood Flow and Metabolism*, vol. 36, no. 8, pp. 1319–37.

Hagberg, L, Cinque, P, Gisslen, M, Brew, BJ, Spudich, S, Bestetti, A, Price, RW & Fuchs, D 2010, 'Cerebrospinal fluid neopterin: An informative biomarker of central nervous system immune activation in HIV-1 infection', *AIDS Research and Therapy*, vol. 7, pp. 1–12.

Han, X & Fischl, B 2007, 'Atlas renormalization for improved brain MR image segmentation across scanner platforms.', *IEEE transactions on medical imaging*, vol. 26, no. 4, pp. 479–86.

Hardy, GAD, Sieg, S, Rodriguez, B, Anthony, D, Asaad, R, Jiang, W, Mudd, J, Schacker, T, Funderburg, NT, Pilch-Cooper, HA, Debernardo, R, Rabin, RL, Lederman, MM & Harding, C V. 2013, 'Interferon-α is the primary plasma type-I IFN in HIV-1 infection and correlates with immune activation and disease markers.', *PloS one*, vol. 8, no. 2, p. e56527.

Harper, J, Ribeiro, SP, Chan, CN, Aid, M, Deleage, C, Micci, L, Pino, M, Cervasi, B, Raghunathan, G, Rimmer, E, Ayanoglu, G, Wu, G, Shenvi, N, Barnard, RJO, Del Prete, GQ, Busman-Saha, K, Silvestri, G, Kulpa, DA, Bosinger, SE, Easley, KA, Howell, BJ, Gorman, D, Hazuda, DJ, Estes, JD, Sekaly, RP & Paiardini, M 2022, 'Interleukin-10 contributes to reservoir establishment and persistence in SIV-infected macaques treated with antiretroviral therapy', *Journal of Clinical Investigation*, vol. 132, no. 8.

Hasan, KM & Pedraza, O 2009, 'Improving the reliability of manual and automated methods for hippocampal and amygdala volume measurements.', *NeuroImage*, vol. 48, Elsevier Inc., no. 3, pp. 497–8.

Heany, SJ, Phillips, N, Brooks, S, Fouche, JP, Myer, L, Zar, H, Stein, DJ & Hoare, J 2020, 'Neural correlates of maintenance working memory, as well as relevant structural qualities, are associated with earlier antiretroviral treatment initiation in vertically transmitted HIV', *Journal of NeuroVirology*, vol. 26, Journal of NeuroVirology, no. 1, pp. 60–69.

Hoare, J, Ransford, GL, Phillips, N, Amos, T, Donald, K & Stein, DJ 2014, 'Systematic review of neuroimaging studies in vertically transmitted HIV positive children and adolescents.', *Metabolic brain disease*, vol. 29, no. 2, pp. 221–9.

Van Den Hof, M, Ter Haar, AM, Caan, MWA, Spijker, R, Van Der Lee, JH & Pajkrt, D 2019, 'Brain structure of perinatally HIV-infected patients on long-term treatment: A systematic review', *Neurology: Clinical Practice*, vol. 9, no. 5, pp. 433–442.

Van den Hof, M, Ter Haar, AM, Scherpbier, HJ, van der Lee, JH, Reiss, P, Wit, FWNM, Oostrom, KJ & Pajkrt, D 2020, 'Neurocognitive Development in Perinatally Human Immunodeficiency Virus-infected Adolescents on Long-term Treatment, Compared to Healthy Matched Controls: A Longitudinal Study.', *Clinical infectious diseases : an official publication of the Infectious Diseases Society of America*, vol. 70, no. 7, pp. 1364–1371.

Van den Hof, M, Jellema, PEJ, Ter Haar, AM, Scherpbier, HJ, Schrantee, A, Kaiser, A, Caan, MWA, Majoie, CBLM, Reiss, P, Wit, FWNM, Mutsaerts, HJMM & Pajkrt, D 2021, 'Normal structural brain development in adolescents treated for perinatally acquired HIV: a longitudinal imaging study', *AIDS (London, England)*, vol. 35, no. 8, pp. 1221–1228.

Holmes, MJMJ, Robertson, FCFCFC, Little, F, Randall, SRSRSR, Cotton, MFMF, Van Der Kouwe, AJWAJWAJW, Laughton, B & Meintjes, EMEM 2017, 'Longitudinal increases of brain metabolite levels in 5-10 year old children', in J Harezlak (ed.), *PLOS ONE*, vol. 12, no. 7, p. e0180973.

Horvath, S, Stein, DJ, Phillips, N, Heany, SJ, Kobor, MS, Lin, DTS, Myer, L, Zar, HJ, Levine, AJ & Hoare, J 2018, 'Perinatally acquired HIV infection accelerates epigenetic aging in South African adolescents', *Aids*, vol. 32, no. 11, pp. 1465–1474.

Hoult, DI & Phil, D 2000, 'Sensitivity and power deposition in a high-field imaging

experiment.', *Journal of magnetic resonance imaging : JMRI*, vol. 12, no. 1, pp. 46–67.

Huang, X, Liu, X, Meyers, K, Liu, L, Su, B, Wang, P, Li, Z, Li, L, Zhang, T, Li, N, Chen, H, Li, H & Wu, H 2016, 'Cytokine cascade and networks among MSM HIV seroconverters: Implications for early immunotherapy', *Scientific Reports*, vol. 6, Nature Publishing Group, no. November, pp. 1–9.

Huppertz, H, Kröll-Seger, J, Klöppel, S, Ganz, RE & Kassubek, J 2010, 'Intra- and interscanner variability of automated voxel-based volumetry based on a 3D probabilistic atlas of human cerebral structures.', *NeuroImage*, vol. 49, Elsevier Inc., no. 3, pp. 2216–24.

Iscan, Z, Jin, TB, Kendrick, A, Szeglin, B, Lu, H, Trivedi, M, Fava, M, Mcgrath, PJ, Weissman, M, Kurian, BT, Adams, P, Weyandt, S, Toups, M, Carmody, T, Mcinnis, M, Cusin, C, Cooper, C, Oquendo, MA, Parsey, R V & Delorenzo, C 2015, 'Test – Retest Reliability of FreeSurfer Measurements Within and Between Sites : Effects of Visual Approval Process', vol. 3485, no. August 2014, pp. 3472–3485.

Ivey, NS, MacLean, AG & Lackner, AA 2009, 'Acquired immunodeficiency syndrome and the blood-brain barrier.', *Journal of neurovirology*, vol. 15, no. 2, pp. 111–22.

Jack, CR, Bernstein, MA, Fox, NC, Thompson, P, Alexander, G, Harvey, D, Borowski, B, Britson, PJ, L Whitwell, J, Ward, C, Dale, AM, Felmlee, JP, Gunter, JL, Hill, DLG, Killiany, R, Schuff, N, Fox-Bosetti, S, Lin, C, Studholme, C, DeCarli, CS, Krueger, G, Ward, HA, Metzger, GJ, Scott, KT, Mallozzi, R, Blezek, D, Levy, J, Debbins, JP, Fleisher, AS, Albert, M, Green, R, Bartzokis, G, Glover, G, Mugler, J & Weiner, MW 2008, 'The Alzheimer's Disease Neuroimaging Initiative (ADNI): MRI methods.', *Journal of magnetic resonance imaging : JMRI*, vol. 27, no. 4, pp. 685–91.

Jahanshad, N & Thompson, PM 2017, 'Multimodal neuroimaging of male and female brain structure in health and disease across the life span', *Journal of Neuroscience Research*, vol. 95, no. 1–2, pp. 371–379.

Jankiewicz, M, Holmes, MJ, Taylor, PA, Cotton, MF, Laughton, B, van der Kouwe, AJW & Meintjes, EM 2017, 'White Matter Abnormalities in Children with HIV Infection and Exposure', *Frontiers in Neuroanatomy*, vol. 11, no. September, pp. 1–9.

Jernigan, TL, Trauner, DA, Hesselink, JR & Tallal, PA 1991, 'Maturation of human cerebrum observed in vivo during adolescence.', *Brain : a journal of neurology*, vol. 114 (Pt 5, pp. 2037–49.

Jiao, Y, Zhang, T, Wang, R, Zhang, H, Huang, X, Yin, J, Zhang, L, Xu, X & Wu, H 2012, 'Plasma IP-10 is associated with rapid disease progression in early HIV-1 infection.', *Viral immunology*, vol. 25, no. 4, pp. 333–7.

Johann-Liang, R, Lin, K, Cervia, J, Stavola, J & Noel, G 1998, 'Neuroimaging findings in children perinatally infected with the human immunodeficiency virus.', *The Pediatric infectious disease journal*, vol. 17, no. 8, pp. 753–4.

Johansson, PA, Dziegielewska, KM, Liddelow, SA & Saunders, NR 2008, 'The blood-CSF barrier explained: When development is not immaturity', *BioEssays*, vol. 30, no. 3, pp. 237–248.

Joshi, A 2021, 'IP-10 is a Key Player in HIV Infection', vol. 12, no. December, p. 6113.

Jovicich, J, Marizzoni, M, Sala-Llonch, R, Bosch, B, Bartrés-Faz, D, Arnold, J, Benninghoff,

J, Wiltfang, J, Roccatagliata, L, Nobili, F, Hensch, T, Tränkner, A, Schönknecht, P, Leroy, M, Lopes, R, Bordet, R, Chanoine, V, Ranjeva, JP, Didic, M, Gros-Dagnac, H, Payoux, P, Zoccatelli, G, Alessandrini, F, Beltramello, A, Bargalló, N, Blin, O & Frisoni, GB 2013, 'Brain morphometry reproducibility in multi-center 3T MRI studies: A comparison of cross-sectional and longitudinal segmentations', *NeuroImage*, vol. 83, Elsevier Inc., pp. 472–484.

Kaiser, G 2019, *Microbiology*, COMMUNITY COLLEGE OF BALTIMORE COUNTY, CATONSVILLE.

Kandel, ER, Schwartz, JH & Jessell, TM 2000, *Principles of Neural Science*, 4th edn, McGraw-Hill Medical Publishing Division, New York, NY.

Kangarlu, A, Robitallie, PM, Robitaille, P-ML & Robitallie, PM 2000, 'Biological effects and health implications in magnetic resonance imaging', *Concept Magnetic Res*, vol. 12, no. 5, pp. 321–359.

Kedzierska, K & Crowe, SM 2001, 'Cytokines and HIV-1: Interactions and clinical implications', *Antiviral Chemistry and Chemotherapy*, vol. 12, no. 3, pp. 133–150.

Khobo, IL, Jankiewicz, M, Holmes, MJ, Little, F, Cotton, MF, Laughton, B, van der Kouwe, AJW, Moreau, A, Nwosu, E, Meintjes, EM & Robertson, FC 2022, 'Multimodal magnetic resonance neuroimaging measures characteristic of early cART-treated pediatric HIV: A feature selection approach', *Human Brain Mapping*, vol. 43, no. 13, pp. 4128–4144.

Kiernan, J & Rajakumar, R 2013, 'Barr's The Human Nervous System: An Anatomical Viewpoint', 10th edn, Lippincott Williams & Wilkins, p. 448.

Kim, JY, Chun, SY, Park, J-S, Chung, J-W, Ha, Y-S, Lee, JN & Kwon, TG 2018, 'Laminin and Platelet-Derived Growth Factor-BB Promote Neuronal Differentiation of Human Urine-Derived Stem Cells.', *Tissue engineering and regenerative medicine*, vol. 15, Korean Tissue Engineering and Regenerative Medicine Society, no. 2, pp. 195–209.

Kirchhoff, F 2010, 'Immune evasion and counteraction of restriction factors by HIV-1 and other primate lentiviruses', *Cell Host and Microbe*, vol. 8, Elsevier Inc., no. 1, pp. 55–67.

Knake, S, Triantafyllou, C, Wald, LL, Wiggins, G, Kirk, GP, Larsson, PG, Grant, PE, Stufflebeam, SM, Foley, MT, Shiraishi, H, Dale, AM, Halgren, E, Grant, PE, Stufflebeam, SM, Foley, MT, Shiraishi, H, Dale, AM, Halgren, E & Grant, PE 2005, '3T phased array MRI improves the presurgical evaluation in focal epilepsies: a prospective study.', *Neurology*, vol. 65, no. 7, pp. 1026–31.

Ko, A, Kang, G, Hattler, JB, Galadima, HI, Zhang, J, Li, Q & Kim, WK 2019, 'Macrophages but not Astrocytes Harbor HIV DNA in the Brains of HIV-1-Infected Aviremic Individuals on Suppressive Antiretroviral Therapy', *Journal of Neuroimmune Pharmacology*, vol. 14, Journal of Neuroimmune Pharmacology, no. 1, pp. 110–119.

Kochunov, P, Thompson, PM, Coyle, TR, Lancaster, JL, Kochunov, V, Royall, D, Mangin, J-F, Rivière, D, Fox, PT, Rivie, D, Mangin, J-F, Rivière, D, Fox, PT & Rivie, D 2008, 'Relationship among neuroimaging indices of cerebral health during normal aging.', *Human brain mapping*, vol. 29, no. 1, pp. 36–45.

Kolson, D 2017, 'Neurologic complications of HIV infection in the era of antiretroviral therapy', *Topics in Antiviral Medicine*, vol. 25, no. 3, pp. 97–101.

Kornbluth, RS 2000, 'The emerging role of CD40 ligand in HIV infection', *Journal of*

Leukocyte Biology, vol. 68, no. 3, pp. 373–382.

van der Kouwe, AJW, Benner, T, Salat, DH & Fischl, B 2008, 'Brain morphometry with multiecho MPRAGE.', *NeuroImage*, vol. 40, no. 2, pp. 559–69.

Kramer-Hämmerle, S, Rothenaigner, I, Wolff, H, Bell, JE & Brack-Werner, R 2005, 'Cells of the central nervous system as targets and reservoirs of the human immunodeficiency virus', *Virus Research*, vol. 111, no. 2, pp. 194–213.

Kruggel, F, Turner, J, Muftuler, LT & Alzheimer's Disease Neuroimaging Initiative 2010, 'Impact of scanner hardware and imaging protocol on image quality and compartment volume precision in the ADNI cohort.', *NeuroImage*, vol. 49, no. 3, pp. 2123–33.

Lane, TE, Liu, MT, Chen, BP, Asensio, VC, Samawi, RM, Paoletti, AD, Campbell, IL, Kunkel, SL, Fox, HS & Buchmeier, MJ 2000, ' A Central Role for CD4 + T Cells and RANTES in Virus-Induced Central Nervous System Inflammation and Demyelination ', *Journal of Virology*, vol. 74, no. 3, pp. 1415–1424.

Langerak, NG, du Toit, J, Burger, M, Cotton, MF, Springer, PE & Laughton, B 2014, 'Spastic diplegia in children with HIV encephalopathy: First description of gait and physical status', *Developmental Medicine and Child Neurology*, vol. 56, no. 7, pp. 686–694.

Lanier, ER, Sturge, G, McClernon, D, Brown, S, Halman, M, Sacktor, N, McArthur, J, Atkinson, JH, Clifford, D, Price, RW, Simpson, D, Torres, G, Catalan, J, Marder, K, Power, C, Hall, C, Romero, C & Brew, B 2001, 'HIV-1 reverse transcriptase sequence in plasma and cerebrospinal fluid of patients with AIDS dementia complex treated with Abacavir.', *AIDS (London, England)*, vol. 15, no. 6, pp. 747–51.

Laughton, B, Cornell, M, Boivin, M & Van Rie, A 2013, 'Neurodevelopment in perinatally HIV-infected children: a concern for adolescence', *Journal of the International AIDS Society*, vol. 16, no. 1.

Laughton, B, Cornell, M, Grove, D, Kidd, M, Springer, PE, Dobbels, E, van Rensburg, AJ, Violari, A, Babiker, AG, Madhi, SA, Jean-Philippe, P, Gibb, DM & Cotton, MF 2012, 'Early antiretroviral therapy improves neurodevelopmental outcomes in infants.', *AIDS (London, England)*, vol. 26, IAS 2009, Cape Town, no. 13, pp. 1685–1690.

Laughton, B, Cornell, M, Kidd, M, Springer, PE, Dobbels, EFM-T, Rensburg, AJ Van, Otwombe, K, Babiker, A, Gibb, DM, Violari, A, Kruger, M & Cotton, MF 2018, 'Five year neurodevelopment outcomes of perinatally HIV-infected children on early limited or deferred continuous antiretroviral therapy', *Journal of the International AIDS Society*, vol. 21, no. 5, p. e25106.

Lee, H, Nakamura, K, Narayanan, S, Brown, RA & Arnold, DL 2019, 'Estimating and accounting for the effect of MRI scanner changes on longitudinal whole-brain volume change measurements', *NeuroImage*, vol. 184, no. May 2018, pp. 555–565.

Lehmann, M, Nikolic, DS & Piguet, V 2011, 'How HIV-1 takes advantage of the cytoskeleton during replication and cell-to-cell transmission', *Viruses*, vol. 3, no. 9, pp. 1757–1776.

Lei, J, Yin, X, Shang, H & Jiang, Y 2019, 'Cytokine IP-10 is highly involved in HIV infection', *Cytokine*, vol. 115, Elsevier, no. 155, pp. 97–103.

Lenroot, RK, Gogtay, N, Greenstein, DK, Wells, EM, Wallace, GL, Clasen, LS, Blumenthal,

JD, Lerch, J, Zijdenbos, AP, Evans, AC, Thompson, PM & Giedd, JN 2007, 'Sexual dimorphism of brain developmental trajectories during childhood and adolescence', *NeuroImage*, vol. 36, no. 4, pp. 1065–1073.

Lenroot, RK, Schmitt, JE, Ordaz, SJ, Wallace, GL, Neale, MC, Lerch, JP, Kendler, KS, Evans, AC & Giedd, JN 2009, 'Differences in genetic and environmental influences on the human cerebral cortex associated with development during childhood and adolescence', *Human Brain Mapping*, vol. 30, no. 1, pp. 163–174.

Letendre, SL, McCutchan, JA, Childers, ME, Woods, SP, Lazzaretto, D, Heaton, RK, Grant, I & Ellis, RJ 2004, 'Enhancing antiretroviral therapy for human immunodeficiency virus cognitive disorders.', *Annals of neurology*, vol. 56, no. 3, pp. 416–23.

Lewis-de Los Angeles, CP, Alpert, KI, Williams, PL, Malee, K, Huo, Y, Csernansky, JG, Yogev, R, Van Dyke, RB, Sowell, ER, Wang, L & Pediatric HIV/AIDS Cohort Study (PHACS) 2016, 'Deformed Subcortical Structures Are Related to Past HIV Disease Severity in Youth With Perinatally Acquired HIV Infection.', *Journal of the Pediatric Infectious Diseases Society*, vol. 5, no. suppl 1, pp. S6–S14.

Lewis-de los Angeles, CP, Williams, PL, Huo, Y, Wang, SD, Uban, KA, Herting, MM, Malee, K, Yogev, R, Csernansky, JG, Nichols, S, Van Dyke, RB, Sowell, ER, Wang, L & Pediatric HIV/AIDS Cohort Study (PHACS) and the Pediatric Imaging, Neurocognition, and G (PING) S 2017, 'Lower total and regional grey matter brain volumes in youth with perinatally-acquired HIV infection: Associations with HIV disease severity, substance use, and cognition', *Brain, behavior, and immunity*, vol. 62, Elsevier Inc., pp. 100–109.

Lewis-de los Angeles, CP, Williams, PL, Jenkins, LM, Huo, Y, Malee, K, Alpert, KI, Uban, KA, Herting, MM, Csernansky, JG, Nichols, SL, Van Dyke, RB, Sowell, ER & Wang, L 2020, 'Brain morphometric differences in youth with and without perinatally-acquired HIV: A cross-sectional study', *NeuroImage: Clinical*, vol. 26, Elsevier, no. October 2019, p. 102246.

Lindsey, JC, Malee, KM, Brouwers, P & Hughes, MD 2007, 'Neurodevelopmental functioning in HIV-infected infants and young children before and after the introduction of protease inhibitor-based highly active antiretroviral therapy.', *Pediatrics*, vol. 119, no. 3, pp. e681–e693.

Liu, F, Zhao, H & Crozier, S 2003, 'Calculation of electric fields induced by body and head motion in high-field MRI.', *Journal of magnetic resonance (San Diego, Calif. : 1997)*, vol. 161, no. 1, pp. 99–107.

Liu, S, Hou, B, Zhang, Y, Lin, T, Fan, X, You, H & Feng, F 2020, 'Inter-scanner reproducibility of brain volumetry: influence of automated brain segmentation software.', *BMC neuroscience*, vol. 21, BioMed Central, no. 1, p. 35.

Lobo-Silva, D, Carriche, GM, Castro, AG, Roque, S & Saraiva, M 2016, 'Balancing the immune response in the brain: IL-10 and its regulation', *Journal of Neuroinflammation*, vol. 13, Journal of Neuroinflammation, no. 1, pp. 1–10.

Lu, S-M, Tremblay, M-È, King, IL, Qi, J, Reynolds, HM, Marker, DF, Varrone, JJP, Majewska, AK, Dewhurst, S & Gelbard, HA 2011, 'HIV-1 Tat-induced microgliosis and synaptic damage via interactions between peripheral and central myeloid cells.', *PloS one*, vol. 6, no. 9, p. e23915.

Luders, E, Thompson, PM & Toga, AW 2010, 'The Development of the Corpus Callosum in the Healthy Human Brain', *Journal of Neuroscience*, vol. 30, no. 33, pp. 10985–10990.

Madhi, SA, Adrian, P, Cotton, MF, Mcintyre, JA, Jean-, P, Meadows, S, Nachman, S, Käyhty, H & Klugman, KP 2011, 'pneumococcal conjugate vaccine in infants', vol. 202, no. July 2009, pp. 355–361.

Madhi, SA, Adrian, P, Cotton, MF, McIntyre, JA, Jean-Philippe, P, Meadows, S, Nachman, S, Käyhty, H, Klugman, KP, Violari, A & Comprehensive International Program of Research on AIDS 4 Study Team 2010, 'Effect of HIV infection status and anti-retroviral treatment on quantitative and qualitative antibody responses to pneumococcal conjugate vaccine in infants.', *The Journal of infectious diseases*, vol. 202, no. 3, pp. 355–61.

Madzime, J, Holmes, M, Cotton, MF, Laughton, B, van der Kouwe, AJW, Meintjes, EM & Jankiewicz, M 2021, 'Altered White Matter Tracts in the Somatosensory, Salience, Motor, and Default Mode Networks in 7-Year-Old Children Living with Human Immunodeficiency Virus: A Tractographic Analysis.', *Brain connectivity*.

Mariani, SA, Brigida, I, Kajaste-Rudnitski, A, Ghezzi, S, Rocchi, A, Plebani, A, Vicenzi, E, Aiuti, A & Poli, G 2012, 'HIV-1 envelope-dependent restriction of CXCR4-using viruses in child but not adult untransformed CD4+ T-lymphocyte lines.', *Blood*, vol. 119, no. 9, pp. 2013–23.

Mark Hammer 2014, *MRI Physics: Tissue Contrast in MRI*, XRayPhysics - Interactive Radiology Physics.

Martín-Bejarano, M, Ruiz-Saez, B, Martinez-De-aragón, A, Melero, H, Zamora, B, Malpica, NA, Ramos, JT & Gonzalez-Tomé, MI 2021, 'A systematic review of magnetic resonance imaging studies in perinatally HIV-infected individuals', *AIDS Reviews*, vol. 23, no. 4, pp. 167–185.

Martin, P & Leibovich, SJ 2005, 'Inflammatory cells during wound repair: the good, the bad and the ugly.', *Trends in cell biology*, vol. 15, no. 11, pp. 599–607.

Mberi, F, Jankiewicz, M, Little, F, Cotton, MF, Laughton, B, van der Kouwe, AJW, Meintjes, EM & Holmes, MJ 2018, 'Ongoing White Matter Alterations in HIV Infected and HIV Exposed Children: A DTI Study at 9 Years.', in *22nd International AIDS Conference*, Amsterdam, p. TUPDB0104.

Mbugua, KK, Holmes, MJ, Cotton, MF, Ratai, E-M, Little, F, Hess, AT, Dobbels, E, Van der Kouwe, AJW, Laughton, B & Meintjes, EM 2016, 'HIV-associated CD4+/CD8+ depletion in infancy is associated with neurometabolic reductions in the basal ganglia at age 5 years despite early antiretroviral therapy', *AIDS*, vol. 30, no. 9, pp. 1353–1362.

Mcarthur, JC, Brew, BJ & Nath, A 2005, 'Neurological complications of HIV infection.', *The Lancet. Neurology*, vol. 4, no. 9, pp. 543–55.

McClernon, DR, Lanier, R, Gartner, S, Feaser, P, Pardo, C a, St Clair, M, Liao, Q & McArthur, JC 2001, 'HIV in the brain: RNA levels and patterns of zidovudine resistance.', *Neurology*, vol. 57, no. 8, pp. 1396–401.

McCoig, C, Castrejón, MM, Castaño, E, De Suman, O, Báez, C, Redondo, W, McClernon, D, Danehower, S, Lanier, ER, Richardson, C, Keller, A, Hetherington, S, Sáez-Llorens, X & Ramilo, O 2002, 'Effect of combination antiretroviral therapy on cerebrospinal fluid HIV RNA, HIV resistance, and clinical manifestations of encephalopathy.', *The Journal of pediatrics*, vol. 141, no. 1, pp. 36–44.

McGuire, JL, Gill, AJ, Douglas, SD, Kolson, DL, Hiv, CNS, Effects, AT & CNS HIV Anti-

Retroviral Therapy Effects Research (CHARTER) group 2015, 'Central and peripheral markers of neurodegeneration and monocyte activation in HIV-associated neurocognitive disorders.', *Journal of neurovirology*, vol. 21, no. 4, pp. 439–48.

McMichael, AJ, Borrow, P, Tomaras, GD, Goonetilleke, N & Haynes, BF 2010, 'The immune response during acute HIV-1 infection: Clues for vaccine development', *Nature Reviews Immunology*, vol. 10, Nature Publishing Group, no. 1, pp. 11–23.

Medders, KE & Kaul, M 2011, 'Mitogen-activated protein kinase p38 in HIV infection and associated brain injury.', *Journal of neuroimmune pharmacology : the official journal of the Society on NeuroImmune Pharmacology*, vol. 6, no. 2, pp. 202–15.

Mitchell, W 2001, 'Neurological and developmental effects of HIV and AIDS in children and adolescents.', *Mental retardation and developmental disabilities research reviews*, vol. 7, no. 3, pp. 211–6.

Mitchell, Wendy 2001, 'Neurological and developmental effects of HIV and AIDS in children and adolescents', *Mental retardation and developmental disabilities …*, vol. 216, pp. 211–216.

Mlcochova, P, Watters, S a, Towers, GJ, Noursadeghi, M & Gupta, RK 2014, 'Vpx complementation of "non-macrophage tropic" R5 viruses reveals robust entry of infectious HIV-1 cores into macrophages.', *Retrovirology*, vol. 11, Retrovirology, no. 1, p. 25.

Moberg, PJ, Ding, Y, Hitzemann, R, Smith, G & Logan, J 1998, 'Association between declines in Brain Dopamine Activity with age and Cognitive and Motor Impairment in Healthy Individuals', *American Journal Of Psychiatry*, no. 6, pp. 344–349.

Molero-Luis, M, Casas-Alba, D, Orellana, G, Ormazabal, A, Sierra, C, Oliva, C, Valls, A, Velasco, J, Launes, C, Cuadras, D, Pérez-Dueñas, B, Jordan, I, Cambra, FJ, Ortigoza-Escobar, JD, Muñoz-Almagro, C, Garcia-Cazorla, A, Armangué, T & Artuch, R 2020, 'Cerebrospinal fluid neopterin as a biomarker of neuroinflammatory diseases', *Scientific Reports*, vol. 10, Nature Publishing Group UK, no. 1, pp. 1–9.

Morey, RA, Petty, CM, Xu, Y, Hayes, JP, Wagner, HR, Lewis, D V, LaBar, KS, Styner, M & McCarthy, G 2009, 'A comparison of automated segmentation and manual tracing for quantifying hippocampal and amygdala volumes.', *NeuroImage*, vol. 45, Elsevier B.V., no. 3, pp. 855–66.

Mulder, ER, de Jong, R a, Knol, DL, van Schijndel, R a, Cover, KS, Visser, PJ, Barkhof, F & Vrenken, H 2014, 'Hippocampal volume change measurement: quantitative assessment of the reproducibility of expert manual outlining and the automated methods FreeSurfer and FIRST.', *NeuroImage*, vol. 92, Elsevier Inc., pp. 169–81.

Musich, T, Peters, PJ, Duenas-Decamp, MJ, Gonzalez-Perez, MP, Robinson, J, Zolla-Pazner, S, Ball, JK, Luzuriaga, K & Clapham, PR 2011, 'A conserved determinant in the V1 loop of HIV-1 modulates the V3 loop to prime low CD4 use and macrophage infection.', *Journal of virology*, vol. 85, no. 5, pp. 2397–405.

Musielak, KA & Fine, JG 2016, 'An Updated Systematic Review of Neuroimaging Studies of Children and Adolescents with Perinatally Acquired HIV', *Journal of Pediatric Neuropsychology*, vol. 2, no. 1–2, pp. 34–49.

Nagarajan, R, Sarma, MK, Thomas, MA, Chang, L, Natha, U, Wright, M, Hayes, J, Nielsen-

Saines, K, Michalik, DE, Deville, J, Church, JA, Mason, K, Critton-Mastandrea, T, Nazarian, S, Jing, J & Keller, MA 2012, 'Neuropsychological function and cerebral metabolites in HIV-infected youth.', *Journal of neuroimmune pharmacology : the official journal of the Society on NeuroImmune Pharmacology*, vol. 7, no. 4, pp. 981–90.

Narayanan, PL, Warton, C, Rosella Boonzaier, N, Molteno, CD, Joseph, J, Jacobson, JL, Jacobson, SW, Zöllei, L & Meintjes, EM 2016, 'Improved segmentation of cerebellar structures in children.', *Journal of neuroscience methods*, vol. 262, no. 6, pp. 1–13.

Netter, FH 2002, 'Neuroanatomy: Basal Nuclei (Ganglia)', in *Atlas of Neuroanatomy and Neurophysiology*, Icon Custom Communications, Teterboro, p. 4.

Norris, PJ, Pappalardo, BL, Custer, B, Spotts, G, Hecht, FM & Busch, MP 2006, 'Elevations in IL-10, TNF-α, and IFN-γ from the earliest point of HIV type 1 infection', *AIDS Research and Human Retroviruses*, vol. 22, no. 8, pp. 757–762.

Nozyce, ML, Lee, SS, Wiznia, A, Nachman, S, Mofenson, LM, Smith, ME, Yogev, R, McIntosh, K, Stanley, K & Pelton, S 2006, 'A behavioral and cognitive profile of clinically stable HIV-infected children.', *Pediatrics*, vol. 117, no. 3, pp. 763–770.

Nwosu, EC, Holmes, MJ, Cotton, MF, Dobbels, E, Little, F, Laughton, B, van der Kouwe, A, Meintjes, EM & Robertson, F 2021, 'Cortical structural changes related to early antiretroviral therapy (ART) interruption in perinatally HIV-infected children at 5 years of age', *IBRO Neuroscience Reports*, vol. 10, Elsevier Ltd, no. February, pp. 161–170.

Nwosu, EC, Holmes, MJ, Cotton, MF, Dobbels, E, Little, F, Laughton, B, van der Kouwe, A, Robertson, F & Meintjes, EM 2023, 'Similar cortical morphometry trajectories from 5 to 9 years in children with perinatal HIV who started treatment before age 2 years and uninfected controls', *BMC Neuroscience*, vol. 24, BioMed Central, no. 1, pp. 1–15.

Nwosu, EC, Robertson, FC, Holmes, MJ, Cotton, MF, Dobbels, E, Little, F, Laughton, B, van der Kouwe, A & Meintjes, EM 2018, 'Altered brain morphometry in 7-year old HIV-infected children on early ART', *Metabolic Brain Disease*, vol. 33, Metabolic Brain Disease, no. 2, pp. 523–535.

Nwosu, EC, Robertson, FC & Meintjes, EM 2019, 'Brain morphometry of HIV-infected children on early antiretroviral therapy (ART) from age 5 to 9 years', University of Cape Town.

Ochsenbauer, C, Edmonds, TG, Ding, H, Keele, BF, Decker, J, Salazar, MG, Salazar-Gonzalez, JF, Shattock, R, Haynes, BF, Shaw, GM, Hahn, BH & Kappes, JC 2012, 'Generation of transmitted/founder HIV-1 infectious molecular clones and characterization of their replication capacity in CD4 T lymphocytes and monocyte-derived macrophages.', *Journal of virology*, vol. 86, no. 5, pp. 2715–28.

Okafor, EC, Hullsiek, KH, Williams, DA, Scriven, JE, Rhein, J, Nabeta, HW, Musubire, AK, Rajasingham, R, Muzoora, C, Schutz, C, Meintjes, G, Meya, DB & Boulware, DR 2020, 'Correlation between blood and CSF compartment cytokines and chemokines in subjects with cryptococcal meningitis', *Mediators of Inflammation*, vol. 2020.

Oster, S, Christoffersen, P, Gundersen, HJG, Nielsen, JO, Pakkenberg, B & Pedersen, C 1993, 'Cerebral atrophy in AIDS: a stereological study', *Acta Neuropathologica*, vol. 85, no. 6, pp. 617–622.

Patsalides, AD, Wood, L V., Atac, GK, Sandifer, E, Butman, JA & Patronas, NJ 2002,

‘Cerebrovascular disease in HIV-infected pediatric patients: neuroimaging findings.’, *Journal of Roentgenology*, vol. 179, no. 4, pp. 999–1003.

Paul, ME, Mao, C, Charurat, M, Serchuck, L, Foca, M, Hayani, K, Handelsman, EL, Diaz, C, McIntosh, K, Shearer, WT & Women and Infants Transmission Study 2005, ‘Predictors of immunologic long-term nonprogression in HIV-infected children: Implications for initiating therapy’, *Journal of Allergy and Clinical Immunology*, vol. 115, no. 4, pp. 848–855.

Paul, R, Prasitsuebsai, W, Jahanshad, N, Puthanakit, T, Thompson, P, Aurpibul, L, Hansudewechakul, R, Kosalaraksa, P, Kanjanavanit, S, Ngampiyaskul, C, Luesomboon, W, Lerdlum, S, Pothisri, M, Visrutaratna, P, Valcour, V, Nir, TM, Saremi, A, Kerr, S, Ananworanich, J & Pediatric Randomized Early versus Deferred Initiation in Cambodia and Thailand (PREDICT) Study Group 2018, ‘Structural Neuroimaging and Neuropsychologic Signatures in Children With Vertically Acquired HIV.’, *The Pediatric infectious disease journal*, vol. 37, no. 7, pp. 662–668.

Perdomo-Celis, F, Feria, MG, Taborda, NA & Rugeles, MT 2018, ‘A Low Frequency of IL-17-Producing CD8+ T-Cells Is Associated With Persistent Immune Activation in People Living With HIV Despite HAART-Induced Viral Suppression’, *Frontiers in Immunology*, vol. 9, no. October.

Pérez-Cerdá, F, Sánchez-Gómez, MV & Matute, C 2016, ‘The link of inflammation and neurodegeneration in progressive multiple sclerosis’, *Multiple Sclerosis and Demyelinating Disorders*, vol. 1, Multiple Sclerosis and Demyelinating Disorders, no. 1, p. 9.

Phillips, N, Amos, T, Kuo, C, Hoare, J, Ipser, J, Thomas, KGF & Stein, DJ 2016, ‘HIV-Associated Cognitive Impairment in Perinatally Infected Children: A Meta-analysis.’, *Pediatrics*, vol. 138, no. 5, pp. e20160893–e20160893.

Pillai, SK, Pond, SLK, Liu, Y, Good, BM, Strain, MC, Ellis, RJ, Letendre, S, Smith, DM, Günthard, HF, Grant, I, Marcotte, TD, McCutchan, JA, Richman, DD & Wong, JK 2006, ‘Genetic attributes of cerebrospinal fluid-derived HIV-1 env.’, *Brain : a journal of neurology*, vol. 129, no. Pt 7, pp. 1872–83.

Pollard, VW & Malim, MH 1998, ‘The HIV-1 Rev protein.’, *Annual review of microbiology*, vol. 52, pp. 491–532.

Powell, S, Magnotta, VA, Johnson, H, Jammalamadaka, VK, Pierson, R & Andreasen, NC 2008, ‘Registration and machine learning-based automated segmentation of subcortical and cerebellar brain structures.’, *NeuroImage*, vol. 39, no. 1, pp. 238–47.

Preboske, GM, Gunter, JL, Ward, CP & Jr, CRJ 2006, ‘Common MRI acquisition non-idealities significantly impact the output of the boundary shift integral method of measuring brain atrophy on serial MRI’, vol. 30, pp. 1196–1202.

Pulli, EP, Silver, E, Kumpulainen, V, Copeland, A, Merisaari, H, Saunavaara, J, Parkkola, R, Lähdesmäki, T, Saukko, E, Nolvi, S, Kataja, EL, Korja, R, Karlsson, L, Karlsson, H & Tuulari, JJ 2022, ‘Feasibility of FreeSurfer Processing for T1-Weighted Brain Images of 5-Year-Olds: Semiautomated Protocol of FinnBrain Neuroimaging Lab’, *Frontiers in Neuroscience*, vol. 16, no. May, pp. 1–20.

Ragin, AB, Wu, Y, Ochs, R, Scheidegger, R, Cohen, BA, Edelman, RR, Epstein, LG & McArthur, J 2010, ‘Biomarkers of neurological status in HIV infection: A 3-year study’, *Proteomics - Clinical Applications*, vol. 4, no. 3, pp. 295–303.

Randall, SR, Warton, CMR, Holmes, MJ, Cotton, MF, Laughton, B, van der Kouwe, AJW & Meintjes, EM 2017, 'Larger Subcortical Gray Matter Structures and Smaller Corpora Callosa at Age 5 Years in HIV Infected Children on Early ART.', *Frontiers in neuroanatomy*, vol. 11, no. November, p. 95.

Randall, SR, Warton, CMR, Morgan, L, Moreau, A, Cotton, MF, Laughton, B, van der Kouwe, AJW, Meintjes, EM & Holmes, MJ 2021, 'Assessing Inter-Scanner Reproducibility Using Manual and Automated Segmentation of Subcortical Structures In 9- To 10-Year-Old Children: Under Review'.

Rao, VR, Ruiz, AP & Prasad, VR 2014, 'Viral and cellular factors underlying neuropathogenesis in HIV associated neurocognitive disorders (HAND).', *AIDS research and therapy*, vol. 11, p. 13.

Rapoport, JL, Castellanos, FX, Gogate, N, Janson, K, Kohler, S & Nelson, P 2001, 'Imaging normal and abnormal brain development: new perspectives for child psychiatry.', *The Australian and New Zealand journal of psychiatry*, vol. 35, no. 3, pp. 272–281.

Raskino, C, Pearson, DA, Baker, CJ, Lifschitz, MH, O'Donnell, K, Mintz, M, Nozyce, M, Brouwers, P, McKinney, RE, Jimenez, E & Englund, J a 1999, 'Neurologic, neurocognitive, and brain growth outcomes in human immunodeficiency virus-infected children receiving different nucleoside antiretroviral regimens. Pediatric AIDS Clinical Trials Group 152 Study Team.', *Pediatrics*, vol. 104, no. 3, p. e32.

Reig, S, Sánchez-González, J, Arango, C, Castro, J, González-Pinto, A, Ortuño, F, Crespo-Facorro, B, Bargalló, N & Desco, M 2009, 'Assessment of the increase in variability when combining volumetric data from different scanners', *Human Brain Mapping*, vol. 30, no. 2, pp. 355–368.

Reiss, AL, Abrams, MT, Singer, HS, Ross, JL & Denckla, MB 1996, 'Brain development, gender and IQ in children. A volumetric imaging study.', *Brain : a journal of neurology*, vol. 119 (Pt 5, pp. 1763–74.

Remer, J, Croteau-Chonka, E, Dean, DC, D'Arpino, S, Dirks, H, Whiley, D & Deoni, SCL 2017, 'Quantifying cortical development in typically developing toddlers and young children, 1–6 years of age', *NeuroImage*, vol. 153, Elsevier, no. November 2016, pp. 246–261.

Reuter, M, Schmansky, NJ, Rosas, HD & Fischl, B 2012, 'NeuroImage Within-subject template estimation for unbiased longitudinal image analysis', *NeuroImage*, vol. 61, Elsevier Inc., no. 4, pp. 1402–1418.

Richards, MH, Narasipura, SD, Seaton, MS, Lutgen, V & Al-Harthi, L 2016, 'Migration of CD8+ T Cells into the Central Nervous System Gives Rise to Highly Potent Anti-HIV CD4dimCD8bright T Cells in a Wnt Signaling–Dependent Manner', *The Journal of Immunology*, vol. 196, no. 1, pp. 317–327.

van Rie, A, Harrington, PR, Dow, A & Robertson, K 2007, 'Neurologic and neurodevelopmental manifestations of pediatric HIV/AIDS: a global perspective.', *European journal of paediatric neurology : EJPN : official journal of the European Paediatric Neurology Society*, vol. 11, no. 1, pp. 1–9.

van Rie, A, Mupuala, A & Dow, A 2008, 'Impact of the HIV/AIDS epidemic on the neurodevelopment of preschool-aged children in Kinshasa, Democratic Republic of the Congo.', *Pediatrics*, vol. 122, no. 1, pp. e123-8.

Ritola, K, Robertson, K, Fiscus, SA, Hall, C & Swanstrom, R 2005, 'Increased human immunodeficiency virus type 1 (HIV-1) env compartmentalization in the presence of HIV-1-associated dementia.', *Journal of virology*, vol. 79, no. 16, pp. 10830–4.

Robertson, FC, Holmes, MJ, Cotton, MF, Dobbels, E, Little, F, Laughton, B, van der Kouwe, AJW & Meintjes, EM 2018, 'Perinatal HIV Infection or Exposure Is Associated With Low N-Acetylaspartate and Glutamate in Basal Ganglia at Age 9 but Not 7 Years', *Frontiers in Human Neuroscience*, vol. 12, no. May, pp. 1–10.

Rosca, EC, Rosca, O, Chirileanu, RD & Simu, M 2011, 'HIV & AIDS Review Neurocognitive disorders due to HIV infection', *HIV & AIDS Review*, vol. 10, Polish AIDS Research Society., no. 2, pp. 33–37.

Rosenberg, ES, Billingsley, JM, Caliendo, AM, Boswell, SL, Sax, PE, Kalams, SA & Walker, BD 1997, 'Vigorous HIV-1-specific CD4+ T cell responses associated with control of viremia.', *Science (New York, N.Y.)*, vol. 278, no. 5342, pp. 1447–50.

Rosenfeldt, V, Valerius, NH & Paerregaard, a 2000, 'Regression of HIV-associated progressive encephalopathy of childhood during HAART.', *Scandinavian journal of infectious diseases*, vol. 32, no. 5, pp. 571–574.

Ruhanya, V, Jacobs, GB, Naidoo, S, Paul, RH, Joska, JA, Seedat, S, Nyandoro, G, Engelbrecht, S & Glashoff, RH 2021a, 'Impact of Plasma IP-10/CXCL10 and RANTES/CCL5 Levels on Neurocognitive Function in HIV Treatment-Naive Patients', *AIDS Research and Human Retroviruses*, vol. 37, no. 9, pp. 657–665.

Ruhanya, V, Jacobs, GB, Paul, RH, Joska, JA, George, SS, Engelbrecht, S & Glashoff, RH 2021b, 'Proinflammatory cytokines and chemokines are related to MRI measures of white and gray matter in HIV infection', no. May.

Sacktor, N, Haughey, N, Cutler, R, Tamara, A, Turchan, J, Pardo, C, Vargas, D & Nath, A 2004, 'Novel markers of oxidative stress in actively progressive HIV dementia', *Journal of Neuroimmunology*, vol. 157, pp. 176–184.

Sacktor, NC, Bacellar, H, Hoover, DR, Nance-Sproson, TE, Selnes, OA, Miller, EN, Dal Pan, GJ, Kleeberger, C, Brown, A, Saah, A & McArthur, JC 1996, 'Psychomotor slowing in HIV infection: a predictor of dementia, AIDS and death.', *Journal of neurovirology*, vol. 2, no. 6, pp. 404–10.

Safriel, YI, Haller, JO, Lefton, DR & Obedian, R 2000, 'Imaging of the brain in the HIV-positive child.', *Pediatric radiology*, vol. 30, no. 11, pp. 725–32.

Sánchez-Benavides, G, Gómez-Ansón, B, Sainz, A, Vives, Y, Delfino, M & Peña-Casanova, J 2010, 'Manual validation of FreeSurfer's automated hippocampal segmentation in normal aging, mild cognitive impairment, and Alzheimer Disease subjects.', *Psychiatry research*, vol. 181, Elsevier Ireland Ltd, no. 3, pp. 219–25.

Sarma, MK, Nagarajan, R, Keller, M a, Kumar, R, Nielsen-Saines, K, Michalik, DE, Deville, J, Church, J a & Thomas, MA 2014, 'Regional brain gray and white matter changes in perinatally HIV-infected adolescents.', *NeuroImage. Clinical*, vol. 4, The Authors, pp. 29–34.

Saunders, NR, Liddelow, SA & Dziegielewska, KM 2012, 'Barrier mechanisms in the developing brain', *Frontiers in Pharmacology*, vol. 3 MAR, no. March, pp. 1–18.

Schick, F 2005, 'Whole-body MRI at high field: technical limits and clinical potential.',

European radiology, vol. 15, no. 5, pp. 946–59.

Schnack, HG, Haren, NEM Van, Pol, HEH, Picchioni, M, Weisbrod, M, Sauer, H, Cannon, T, Huttunen, M, Murray, R & Kahn, S 2004, 'Reliability of Brain Volumes from Multicenter MRI Acquisition : A Calibration Study', vol. 320, no. February, pp. 312–320.

Schnell, G, Joseph, S, Spudich, S, Price, RW & Swanstrom, R 2011, 'HIV-1 replication in the central nervous system occurs in two distinct cell types.', *PLoS pathogens*, vol. 7, no. 10, p. e1002286.

Shah, SS, Zimmerman, R a, Rorke, LB & Vezina, LG 1996, 'Cerebrovascular complications of HIV in children.', *AJNR. American journal of neuroradiology*, vol. 17, no. 10, pp. 1913–7.

Shanbhag, MC, Rutstein, RM, Zaoutis, T, Zhao, H, Chao, D & Radcliffe, J 2016, 'Neurocognitive Functioning in Pediatric Human Immunodeficiency Virus Infection', *Archives of pediatrics & adolescent medicine*, vol. 159, no. July 2005, pp. 651–656.

Shearer, WT, Pahwa, S, Read, JS, Chen, J, Wijayawardana, SR, Palumbo, P, Abrams, EJ, Nesheim, SR, Yin, W, Thompson, B & Easley, KA 2007, 'CD4/CD8 T-cell ratio predicts HIV infection in??infants: The National Heart, Lung, and Blood Institute P2C2 Study', *Journal of Allergy and Clinical Immunology*, vol. 120, no. 6, pp. 1449–1456.

Shokouh, M-N 2021, *BiteSized Immunology: Human immunodeficiency virus*, *British Society for Immunology*, British Society for Immunology, Oxford.

Shokouhi, M, Barnes, A, Suckling, J, Moorhead, TW, Brennan, D, Job, D, Lymer, K, Dazzan, P, Reis Marques, T, Mackay, C, McKie, S, Williams, SRC, Lawrie, SM, Deakin, B, Williams, SRC & Condon, B 2011, 'Assessment of the impact of the scanner-related factors on brain morphometry analysis with Brainvisa.', *BMC medical imaging*, vol. 11, no. 1, p. 23.

Silverstein, PS & Kumar, A 2013, 'HIV-1 and Alcohol: Interactions in the Central Nervous System.', *Alcoholism, clinical and experimental research*.

Sowell, ER, Peterson, BS, Thompson, PM, Welcome, SE, Henkenius, AL & Toga, AW 2003, 'Mapping cortical change across the human life span.', *Nature Neuroscience*, vol. 6, no. 3, pp. 309–15.

Sowell, ER, Thompson, PM, Leonard, CM, Welcome, SE, Kan, E & Toga, AW 2004, 'Longitudinal mapping of cortical thickness and brain growth in normal children.', *The Journal of neuroscience : the official journal of the Society for Neuroscience*, vol. 24, no. 38, pp. 8223–31.

Sowell, ER, Trauner, DA, Gamst, A & Jernigan, TL 2002, 'Development of cortical and subcortical brain structures in childhood and adolescence: A structural MRI study', *Developmental Medicine and Child Neurology*, vol. 44, no. 1, pp. 4–16.

Stampanoni Bassi, M, Iezzi, E, Marfia, GA, Simonelli, I, Musella, A, Mandolesi, G, Fresegna, D, Pasqualetti, P, Furlan, R, Finardi, A, Mataluni, G, Landi, D, Gilio, L, Centonze, D & Buttari, F 2018, 'Platelet-derived growth factor predicts prolonged relapse-free period in multiple sclerosis.', *Journal of neuroinflammation*, vol. 15, Journal of Neuroinflammation, no. 1, p. 108.

Stevens, JP 1992, *Applied multivariate statistics for the social sciences (5th ed.)*, *Routledge/Taylor & Francis Group.*, vol. 43, no. 1.

Strain, MC, Letendre, S, Pillai, SK, Russell, T, Ignacio, CC, Günthard, HF, Good, B, Smith,

DM, Wolinsky, SM, Furtado, M, Marquie-Beck, J, Durelle, J, Grant, I, Richman, DD, Marcotte, T, McCutchan, JA, Ellis, RJ, Wong, JK, Gu, HF, Good, B, Smith, DM, Wolinsky, SM, Furtado, M, Durelle, J, Grant, I, Richman, DD, Marcotte, T, McCutchan, JA, Ellis, RJ, Wong, JK, Günthard, HF, Good, B, Smith, DM, Wolinsky, SM, Furtado, M, Marquie-Beck, J, Durelle, J, Grant, I, Richman, DD, Marcotte, T, McCutchan, JA, Ellis, RJ & Wong, JK 2005, 'Genetic composition of human immunodeficiency virus type 1 in cerebrospinal fluid and blood without treatment and during failing antiretroviral therapy.', *Journal of virology*, vol. 79, no. 3, pp. 1772–88.

Strazza, M, Pirrone, V, Wigdahl, B & Nonnemacher, MR 2011, 'Breaking down the barrier : The effects of HIV-1 on the blood – brain barrier', *Brain Research*, vol. 1399, Elsevier B.V., pp. 96–115.

Sugawara, S, Thomas, DL & Balagopal, A 2019, 'HIV-1 Infection and Type 1 Interferon: Navigating Through Uncertain Waters', *AIDS Research and Human Retroviruses*, vol. 35, no. 1, pp. 25–32.

Tabachnick, BG, Fidell, LS & Ullman, JB 2018, *Using Multivariate Statistics*, *Pearson*, 7th edn.

Tae, WS, Kim, SS, Lee, KU, Nam, E-C & Kim, KW 2008, 'Validation of hippocampal volumes measured using a manual method and two automated methods (FreeSurfer and IBASPM) in chronic major depressive disorder.', *Neuroradiology*, vol. 50, no. 7, pp. 569–81.

Takahashi, K, Wesselingh, SL, Griffin, DE, McArthur, JC, Johnson, RT & Glass, JD 1996, 'Localization of HIV-1 in human brain using polymerase chain reaction/in situ hybridization and immunocytochemistry', *Annals of Neurology*, vol. 39, no. 6, pp. 705–711.

Takemoto, JK, Miller, TL, Wang, J, Jacobson, DL, Geffner, ME, Van Dyke, RB & Gerschenson, M 2017, 'Insulin resistance in HIV-infected youth is associated with decreased mitochondrial respiration', *Aids*, vol. 31, no. 1, pp. 15–23.

Tamula, MAT, Wolters, PL, Walsek, C, Zeichner, S & Civitello, L 2003, 'Cognitive decline with immunologic and virologic stability in four children with human immunodeficiency virus disease.', *Pediatrics*, vol. 112, no. 3 Pt 1, pp. 679–84.

Tardieu, M, Brunelle, F, Raybaud, C, Ball, W, Barret, B, Pautard, B, Lachassine, E, Mayaux, M & Blanche, S 2005, 'Cerebral MR imaging in uninfected children born to HIV-seropositive mothers and perinatally exposed to zidovudine.', *AJNR. American journal of neuroradiology*, vol. 26, no. 4, pp. 695–701.

Tardieu, M, Le Chenadec, J, Persoz, A, Meyer, L, Blanche, S & Mayaux, M-J 2000, 'HIV-1-related encephalopathy in infants compared with children and adults', *Neurology*, vol. 54, no. 5, pp. 1089–1095.

Thompson, PM, Dutton, R a., Hayashi, KM, Lu, A, Lee, SE, Lee, JY, Lopez, OL, Aizenstein, HJ, Toga, AW & Becker, JT 2006, '3D mapping of ventricular and corpus callosum abnormalities in HIV/AIDS.', *NeuroImage*, vol. 31, no. 1, pp. 12–23.

Thompson, PM, Giedd, JN, Woods, RP, MacDonald, D, Evans, AC & Toga, AW 2000, 'Growth patterns in the developing brain detected by using continuum mechanical tensor maps.', *Nature*, vol. 404, no. 6774, pp. 190–3.

Thurman, M, Johnson, S, Acharya, A, Pallikkuth, S, Mahesh, M & Byrareddy, SN 2020, 'Biomarkers of Activation and Inflammation to Track Disparity in Chronological and

Physiological Age of People Living With HIV on Combination Antiretroviral Therapy', *Frontiers in Immunology*, vol. 11, no. October, pp. 1–11.

Tisdall, MD, Hess, AT, Reuter, M, Meintjes, EM, Fischl, B & van der Kouwe, AJW 2012, 'Volumetric navigators for prospective motion correction and selective reacquisition in neuroanatomical MRI.', *Magnetic resonance in medicine*, vol. 68, no. 2, pp. 389–99.

Toich, JTF, Taylor, PA, Holmes, MJ, Gohel, S, Cotton, MF, Dobbels, E, Laughton, B, Little, F, van der Kouwe, AJW, Biswal, B & Meintjes, EM 2018, 'Functional Connectivity Alterations between Networks and Associations with Infant Immune Health within Networks in HIV Infected Children on Early Treatment: A Study at 7 Years', *Frontiers in Human Neuroscience*, vol. 11, no. January, pp. 1–15.

Tornatore, C, Chandra, R, Berger, JR & Major, EO 1994, 'HIV-1 infection of subcortical astrocytes in the pediatric central nervous system.', *Neurology*, vol. 44, no. 3 Pt 1, pp. 481–7.

Tsialios, P, Thrippleton, M, Glatz, A & Pernet, C 2017, 'Evaluation of MRI sequences for quantitative T1 brain mapping', *Journal of Physics: Conference Series*, vol. 931, no. 1, pp. 0–4.

Tyborowska, A, Volman, I, Niermann, HCM, Pouwels, JL, Smeekens, S, Cillessen, AHN, Toni, I & Roelofs, K 2018, 'Early-life and pubertal stress differentially modulate grey matter development in human adolescents', *Scientific Reports*, vol. 8, no. 1, pp. 1–11.

Vannucci, RC, Barron, TF & Vannucci, SJ 2017, 'Development of the Corpus Callosum: An MRI Study', *Developmental Neuroscience*, vol. 39, no. 1–4, pp. 97–106.

Violari, A, Cotton, MF, Gibb, DM, Babiker, AG, Steyn, J, Madhi, SA, Jean-Philippe, P, McIntyre, JA & CHER Study Team 2008, 'Early antiretroviral therapy and mortality among HIV-infected infants.', *The New England journal of medicine*, vol. 359, no. 21, pp. 2233–44.

Wade, BSC, Valcour, VG, Puthanakit, T, Saremi, A, Gutman, BA, Nir, TM, Watson, C, Aurpibul, L, Kosalaraksa, P, Ounchanum, P, Kerr, S, Dumrongpisutikul, N, Visrutaratna, P, Srinakarin, J, Pothisri, M, Narr, KL, Thompson, PM, Ananworanich, J, Paul, RH & Jahanshad, N 2019, 'Mapping abnormal subcortical neurodevelopment in a cohort of Thai children with HIV', *NeuroImage: Clinical*, vol. 23, Elsevier, no. March, p. 101810.

Wahl, A & Al-Harthi, L 2023, 'HIV infection of non-classical cells in the brain', *Retrovirology*, vol. 20, BioMed Central, no. 1, pp. 1–13.

Walot, I, Miller, BL, Chang, L & Mehringer, CM 1996, 'Neuroimaging Findings in Patients with AIDS', *Clinical Infectious Diseases*, vol. 22, no. 6, pp. 906–919.

Walsh, KA, Megyesi, JF, Wilson, JX, Crukley, J, Laubach, VE & Hammond, RR 2004, 'Antioxidant protection from HIV-1 gp120-induced neuroglial toxicity.', *Journal of neuroinflammation*, vol. 1, no. 1, p. 8.

Wang, Z, Yin, X, Ma, M, Ge, H, Lang, B, Sun, H, He, S, Fu, Y, Sun, Y, Yu, X, Zhang, Z, Cui, H, Han, X, Xu, J, Ding, H, Chu, Z, Shang, H, Wu, Y & Jiang, Y 2021, 'IP-10 Promotes Latent HIV Infection in Resting Memory CD4+ T Cells via LIMK-Cofilin Pathway', *Frontiers in Immunology*, vol. 12, no. August, pp. 1–15.

Wedderburn, CJ, Weldon, E, Bertran-Cobo, C, Rehman, AM, Stein, DJ, Gibb, DM, Yeung, S, Prendergast, AJ & Donald, KA 2022, 'Early neurodevelopment of HIV-exposed uninfected children in the era of antiretroviral therapy: a systematic review and meta-analysis', *The Lancet Child and Adolescent Health*, vol. 6, The Author(s). Published by Elsevier Ltd. This is an

Open Access article under the CC BY 4.0 license, no. 6, pp. 393–408.

Wedderburn, CJ, Yeung, S, Rehman, AM, Stadler, JAM, Nhapi, RT, Barnett, W, Myer, L, Gibb, DM, Zar, HJ, Stein, DJ & Donald, KA 2019, 'Neurodevelopment of HIV-exposed uninfected children in South Africa: outcomes from an observational birth cohort study', *The Lancet Child and Adolescent Health*, vol. 3, The Author(s). Published by Elsevier Ltd. This is an Open Access article under the CC BY 4.0 license, no. 11, pp. 803–813.

Westerhausen, R, Luders, E, Specht, K, Ofte, SH, Toga, AW, Thompson, PM, Helland, T & Hugdahl, K 2011, 'Structural and functional reorganization of the corpus callosum between the age of 6 and 8 years', *Cerebral Cortex*, vol. 21, no. 5, pp. 1012–1017.

WHO-UNAIDS 2019, *UNAIDS SOUTH AFRICA 2019 FACTSHEET: HIV and AIDS Estimates*, UNAIDS Report.

— 2020, *WHO UNAIDS - SOUTH AFRICA 2020*.

WHO 2013, 'Consolidated guidelines on the use of antiretroviral drugs for treating and preventing HIV infection: recommendations for a public health approach', *Recommendations for a Public Health Approach*, no. June, p. 272.

WHO UNAIDS & World Health Organisation 2014, *Guidelines on post-exposure prophylaxis for hiv and the use of co-trimoxazole prophylaxis for hiv-related infections among adults, adolescents and children: recommendations for a public health approach*, *WHO UNAIDS*, WHO UNAIDS, no. 2013 consolidated guidelines.

Wiley, C a, Schrier, RD, Nelson, J a, Lampert, PW & Oldstone, MB 1986, 'Cellular localization of human immunodeficiency virus infection within the brains of acquired immune deficiency syndrome patients.', *Proceedings of the National Academy of Sciences of the United States of America*, vol. 83, no. 18, pp. 7089–93.

Williams, ME, Van Rensburg, AJ, Loots, DT, Naudé, PJW & Mason, S 2021, 'Immune Dysregulation Is Associated with Neurodevelopment and Neurocognitive Performance in HIV Pediatric Populations—A Scoping Review', *Viruses*, vol. 13, no. 12.

Woods, RP 2003, 'Multitracer: a Java-based tool for anatomic delineation of grayscale volumetric images', *NeuroImage*, vol. 19, no. 4, pp. 1829–1834.

Woods, RP 2005, *Multitracer Software*, 1, UCLA Laboratory of Neuroimaging, California.

Yadav, SK, Gupta, RK, Garg, RK, Venkatesh, V, Gupta, PK, Singh, AK, Hashem, S, Al-Sulaiti, A, Kaura, D, Wang, E, Marincola, FM & Haris, M 2017, 'Altered structural brain changes and neurocognitive performance in pediatric HIV.', *NeuroImage. Clinical*, vol. 14, The Author(s), no. 9, pp. 316–322.

Yazdanian, M 1999, 'Blood-brain barrier properties of human immunodeficiency virus antiretrovirals.', *Journal of pharmaceutical sciences*, vol. 88, no. 10, pp. 950–4.

Yu, X, Gao, L, Wang, H, Yin, Z, Fang, J, Chen, J, Li, Q, Xu, H & Gui, X 2019, 'Neuroanatomical Changes Underlying Vertical HIV Infection in Adolescents.', *Frontiers in immunology*, vol. 10, no. MAR, p. 814.

Zayas, JP & Mamede, JI 2022, 'HIV Infection and Spread between Th17 Cells', *Viruses*, vol. 14, no. 2.

Zhang, L, Yu, W, He, T, Yu, J, Caffrey, RE, Dalmasso, E a, Fu, S, Pham, T, Mei, J, Ho, JJ, Zhang,

W, Lopez, P & Ho, DD 2002, 'Contribution of human alpha-defensin 1, 2, and 3 to the anti-HIV-1 activity of CD8 antiviral factor.', *Science (New York, N.Y.)*, vol. 298, no. 5595, pp. 995–1000.

Zhang, R, Fichtenbaum, CJ, Hildeman, DA, Lifson, JD & Chougnet, C 2004, 'CD40 Ligand Dysregulation in HIV Infection: HIV Glycoprotein 120 Inhibits Signaling Cascades Upstream of CD40 Ligand Transcription', *The Journal of Immunology*, vol. 172, no. 4, pp. 2678–2686.

Zlokovic, B V. 2008, 'The Blood-Brain Barrier in Health and Chronic Neurodegenerative Disorders', *Neuron*, vol. 57, no. 2, pp. 178–201.

CHAPTER 10 Appendices

10.1 Appendix A: ARV Drugs and Their Action: CHER Trial (Cotton et al. 2013)

First Line ART

Zidovudine (Esposito, Corona & Tramontano 2012; Ghodke et al. 2012)

Zidovudine is a member of the nucleoside analogue reverse transcriptase inhibitors (NRTIs) family. It competes with thymidine triphosphate, a nucleotide that is utilised by reverse transcriptase during conversion from ssRNA to dsDNA, leading to incorporation of zidovudine (which lacks the 3' hydroxyl group) instead of thymidine triphosphate causing chain termination. It inhibits the replication of HIV-1 by causing chain termination.

Lamivudine (Esposito, Corona & Tramontano 2012)

Same as above but competes with cytosine triphosphate instead of thymidine triphosphate. It inhibits the replication of HIV-1 by causing chain termination.

Lopinavir-ritonavir (Bazzoli et al. 2010)

Lopinavir-ritonavir are protease inhibitors, which prevent the cleavage of the precursor proteins by HIV proteases to form activated proteins required in the construction of new virions.

Second Line ART

Didanosine (Esposito, Corona & Tramontano 2012)

Same as Zidovudine, an NRTI, but is an adenine analogue instead of thymidine triphosphate. It inhibits the replication of HIV-1 by causing chain termination.

Abacavir (Esposito, Corona & Tramontano 2012)

Same as Zidovudine but is a guanosine analogue instead of thymidine triphosphate. It inhibits the replication of HIV-1 by causing chain termination.

Nevirapine and Efavirenz (Esposito, Corona & Tramontano 2012)

Both nevirapine and efavirenz are part of the non-nucleoside reverse transcriptase inhibitors (NNRTIs) family. This group noncompetitively binds to a hydrophobic pocket in the reverse transcriptase structure. The pocket is located near the polymerase active site and binding leads to conformational (structural) changes in reverse transcriptase, which in turn inhibits the elongation of DNA during DNA synthesis.

10.2 Appendix B: 5 Year HIV Cross-sectional Article

frontiers in Neuroanatomy

ORIGINAL RESEARCH
published: 02 November 2017
doi: 10.3389/fnana.2017.00095

Larger Subcortical Gray Matter Structures and Smaller Corpora Callosa at Age 5 Years in HIV Infected Children on Early ART

Steven R. Randall[1], Christopher M. R. Warton[1], Martha J. Holmes[2], Mark F. Cotton[3], Barbara Laughton[3], Andre J. W. van der Kouwe[4] and Ernesta M. Meintjes[2]*

[1] Department of Human Biology, Faculty of Health Sciences, University of Cape Town, Cape Town, South Africa, [2] MRC/UCT Medical Imaging Research Unit, Division of Biomedical Engineering, Department of Human Biology, Faculty of Health Sciences, University of Cape Town, Cape Town, South Africa, [3] Children's Infectious Diseases Clinical Research Unit, Department of Paediatrics and Child Health, Tygerberg Children's Hospital & Faculty of Medicine and Health Sciences, Stellenbosch University, Cape Town, South Africa, [4] Athinoula A. Martinos Center for Biomedical Imaging, Massachusetts General Hospital, Charlestown, MA, United States

OPEN ACCESS

Edited by:
Nourla Lakhdar-Ghazal, Faculty of Science, Mohammed V University, Morocco

Reviewed by:
Owen Carmichael, Pennington Biomedical Research Center, United States
Francesco Sammartino, Ohio State University Columbus, United States

***Correspondence:**
Steven R. Randall
srandall884@gmail.com

Received: *30 July 2017*
Accepted: *16 October 2017*
Published: *02 November 2017*

Citation:
Randall SR, Warton CMR, Holmes MJ, Cotton MF, Laughton B, van der Kouwe AJW and Meintjes EM (2017) Larger Subcortical Gray Matter Structures and Smaller Corpora Callosa at Age 5 Years in HIV Infected Children on Early ART. Front. Neuroanat. 11:95. doi: 10.3389/fnana.2017.00095

Sub-Saharan Africa is home to 90% of HIV infected (HIV+) children. Since the advent of antiretroviral therapy (ART), HIV/AIDS has transitioned to a chronic condition where central nervous system (CNS) damage may be ongoing. Although, most guidelines recommend early ART to reduce CNS viral reservoirs, the brain may be more vulnerable to potential neurotoxic effects of ART during the rapid development phase in the first years of life. Here we investigate differences in subcortical volumes between 5-year-old HIV+ children who received early ART (before age 18 months) and uninfected children using manual tracing of Magnetic Resonance Images. Participants included 61 Xhosa children (43 HIV+/18 uninfected, mean age = 5.4 ± 0.3 years, 25 male) from the children with HIV early antiretroviral (CHER) trial; 27 children initiated ART before 12 weeks of age (ART-Before12Wks) and 16 after 12 weeks (ART-After12Wks). Structural images were acquired on a 3T Allegra MRI in Cape Town and manually traced using MultiTracer. Volumetric group differences (HIV+ vs. uninfected; ART-Before12Wks vs. ART-After12Wks) were examined for the caudate, nucleus accumbens (NA), putamen (Pu), globus pallidus (GP), and corpus callosum (CC), as well as associations within infected children of structure volumes with age at ART initiation and CD4/CD8 as a proxy for immune health. HIV+ children had significantly larger NA and Pu volumes bilaterally and left GP volumes than controls, whilst CC was smaller. Bilateral Pu was larger in both treatment groups compared to controls, while left GP and bilateral NA were enlarged only in ART-After12Wks children. CC was smaller in both treatment groups compared to controls, and smaller in ART-After12Wks compared to ART-Before12Wks. Within infected children, delayed ART initiation was associated with larger Pu volumes, effects that remained significant when controlling for sex and duration of treatment interruption (left $\beta = 0.447$, $p = 0.005$; right $\beta = 0.325$, $p = 0.051$), and lower

CD4/CD8 with larger caudates controlling for sex (left $\beta = -0.471$, $p = 0.002$; right $\beta = -0.440$, $p = 0.003$). Volumetric differences were greater in children who initiated ART after 12 weeks. Results suggest damage is ongoing despite early ART and viral load suppression; however, earlier treatment is neuroprotective.

Keywords: HIV/AIDS, antiretroviral, MRI, volumetric segmentation, WM, GM, pediatric

INTRODUCTION

Since the advent of combination antiretroviral (ARV) therapy (ART), human immunodeficiency virus (HIV) infection has become a chronic condition with ongoing damage to the body and central nervous system (CNS), especially in the developing brain of the fetus, infant and young child (van Rie et al., 2007). As CNS penetration by ART is limited, the brain may become a reservoir for the virus, with few drugs available to impact these reservoirs (van Rie et al., 2007). Substantial brain development in the first few years of life puts infected children at greater risk of neurological impairment compared to HIV infected (HIV+) adults (Tardieu et al., 2000; Mitchell, 2001). For example, language functions are more impaired in HIV+ children than in adults (van Rie et al., 2007).

To minimize effects of HIV in children, new guidelines recommend that life-long ART be initiated as soon as possible (WHO, 2013). However, some ARVs can cause neurodevelopmental impairment despite virological suppression in the CNS (Tardieu et al., 2005; van Rie et al., 2007). For example, prenatal exposure to zidovudine has been linked to mitochondrial dysfunction within the CNS (Tardieu et al., 2005), as well as chronic ARV treatment in the form of combination therapy results in abnormal BOLD response within frontal brain regions (Chang et al., 2008). Few studies have examined the long-term neurological effects of HIV infection in children in whom plasma viral loads (VL) are suppressed following early ART (before 18 months of age; Le Doaré et al., 2012; Laughton et al., 2013; Phillips et al., 2016), and very little is known about the complex nature of brain recovery following ART initiation and subsequent brain development (Tamula et al., 2003; Shanbhag et al., 2005; van Rie et al., 2007; Govender et al., 2011; Laughton et al., 2012; Whitehead et al., 2014).

Although neuroimaging can provide insights into the mechanisms underpinning neurobehavioral outcomes in HIV+ children (Hoare et al., 2014; Musielak and Fine, 2016), such studies are rare, even in developed countries, and have typically included children across wide age ranges who either started ART late (Hoare et al., 2015) or some on early ART but small numbers with VL suppression (van Arnhem et al., 2013; Sarma et al., 2014). Studies in children and youths where most (>85%) have suppressed viral loads, and some received early ART, have demonstrated lower global and local cortical and total gray matter (GM) volumes (Cohen et al., 2016; Lewis-de Los Angeles et al., 2017), white matter (WM) alterations (Ackermann et al., 2014, 2016; Andronikou et al., 2014; Uban et al., 2015), and volume reductions (Cohen et al., 2016), both subcortical volume increases and decreases and shape deformations (Lewis-de Los Angeles et al., 2016; Yadav et al., 2017), altered cortical thickness (Yadav et al., 2017), and effects of immunocompromise in infancy on basal ganglia metabolism at 5 years (Mbugua et al., 2016). These findings suggest that HIV- and/or ART-related damage may be irreversible or ongoing.

In this study we compare over a narrow age range (4.9–6.5 years of age) manually traced volumes of select subcortical structures and the corpus callosum in a unique cohort of HIV-infected children, all of whom initiated ART before 76 weeks of age and were followed since birth, to HIV-uninfected children from the same community. This is the first study using gold-standard manual tracing (Morey et al., 2009) to assess structural brain changes in perinatally acquired HIV on early ART (Hoare et al., 2014; Musielak and Fine, 2016). Amongst HIV+ children from this cohort, initiating treatment before 12 weeks showed improved cognitive performance at 11 months and improved overall health compared to starting treatment after 12 weeks (Violari et al., 2008; Laughton et al., 2012; Cotton et al., 2013). We also examined the effect of timing of treatment initiation on volume alterations. We hypothesized that HIV+ children on early treatment would experience similar perturbations observed previously in both children and adults, with neuronal thinning, resulting overall in global atrophy and loss of gray matter and white matter volume. In addition, we hypothesized that earlier treatment would mitigate the effects of HIV and accompanying brain damage leading to smaller reductions in volume in children initiating ART earlier.

MATERIALS AND METHODS

This study included 43 HIV+ Xhosa children from the randomized CHER (Children with HIV early antiretroviral) trial in follow-up at the Children's Infectious Diseases Clinical Research Unit, Tygerberg Children's Hospital, Cape Town (Laughton et al., 2012). As part of the CHER trial, infants with CD4 percentage (CD4%) of at least 25% were randomized to one of the following three treatment arms: ART-Def (ART Deferred until CD4% < 25% in first year or CD4% < 20% thereafter, or if clinical disease progression criteria presented); ART-40W (ART initiated before 12 weeks of age and interrupted after 40 weeks); and ART-96W (ART initiated before 12 weeks of age and interrupted after 96 weeks). ART was restarted in ART-40W and ART-96W for CD4% decline or clinical evidence of disease progression. (Violari et al., 2008; Cotton et al., 2013). One child not adhering to ART was excluded. Since some children in the ART-Def arm met criteria for almost immediate initiation of ART, the children were grouped here based on age at treatment initiation, specifically those who received ART at or before 12 weeks (ART-Before12wks) and those who received

treatment after 12 weeks (ART-After12wks). Of the 27 who received ART before 12 weeks, 9 remained on continuous ART in line with clinical criteria governing interruption. Treatment was interrupted in 18, two of whom had not met ART restart criteria at the time of scan as they remained clinically well with CD4% of at least 20%.

Eighteen HIV uninfected Xhosa children were recruited from an interlinked vaccine trial as controls (Madhi et al., 2010). They comprised 12 HIV exposed uninfected (HEU) children born to HIV+ mothers but who tested HIV negative (PCR) at baseline and 30 days after the third dose of vaccine, and 6 HIV unexposed and uninfected children (HU) born to HIV seronegative mothers (tested after 24 weeks gestation) who remained seronegative at enrolment.

All children received MRI scanning on a 3T Allegra MRI (Siemens, Erlangen, Germany) at the Cape Universities Brain Imaging Centre (CUBIC) according to protocols approved by the Human Research Ethics Committees of the Universities of Cape Town and Stellenbosch. All parents provided written informed consent and all children provided oral assent. High-resolution T1 weighted images were acquired using a volumetric echo-planar imaging (EPI) navigated (Tisdall et al., 2012) multi echo magnetization prepared rapid gradient echo (MEMPRAGE) sequence (van der Kouwe et al., 2008). Imaging parameters were: FOV: 224 × 224 mm^2; 144 sagittal slices, TR: 2,530 ms; TE: 1.53/3.19/4.86/6.53 ms; TI: 1,160 ms; Flip angle: 7°; voxel size: 1.3 × 1.0 × 1.0 mm^3, scan time 5:20 min. The 3D EPI navigator provided real-time motion tracking and correction. BrainVoyager QX software (Brain Innovation, Maastricht) was used to transform DICOM files into the AC-PC plane and rotate images for hemispherical symmetry.

Due to its frequency in the HIV literature, the basal ganglia (**Figure 1A**) was the primary subcortical region of interest (ROI), with the corpus callosum (**Figure 1B**) functioning as the white matter analog. All gray matter structures within the basal ganglia were manually segmented, with the exception of the substantia nigra and subthalamic nuclei. The structures included the caudate head, nucleus accumbens (NA), globus pallidus (GP), and putamen (Pu). All structures were manually traced using MultiTracer software (http://bishopw.loni.ucla.edu/MultiTracer/) on a Lenovo ThinkPad X200 tablet and integrated active digitizer stylus.

All tracings were performed at 4X magnification as further magnification resulted in visible pixelation of the images. Image files were scaled according to the prescribed voxel intensity range (Woods, 2003); the contrast used in this study ranged from Pixel Intensity Units of 13,000 to 18,000 dependent on the structure. Screen brightness for the tracing tablet was set to 100% and brightness of images was set to 1.34 (49% of a maximum unadjusted default scale value of 2.72) for most structures (Woods, 2003).

The contours of selected brain structures were completed by manually outlining the structures on MR images, slice by slice. For standardization purposes, tracing of all subcortical gray matter structures were performed in the coronal plane. Based on this tracing, we present the frust volumes output by MultiTracer. The expert neuroanatomist (SR) who performed all tracings was blinded to all participant data. Inter-rater and intra-rater reliabilities were assessed for each structure using independent measurements for 10 participants who were randomly selected by another expert neuroanatomist (CW) and the primary tracer (SR), respectively, and assessed via Pearson and intra-class correlation.

Data and statistical analyses were performed in IBM SPSS Statistics 23. ANOVA was used to compare structure volumes of uninfected children to infected children, and to children who initiated ART before and after 12 weeks. Additionally, amongst infected children, we used linear regression to examine associations of structure volumes with timing of ART initiation. Since treatment was interrupted in a subset of the children who received ART before 12 weeks and interruption is characterized by a subsequent drop in CD4 cell count and increased VL,

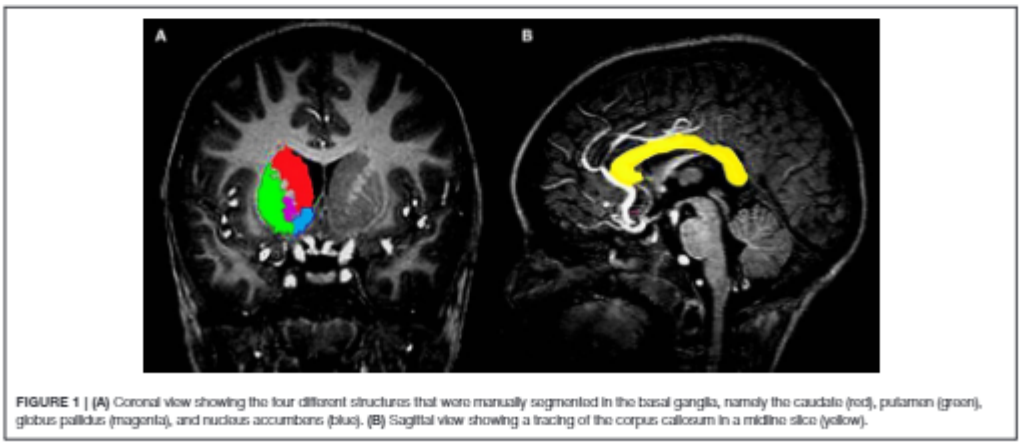

FIGURE 1 | (A) Coronal view showing the four different structures that were manually segmented in the basal ganglia, namely the caudate (red), putamen (green), globus pallidus (magenta), and nucleus accumbens (blue). **(B)** Sagittal view showing a tracing of the corpus callosum in a midline slice (yellow).

which may negate the potential benefits of earlier ART, multiple regression was used to control for duration of interruption. Duration of interruption was set to zero for children in whom treatment was not interrupted. Sex was controlled for in all analyses as it affects brain development (Gur et al., 1999; Gilmore et al., 2007). Finally, to explore whether volume alterations may be due to an inflammatory response, we examined relationships between structure volumes and CD4/CD8 ratio as a proxy for immune health, both at enrolment and at scan. Due to the fact that statistical analyses were repeated for 9 anatomical structures, we indicate for each test which results survive Bonferroni correction ($p < 0.0056$).

Since lower total GM and WM volumes have been reported in HIV+ youths (Cohen et al., 2016; Lewis-de Los Angeles et al., 2017), total intracranial volumes (ICVs) were derived for all children using FreeSurfer (Fischl, 2012) and considered a potential confounder. Additional control variables considered included age at scan and birthweight. Control variables showing group differences were controlled for using analysis of covariance (ANCOVA) and multiple regression.

RESULTS

We present data for 61 Xhosa children (mean age ± s.e. = 5.4 ± 0.04; 25 male). Of 18 uninfected controls, 12 were HEU and 6 HU. Of the 43 infected children, 27 received ART before 12 weeks, and 16 after. Sample characteristics are summarized in **Table 1**. Since uninfected children were slightly older than infected children, and children who received ART before 12 weeks had smaller ICVs than uninfected controls, we controlled for ICV and age at scan in all analyses involving uninfected and infected children. While no children had suppressed VLs at enrolment, VL was suppressed in 93% of infected children at time of scanning. Children receiving ART before and after 12 weeks did not differ on any of the clinical variables. No significant effect of interruption on structure volume was observed, nor did duration of interruption show any relation with structure volumes (all p's > 0.18).

All inter-rater Pearson correlations for manually traced volumes were significant (all p's < 0.05) and ranged from $r = 0.71$ for the left caudate to $r = 0.93$ for the corpus callosum. Cronbach's α's were above 0.8 in all regions. Intra-rater Pearson correlations were greater than $r = 0.82$ (all p's < 0.001), and Cronbach's α's were all above 0.83.

In **Table 2** we compare structure volumes between HIV+ and uninfected children, and in **Figure 2** between uninfected children and children who received ART before and after 12 weeks, controlling for sex, ICV, and age at scan. Infected children showed gray matter (GM) volume increases in left (L) NA, albeit below conventional levels of significance, right (R) NA, bilaterally in Pu, and L GP, effects that appear to be largely attributable to volume increases in children who initiated ART after 12 weeks. In contrast to GM volume increases, CC was smaller in infected children with reductions evident both in children initiating ART before and after 12 weeks. Only in CC did volumes differ significantly between children initiating ART before and after 12 weeks, with the latter showing greater volume reductions compared to uninfected controls than children who initiated ART before 12 weeks. HIV-related volume increases in the Pu and reductions in the CC remain significant after Bonferroni correction for multiple comparisons.

Amongst infected children, increasing age of ART initiation was associated with larger Pu volumes bilaterally (**Figure 3, Table 3**), with the association on the left surviving Bonferroni correction for multiple comparisons. Although caudate volumes did not show any group differences or relation with timing of ART initiation, amongst infected children, lower CD4/CD8 ratio at the time of scanning was associated with caudate volume increases bilaterally (left $r = -0.487$, $p = 0.007$; right $r = -0.469$, $p = 0.001$; **Figure 4**), effects that remained significant when controlling for sex (left $\beta = -0.471$, $p = 0.002$; right $\beta = -0.440$, $p = 0.003$) and adjusting for multiple comparisons. Lower enrolment CD4/CD8 was also weakly associated with greater caudal volumes at age 5 years (left $r = -0.252$ $p = 0.107$; right $r = -0.298$ $p = 0.056$), although these relations did not survive when controlling for sex (left $\beta = -0.217$, $p = 0.201$; right $\beta = -0.226$, $p = 0.172$). No other regions showed association between volumes and immune health at enrolment (all p's > 0.2) or at scan (all p's > 0.5).

DISCUSSION

This is the first study to examine over a narrow age range the impact of HIV on subcortical gray matter and corpus callosum volumes in a cohort of children receiving ART before 18 months of age and VL suppression by 109 weeks in all but three children. In contrast to most previous studies in HIV+ adults and children that reported gray matter atrophy (Tardieu et al., 2000; Crain et al., 2010; Becker et al., 2011; Chang et al., 2011; Cohen et al., 2016; Musielak and Fine, 2016; Lewis-de Los Angeles et al., 2017), we found HIV-related subcortical GM volume increases at 5 years in the left GP and bilaterally in the NA and Pu, but CC reductions. Association of increasing age of ART initiation with greater volumes in the Pu suggest that treatment timing plays a role in these observed volume increases. The fact that both GM and WM volume differences were largest in children who initiated ART after 12 weeks point to greater protection from earlier treatment, which is consistent with the findings from other studies in this cohort (Laughton et al., 2012; Mbugua et al., 2016). The fact that associations of Pu and NA volumes with treatment timing strengthened after adjustment for interruption supports findings from a previous DTI study in the same cohort that found the lowest fractional anisotropy in a region in the corticospinal tract in treatment-interrupted children suggesting that ART interruption may negate the benefit of earlier ART (Ackermann et al., 2016).

Even though most studies in children find cortical and total gray matter atrophy in HIV infection (Cohen et al., 2016; Lewis-de Los Angeles et al., 2017), regional GM volume increases have been reported (Sarma et al., 2014). Although, few studies have examined subcortical volumes specifically, two recent studies reported HIV-related regional subcortical GM increases. Blokhuis et al. (2017) found trend-level Pu increases

TABLE 1 | Sample characteristics.

Biographical Data		Uninfected Controls (n = 18)	HIV infected (n = 43)			F / χ2	p
			Total Infected (n = 43)	ART-Before12Wks (n = 27)	ART-After12Wks (n = 16)		
Sex: Male	n (%)	8 (44)	17 (40)	11 (41)	6 (38)	0.17	0.918
Age: Scan [Yrs][a]	Mean (SD)	6.6 (3.59)	5.4 (3.28)	5.4 (3.20)	5.3 (3.52)	4.61	0.014
	(Range)	(5.1–6.8)	(4.8–6.9)	(5.0–6.9)	(4.9–6.9)		
Birth weight [g]	Mean (SD)	3,108 (842)	3,104 (402)	3,094 (426)	3,122 (360)	0.02	0.883
ICV [mm³][b]	Mean	1.36×10^6	1.27×10^6	1.26×10^6	1.31×10^6	6.66	0.029
	(SD)	(0.11×10^6)	(0.11×10^6)	(0.12×10^6)	(0.08×10^6)		
HIV-INFECTED CLINICAL DATA							
Treatment							
Cumulative Treatment [Wks][c]	Median (IQR)		240.9 (99.0)	236.3 (147.8)	241.4 (204.0)	0.12	0.728
Age at ART Initiation [Yrs][c]	Mean (SD)		1.8.9 (1.6.4)	0.3 (1.8)	3.5.7 (1.6.0)	78.78	<0.001
	(Range)		(0.5–7.5.8)	(0.5–1.2.0)	(1.8.37–7.5.8)		
Age VL Suppression [Yrs]	Median (IQR)		4.3.1 (4.1.4)	3.3.5 (1.6.0)	6.1.9 (3.0.0)	9.71	0.002
	(Range)		(2.9.0–1.6.1.0)	(0.5.–1.0.7.0)	(2.9.0–1.6.1.0)		
Number ART Interrupted	(n)		1.8	1.8	0		
Age at Interruption [Wks][d]	Median (IQR)		6.0.8 (5.4.8)	6.5.8 (5.4.8)	Not interrupted		
	(Range)		(4.6.–1.1.4.6)	(4.6.–1.1.4.6)			
Length of Interruption [Wks][d]	Median (IQR)		4.6.8 (7.4.4)	4.6.8 (7.4.4)			
	(Range)		(1.1.0–2.0.8.1.)	(1.1.0–2.0.8.1.)			
ENROLLMENT[e]							
CD4%	Mean (SD)		3.6 (6)	3.6 (6)	3.7 (7)	0.44	0.511
CD4/CD8 Ratio	Mean (SD)		1.44 (0.78)	1.42 (0.82)	1.45 (0.64)	0.06	0.813
CD4 Count (Cells/mL)	Median (IQR)		1,836 (1,219)	1,693 (1,385)	1,889 (799)	0.23	0.633
CD8 Count (Cells/mL)	Median (IQR)		1,398 (1,284)	1,493 (1,191)	1,397 (1,643)	0.04	0.844
Plasma Viral Load (RNA/ml			Total				
High (≥750,01)	n (%)		23 (53)	12 (44)	11 (81)	2.39	0.122
Low (400–750,000)	n (%)		20 (47)	15 (56)	5 (31)		
S-processes (≤399)	n (%)		0 (0)	0 (0)	0 (0)		
PRESCAN							
Stimulus Scan [Days]	Median (IQR)		28 (31.5)	28 (35.5)	30 (10.5)	0.667	0.327
	(Range)		(0–223)	(0–223)	(0–1.4.5)		
CD4%	Mean (SD)		3.7 (8.02)	3.6 (8)	3.7 (7)	1.24	0.271
CD4/CD8 Ratio	Mean (SD)		1.32 (0.66)	1.32 (0.66)	1.33 (0.48)	0.15	0.702
CD4 Count (Cells/mL)	Median (IQR)		1,029 (677)	1,029 (677)	931 (622)	0.02	0.880
CD8 Count (Cells/mL)	Median (IQR)		1,011 (592)	979 (299)	993 (778)	0.02	0.900
Plasma Viral Load (RNA/ml[f]			Total				
High (≥750,01)	n (%)		1 (2)	0 (0)	1 (6)	1.86	0.378
Low (400–750,000)	n (%)		4 (9)	3 (11)	1 (6)		
S-processes (≤399)	n (%)		38 (88)	24 (89)	14 (88)		

Values are Mean (SD), Median (IQR), number (%).

$\chi 2$ from Kruskal–Wallis ANOVA or categorical Associations; F statistic from Univariate ANOVA for parametric data between treatment groups and controls; ICV, Intracranial Volume; Yrs, Years; Wks, Weeks; g, Grams; mm, millimeters; SD, Standard deviation; IQR, Interquartile Range.

[a] ART-Before12 wks < Uninfected Controls (both $p's < 0.05$).

[b] ART-Before12 wks < Uninfected Controls ($p < 0.01$).

[c] Only including 18 children from the ART-Before12 wks group who were interrupted; 2 had not yet restarted ART at time of scanning.

[d] IQR count at enrolment data missing for 1 ART-After12 wks pt.

[e] Plasma Viral Load Cnt Tests had fewer than 5 cases.

TABLE 2 | Comparison of structure volumes between HIV infected and uninfected children.

ROI (mm^3)	Uninfected Controls ($n = 16$)		HIV infected ($n = 43$)		F	p
	Mean	(*SD*)	Mean	(*SD*)		
L Caudate	4,045	(551)	4,065	(419)	0.312	0.58
R Caudate	4,216	(527)	4,253	(418)	0.904	0.35
L NA	520	(124)	587	(127)	3.587	0.06
R NA	556	(107)	620	(118)	5.205	0.03
CC	470	(71)	357	(65)	19.216	<0.001
L Pu	4,892	(578)	5,246	(516)	15.768	<0.001
R Pu	4,897	(530)	5,272	(518)	18.097	<0.001
L GP	1,804	(166)	1,852	(210)	3.907	0.05
R GP	1,818	(181)	1,816	(215)	2.016	0.16

F-value from Analysis of Covariance adjusted for sex, intracranial volume and age at scan.

TABLE 3 | Associations in infected children of structure volume with age at ART initiation.

ROI	Association with Age at ART Initiation ($n = 43$)					
	r	p	$\beta 1$	p	$\beta 2$	p
L Caudate	0.071	0.651	0.060	0.701	0.193	0.230
R Caudate	0.150	0.336	0.134	0.380	0.227	0.161
L NA	0.272	0.078	0.269	0.085	0.296	0.060
R NA	0.230	0.138	0.235	0.133	0.286	0.091
CC	−0.030	0.847	−0.038	0.808	0.016	0.924
L Pu	0.398	0.007	0.385	0.010	0.447	0.005
R Pu	0.295	0.055	0.288	0.063	0.325	0.051
L GP	0.256	0.098	0.240	0.113	0.233	0.155
R GP	0.209	0.178	0.193	0.204	0.264	0.104

r is the Pearson correlation coefficient; β1 is the standardized regression coefficient adjusted for sex; β2 is the standardized regression coefficient adjusted for sex and duration of interruption.

in HIV+ children, and Yadav and colleagues larger nucleus accumbens and smaller hippocampi (Yadav et al., 2017). The authors postulated inflammatory processes and chronic stress as possible explanations for the volume increases. Putamen hypertrophy in HIV+ adults has also been attributed to possible inflammation and dopaminergic system dysfunction (Castelo et al., 2007). The absence of association of CD4/CD8 ratio, as a marker of immune health, with volumes in regions showing HIV-related increases in our study, suggest that observed volume increases are not necessarily due to inflammatory processes in these specific regions.

Compared to the relative abundance of literature attributing structural atrophy to gliosis and inflammation (Bates et al., 2002; Miller et al., 2002; Mehta et al., 2003; Pekny and Pekna, 2016; Pérez-Cerdá et al., 2016), the mechanisms for pathology-induced hypertrophy of brain structures are not well-understood. Although enlargement of the striatum has been associated with dopaminergic system dysfunction in recreational and antipsychotic drug use (Selemon et al., 1999; Jacobsen et al., 2001; Dazzan et al., 2005; Jernigan et al., 2005), and linked specifically to elevated glial densities in rhesus monkeys administered antipsychotic drugs (Selemon et al., 1999), smaller volume differences in children who initiated ART earlier in our study suggests that the gray matter hypertrophy observed here is not due to gliosis resulting from ART drug interactions. Notably, gray matter hypertrophy has been observed in patients with obstructive sleep apnea (Rosenzweig et al., 2013). Since short-term hypoxic events have been shown to induce reactive gliosis and neuronal death in rats (Aviles-Reyes et al., 2010), ischaemic preconditioning may cause long-lasting neuronal changes within the brain. This may be relevant here as cerebrovascular alterations have been reported in HIV+ children (Shah et al., 1996; Patsalides et al., 2002). Increased metabolic demand in the presence of reactive gliosis (Epstein and Gelbard, 1999; Walsh et al., 2004) and mitochondrial dysfunction in HIV+ children (Tardieu et al., 2005; Crain et al., 2010; Takemoto et al., 2017) may create localized subclinical ischaemic/hypoxic stress within the CNS. Angiogenesis from ischaemic preconditioning may be exacerbated by the *HIV-Tat* gene, a heparin-binding angiogenic growth factor (Das et al., 2016), expressed by infected cells. The exact mechanisms of gray matter hypertrophy in HIV+ children requires further investigation.

Volumetric MRI studies in HIV have mostly relied on automated/semi-automated techniques (Hoare et al., 2014; Sarma et al., 2014; Musielak and Fine, 2016), which typically involve some form of co-registration to a template based on an adult brain, using contrast or other feature discriminators. These techniques may be suboptimal for diagnoses where regional or global brain volumes may be affected, or when examining children. It has been shown that using age-matched pediatric brain templates in pediatric studies lead to considerably different tissue distribution from that obtained with an adult-based template (Yoon et al., 2009). This may explain why previous studies of subcortical volumes using FreeSurfer either failed to detect group differences (Lewis-de Los Angeles et al., 2016), or detected fewer and less significant differences (Blokhuis et al., 2017; Yadav et al., 2017) than in our study. Using FreeSurfer automated segmentation in our cohort, within the gray and white matter structures investigated, there were no significant volumetric differences between groups, apart from the left globus pallidus (GP) which was smaller in infected children (L GP: Mean (*SD*): HIV 1,775 ± 192 mm^3, controls 1,949 ± 255 mm^3, $F = 7.848$, $p = 0.007$), and the CC that tended to be larger (HIV 469 ± 89 mm^3, controls 431 ± 68 mm^3, $F = 2.871$, $p = 0.096$). In both structures, the findings were opposite to those generated using manual segmentation, indicating that automated methods may be inappropriate for pediatric populations, especially in the presence of pathology, and that manual segmentation may be more sensitive to detect subtle changes.

The highest concentration of HIV is observed in the caudate nuclei and CC (Thompson et al., 2006; Ances et al., 2012), possibly due to their proximity to the ventricles. The proximity of these structures to the ventricles, and thus CSF, allows for easier penetration of HIV-infected mononuclear cells permitting higher concentrations of HIV toxins in these sites (Oster et al., 1993; McClernon et al., 2001; Thompson et al., 2006; Kumar et al., 2007; Ances et al., 2012; Andronikou et al., 2014). This would

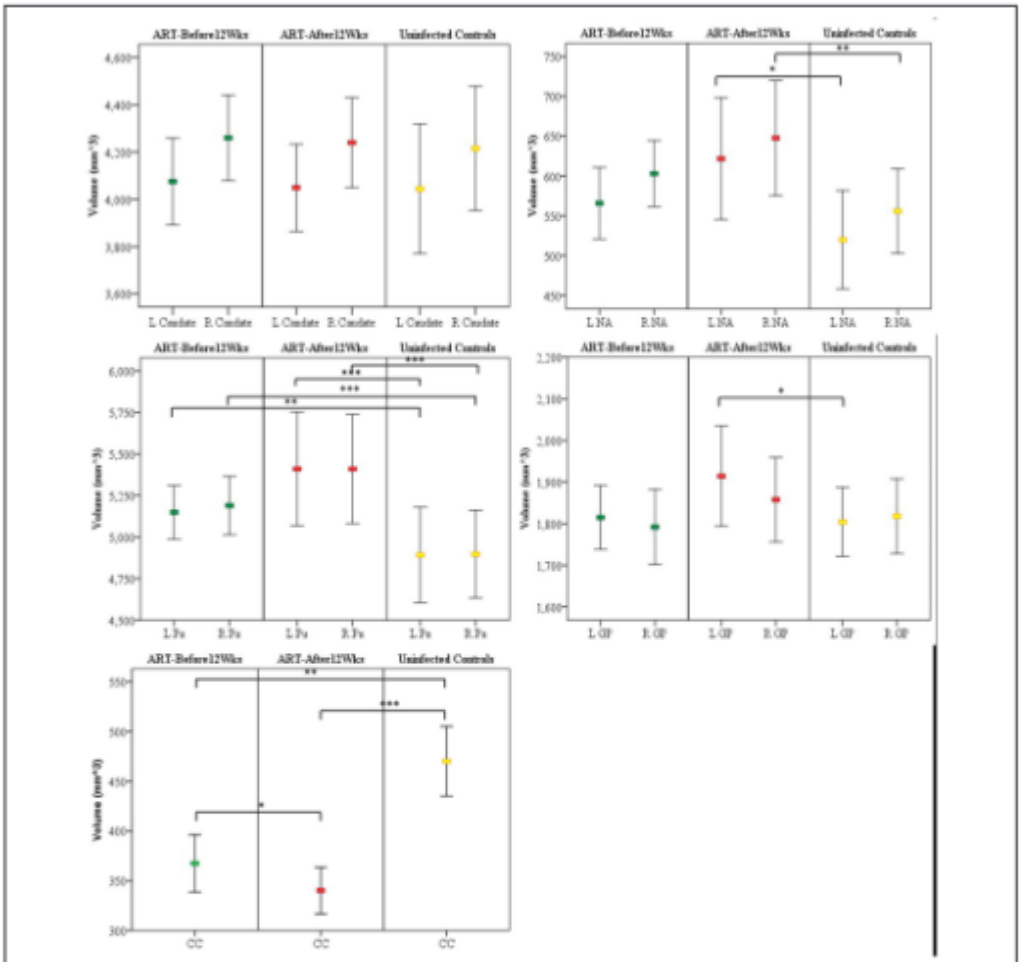

FIGURE 2 | Mean and confidence interval of structure volumes in children who initiated ART before and after 12 weeks and uninfected controls. Volumes were compared using ANCOVA adjusted for sex, intracranial volume, and age at scan. **(A)** Caudate **(B)** nucleus accumbens (NA) **(C)** Putamen (Pu) **(D)** Globus pallidus (GP) **(E)** Corpus callosum (CC) (L, left; R, right); $^{*}p < 0.05$, $^{**}p < 0.01$, $^{***}p < 0.001$.

in turn also apply to certain ARVs that more readily permeate through the blood-brain-barrier (BBB) and pass within the CSF to these sites. As such, location may explain the association seen in the left and right caudate with CD4/CD8 ratio at the time of scanning as a measure of immune health in which the more immunocompromised children at the time of scan had larger caudate volumes bilaterally. This relationship, which survives correction for multiple comparisons, suggests that at this age the caudate is particularly susceptible to the concurrent immune state.

Due to their greater distance from the ventricles, the Pu and NA may be less readily penetrated by the HIV-infected mononuclear cells. However, higher cerebral blood flow of these areas have been observed in HIV+ children (Blokhuis et al., 2017). Another hypothesis may be that once HIV invades the area and viral infection spreads, removal of metabolic waste

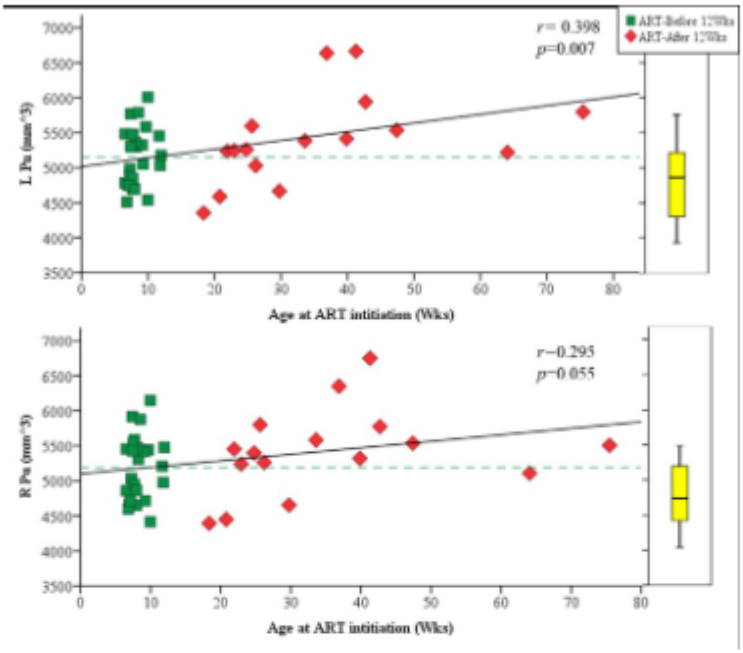

FIGURE 3 | Plots showing the association of volume in the left **(Top)** and right **(Bottom)** putamen with age of ART initiation. The box plot on the right indicates the median volume and IQR for uninfected controls in the same age range as the infected children.

and virions may be slower in these structures compared to the caudate. This may explain the larger Pu and NA observed in HIV+ children. Thus, presence of inflammation in the form of reactive gliosis and leukocyte infiltration, resulting in slightly increased structure size, may be because of prolonged HIV exposure in the Pu and NA rather than a present acute, transient, and compromised immunological state, as in the left and right caudate.

Our finding of reduced CC volume in HIV infection is consistent with that of most previous studies (Thompson et al., 2006; Chiang et al., 2007; Hasan et al., 2009; Dewey et al., 2010; Heaps et al., 2012; Hoare et al., 2012; Sarma et al., 2014; Yadav et al., 2017), although CC volume and thickness were similar to those in controls in a study by Andronikou et al. (2015) including infected children from the same cohort studied here. In our study, the largest volume difference between infected and uninfected children was observed in the CC, with the CC of HIV+ children being on average 24% smaller at 5 years of age than in their uninfected counterparts. Thompson et al. (2006), who similarly found a 25% decrease in the thickness of the CC in HIV+ adults compared to uninfected controls (Thompson et al., 2006), postulated that the overall thickness of the CC is impacted by the loss of peripheral WM. It has been suggested that callosal thickness and volume may be used as biomarkers of overall global WM integrity (Thompson et al., 2006; Andronikou et al., 2014). However, DTI in children from the same cohort studied here revealed no differences in WM integrity between infected and uninfected children in the CC at 5 years of age (Ackermann et al., 2016), despite volume reductions. Since DTI analyses involve co-registration to a template before performing voxel wise statistical comparisons, DTI outcomes would not be impacted by volume differences. As such, making inferences regarding microstructural integrity from macrostructural data may be inappropriate.

The clinical manifestations of HIV infection in these children do not paint a clear picture of causation. VL was suppressed (≤399 RNA/ml) in 93% of children at time of scanning. A previous study in 128 perinatally infected children, who were born prior to the adoption of preventative treatment or ART guidelines, found that 21% showed characteristic evidence of HIV infection induced encephalopathy, despite at least 74% of these children having VL suppression at the time of diagnosis (Cooper et al., 1998). Findings of VL suppression in plasma may, however, not be representative of the compartmentalized and unique viral reservoirs in the CNS (Strain et al., 2005; Pillai et al., 2006). Further, there could be ongoing effects from damage or

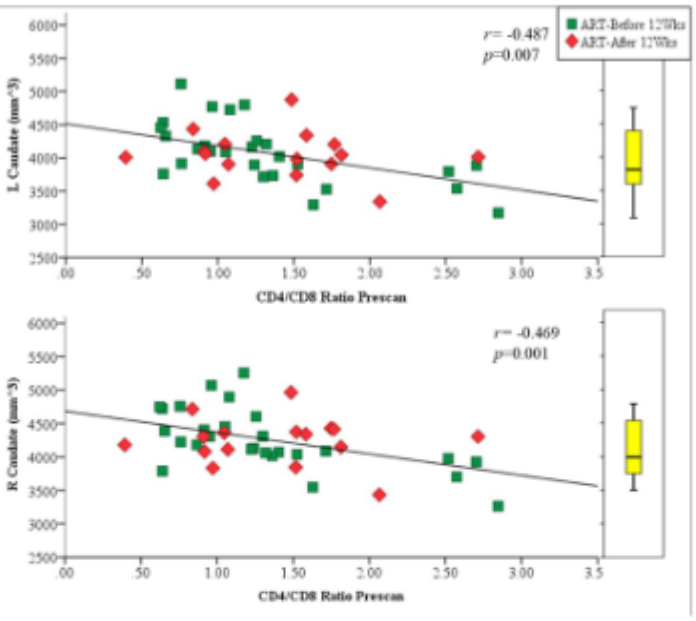

FIGURE 4 | Association of left **(Top)** and right **(Bottom)** caudal volumes with CD4/CD8 ratio at scan as a proxy for immune health. The box plot indicates the distribution of caudate volumes in healthy uninfected controls, excluding the 6 children older than 6 years to match the age range of the uninfected children.

delayed development arising during the initial phases of HIV invasion, prior to ART initiation, which may have occurred *in utero* in some participants. In our study, all HIV+ treatment groups had elevated VL at study entry (7 weeks of age) thus possibly facilitating HIV entry into the CNS early on (Ivey et al., 2009). Neuroinvasion by HIV can occur as early as the initial 10 days post-infection (Lackner et al., 1994). Early ART administered at around 8.4 ± 1.6 weeks of age is perhaps too late for individuals already experiencing high viral loads. Damage to the basal ganglia, and thus corpus striatum is dictated by the rate of initial insult (Brouwers et al., 2000; Becker et al., 2011). This may be evidenced by our observation of CD4/CD8 ratio at enrolment showing weak trend-like association with the size of the left and right caudate. This ties in with spectroscopy findings involving the same cohort at the same age, where basal ganglia metabolite levels (choline, NAA) were associated with CD4/CD8 at enrolment, suggesting that early infiltration and damage caused by HIV persists into early childhood (Mbugua et al., 2016). A confounding issue here may be the duration of ART itself. A trend of duration of ART with prefrontal CC thickness was observed in this cohort previously (Ackermann et al., 2014; Andronikou et al., 2014). It has also been shown that ART decreases motor and working memory performance in both children and adults (von Giesen et al., 2003; Chang et al., 2008; Laughton et al., 2012) which suggests that there may be some complicated interplay between the benefits and risks associated with early ART.

A limitation to the study is the inclusion of total ICV calculated using FreeSurfer automated methods. Intrinsically, using an automated measure to standardize manually derived volumes may add to inaccuracies (Morey et al., 2009; Yoon et al., 2009; Dewey et al., 2010; Narayanan et al., 2016). However, our results do not change significantly without the inclusion of ICV. In addition, a limitation in sampling bias may exist. As the HIV+ Xhosa children formed part of a longitudinal cohort followed since birth with regular follow-up visits to the clinic, it is possible that they are at an added advantage as they could be receiving better health care than the normal standard community care, despite standardized treatment as per the current WHO guidelines. These children also received neuropsychological and behavioral testing giving them additional opportunities for individual case specific and HIV-related support. Children who maintained participation may also have nuanced home environments which allowed them to continue longitudinally.

Overall findings of this study suggest that perinatal HIV infection targets select structures of the basal ganglia, and that these effects are observable at 5 years of age despite early ART and VL suppression. In HIV+ children, both the NA and Pu are enlarged bilaterally, as well as the left GP. In contrast, the CC is smaller compared to uninfected children. Our results suggest

that earlier treatment is neuroprotective. Early therapy before severe viral replication would be advantageous, as evidenced by increased structure size of the bilateral Pu with increased delay to initiate ART.

AUTHOR CONTRIBUTIONS

SR, CW, and EM designed this study and developed the methodology. SR, MH, and EM drafted the manuscript. EM, AvdK, and BL are Principal Investigators. AvdK provided Technical expertise and data processing. SR conducted manual segmentation and performed statistical analyses. CW trained SR in manual segmentation protocol and conducted initial inter-rater reliabilities. MC and BL offered clinical expertise, and monitored and collected clinical data of participants longitudinally. All authors contributed to the manuscript and revised it critically.

ACKNOWLEDGMENTS

We thank the participants and their parents for being willing to take part in this study and research assistants Lunges Khethelo and Thandiwe Hamana for their expertise in supporting the children during neuroimaging, and Stevie Bifen for Inter-rater segmentation.

This work was supported by NIH grants R01HD071664, R21MH096559, and R21MH108346; South African Medical Research Council (SAMRC); South African National Research Foundation (NRF) grants CPR20110614000019421 and CPRR150723129691; and the NRF/DST South African Research Chairs Initiative. Support for the CHER study, which provided the infrastructure for the neurodevelopmental substudy, was provided by the US National Institute of Allergy and Infectious Diseases through the CIPRA network, Grant U19 AI53217; the Departments of Health of the Western Cape and Gauteng, South Africa; and GlaxoSmithKline/Viiv Healthcare. Additional support was provided with Federal funds from the National Institute of Allergy and Infectious Diseases, National Institutes of Health, United States Department of Health and Human Services, under Contract No. HHSN272200800014C.

Permission to conduct the substudy on this cohort was granted by Doctors Avy Violari, Shabir Madhi, and Mark Cotton and the CHER steering committee.

REFERENCES

Ackermann, C., Andronikou, S., Laughton, B., Kidd, M., Dobbels, E., Innes, S., et al. (2014). White matter signal abnormalities in children with suspected HIV-related neurologic disease on early combination antiretroviral therapy. *Pediatr. Infect. Dis. J.* 33, e207–e212. doi: 10.1097/INF.0000000000000288

Ackermann, C., Andronikou, S., Saleh, M. G., Laughton, B., Alhamud, A. A., van der Kouwe, A., et al. (2016). Early antiretroviral therapy in hiv-infected children is associated with diffuse white matter structural abnormality and corpus callosum sparing. *Am. J. Neuroradiol.* 37, 2363–2369. doi: 10.3174/ajnr.A4921

Ances, B. M., Ortega, M., Vaida, F., Heaps, J., and Paul, R. (2012). Independent effects of HIV, aging, and HAART on brain volumetric measures. *J. Acquir. Immune Defic. Syndr.* 59, 469–477. doi: 10.1097/QAI.0b013e318249db17

Andronikou, S., Ackermann, C., Laughton, B., Cotton, M., Tomazos, N., Spottiswoode, B., et al. (2014). Correlating brain volume and callosal thickness with clinical and laboratory indicators of disease severity in children with HIV-related brain disease. *Childs Nerv. Syst.* 30, 1549–1557. doi: 10.1007/s00381-014-2434-3

Andronikou, S., Ackermann, C., Laughton, B., Cotton, M., Tomazos, N., Spottiswoode, B., et al. (2015). Corpus callosum thickness on mid-sagittal MRI as a marker of brain volume: a pilot study in children with HIV-related brain disease and controls. *Pediatr. Radiol.* 45, 1016–1025. doi: 10.1007/s00247-014-3255-y

Aviles-Reyes, R. X., Angelo, M. F., Villarreal, A., Rios, H., Lazarowski, A., and Ramos, A. J. (2010). Intermittent hypoxia during sleep induces reactive gliosis and limited neuronal death in rats: implications for sleep apnea. *J. Neurochem.* 112, 854–869. doi: 10.1111/j.1471-4159.2009.06535.x

Bates, K. A., Fonte, J., Robertson, T. A., Martins, R. N., and Harvey, A. R. (2002). Chronic gliosis triggers Alzheimer's disease-like processing of amyloid precursor protein. *Neuroscience* 113, 785–796. doi: 10.1016/S0306-4522(02)00230-0

Becker, J. T., Sanders, J., Madsen, S. K., Ragin, A., Kingsley, L., Maruca, V., et al. (2011). Subcortical brain atrophy persists even in HAART-regulated HIV disease. *Brain Imaging Behav.* 5, 77–85. doi: 10.1007/s11682-011-9113-8

Blokhuis, C., Mutsaerts, H. J. M. M., Cohen, S., Scherpbier, H. J., Caan, M. W. A., Majoie, C. B. L. M., et al. (2017). Higher subcortical and white matter cerebral blood flow in perinatally HIV-infected children. *Medicine* 96:e5891. doi: 10.1097/MD.0000000000005891

Brouwers, P., Civitello, L., DeCarli, C., Wolters, P., and Sei, S. (2000). Cerebrospinal fluid viral load is related to cortical atrophy and not to intracerebral calcifications in children with symptomatic HIV disease. *J. Neurovirol.* 6, 390–397. doi: 10.3109/13550280009018303

Castelo, J. M. B., Courtney, M. G., Melrose, R. J., and Stern, C. E. (2007). Putamen hypertrophy in nondemented patients with human immunodeficiency virus infection and cognitive compromise. *Arch. Neurol.* 64, 1275–1280. doi: 10.1001/archneur.64.9.1275

Chang, L., Andres, M., Sadino, J., Jiang, C. S., Nakama, H., Miller, E., et al. (2011). Impact of apolipoprotein E ε4 and HIV on cognition and brain atrophy: antagonistic pleiotropy and premature brain aging. *Neuroimage* 58, 1017–1027. doi: 10.1016/j.neuroimage.2011.07.010

Chang, L., Yakupov, R., Nakama, H., Stokes, B., and Ernst, T. (2008). Antiretroviral treatment is associated with increased attentional load-dependent brain activation in HIV patients. *J. Neuroimmune Pharmacol.* 3, 95–104. doi: 10.1007/s11481-007-9092-0

Chiang, M.-C., Dutton, R. A., Hayashi, K. M., Lopez, O. L., Aizenstein, H. J., Toga, A. W., et al. (2007). 3D pattern of brain atrophy in HIV/AIDS visualized using tensor-based morphometry. *Neuroimage* 34, 44–60. doi: 10.1016/j.neuroimage.2006.08.030

Cohen, S., Caan, M. W. A., Mutsaerts, H.-J., Scherpbier, H. J., Kuijpers, T. W., Reiss, P., et al. (2016). Cerebral injury in perinatally HIV-infected children compared to matched healthy controls. *Neurology* 86, 19–27. doi: 10.1212/WNL.0000000000002209

Cooper, E. R., Hanson, C., Diaz, C., Mendez, H., Abboud, R., Nugent, R., et al. (1998). Encephalopathy and progression of human immunodeficiency virus disease in a cohort of children with perinatally acquired human immunodeficiency virus infection. Women and infants transmission study group. *J. Pediatr.* 132, 808–812. doi: 10.1016/S0022-3476(98)70308-7

Cotton, M. F., Violari, A., Otwombe, K., Panchia, R., Dobbels, E., Rabie, H., et al. (2013). Early time-limited antiretroviral therapy versus deferred therapy in South African infants infected with HIV: results from the children with HIV early antiretroviral (CHER) randomised trial. *Lancet* 382, 1555–1563. doi: 10.1016/S0140-6736(13)61409-9

Crain, M. J., Chernoff, M. C., Oleske, J. M., Brogly, S. B., Malee, K. M., Borum, P. R., et al. (2010). Possible mitochondrial dysfunction and its association with antiretroviral therapy use in children perinatally infected with HIV. *J. Infect. Dis.* 202, 291–301. doi: 10.1086/653497

Das, J. R., Gutkind, J. S., and Ray, P. E. (2016). Circulating fibroblast growth factor-2, HIV-Tat, and vascular endothelial cell growth factor-A in HIV-infected children with renal disease activate Rho-A and Src in cultured renal endothelial cells. *PLoS ONE* 11:e0153837. doi: 10.1371/journal.pone.0153837

Dazzan, P., Morgan, K. D., Orr, K., Hutchinson, G., Chitnis, X., Suckling, J., et al. (2005). Different effects of typical and atypical antipsychotics on grey matter in first episode psychosis: the AESOP study. *Neuropsychopharmacology* 30, 765–774. doi: 10.1038/sj.npp.1300603

Dewey, J., Hana, G., Russell, T., Price, J., McCaffrey, D., Harezlak, J., et al. (2010). Reliability and validity of MRI-based automated volumetry software relative to auto-assisted manual measurement of subcortical structures in HIV-infected patients from a multisite study. *Neuroimage* 51, 1334–1344. doi: 10.1016/j.neuroimage.2010.03.033

Epstein, L. G., and Gelbard, H. A. (1999). HIV-1-induced neuronal injury in the developing brain. *J. Leukoc. Biol.* 65, 453–457.

Fischl, B. (2012). FreeSurfer. *Neuroimage* 62, 774–781. doi: 10.1016/j.neuroimage.2012.01.021

Gilmore, J. H., Lin, W., Prastawa, M. W., Looney, C. B., Vetsa, Y. S. K., Knickmeyer, R. C., et al. (2007). Regional gray matter growth, sexual dimorphism, and cerebral asymmetry in the neonatal brain. *J. Neurosci.* 27, 1255–1260. doi: 10.1523/JNEUROSCI.3339-06.2007

Govender, R., Eley, B., Walker, K., Petersen, R., and Wilmshurst, J. M. (2011). Neurologic and neurobehavioral sequelae in children with human immunodeficiency virus (HIV-1) infection. *J. Child Neurol.* 26, 1355–1364. doi: 10.1177/0883073811405203

Gur, R. C., Turetsky, B. I., Matsui, M., Yan, M., Bilker, W., Hughett, P., et al. (1999). Sex differences in brain gray and white matter in healthy young adults: correlations with cognitive performance. *J. Neurosci.* 19, 4065–4072.

Hasan, K. M., Kamali, A., Iftikhar, A., Kramer, L., Papanicolaou, A. C., Fletcher, J. M., et al. (2009). Diffusion tensor tractography quantification of the human corpus callosum fiber pathways across the lifespan. *Brain Res.* 1249, 91–100. doi: 10.1016/j.brainres.2008.10.026

Heaps, J. M., Joska, J., Hoare, J., Ortega, M., Agrawal, A., Seedat, S., et al. (2012). Neuroimaging markers of human immunodeficiency virus infection in South Africa. *J. Neurovirol.* 18, 151–156. doi: 10.1007/s13365-012-0090-5

Hoare, J., Fouche, J.-P., Phillips, N., Joska, J. A., Paul, R., Donald, K. A., et al. (2015). White matter micro-structural changes in ART-naive and ART-treated children and adolescents infected with HIV in South Africa. *AIDS* 29, 1793–1801. doi: 10.1097/QAD.0000000000000766

Hoare, J., Fouche, J.-P., Spottiswoode, B., Donald, K., Philipps, N., Bezuidenhout, H., et al. (2012). A diffusion tensor imaging and neurocognitive study of HIV-positive children who are HAART-naïve "slow progressors". *J. Neurovirol.* 18, 205–212. doi: 10.1007/s13365-012-0099-9

Hoare, J., Ransford, G. L., Phillips, N., Amos, T., Donald, K., and Stein, D. J. (2014). Systematic review of neuroimaging studies in vertically transmitted HIV positive children and adolescents. *Metab. Brain Dis.* 29, 221–229. doi: 10.1007/s11011-013-9456-5

Ivey, N. S., MacLean, A. G., and Lackner, A. A. (2009). Acquired immunodeficiency syndrome and the blood-brain barrier. *J. Neurovirol.* 15, 111–122. doi: 10.1080/13550280902769764

Jacobsen, L. K., Giedd, J. N., Gottschalk, C., Kosten, T. R., and Krystal, J. H. (2001). Quantitative morphology of the caudate and putamen in patients with cocaine dependence. *Am. J. Psychiatry* 158, 486–489. doi: 10.1176/appi.ajp.158.3.486

Jernigan, T. L., Gamst, A. C., Archibald, S. L., Fennema-Notestine, C., Mindt, M. R., Marcotte, T. D., et al. (2005). Effects of methamphetamine dependence and HIV infection on cerebral morphology. *Am. J. Psychiatry* 162, 1461–1472. doi: 10.1176/appi.ajp.162.8.1461

Kumar, A. M., Borodowsky, I., Fernandez, B., Gonzalez, L., and Kumar, M. (2007). Human immunodeficiency virus type 1 RNA Levels in different regions of human brain: quantification using real-time reverse transcriptase-polymerase chain reaction. *J. Neurovirol.* 13, 210–224. doi: 10.1080/13550280701327038

Lackner, A. A., Vogel, P., Ramos, R. A., Kluge, J. D., and Marthas, M. (1994). Early events in tissues during infection with pathogenic (SIVmac239) and nonpathogenic (SIVmac1A11) molecular clones of simian immunodeficiency virus. *Am. J. Pathol.* 145, 428–439.

Laughton, B., Cornell, M., Boivin, M., and Van Rie, A. (2013). Neurodevelopment in perinatally HIV-infected children: a concern for adolescence. *J. Int. AIDS Soc.* 16:18603. doi: 10.7448/IAS.16.1.18603

Laughton, B., Cornell, M., Grove, D., Kidd, M., Springer, P. E., Dobbels, E., et al. (2012). Early antiretroviral therapy improves neurodevelopmental outcomes in infants. *AIDS* 26, 1685–1690. doi: 10.1097/QAD.0b013e328355d0ce

Le Doaré, K., Bland, R., and Newell, M.-L. (2012). Neurodevelopment in children born to HIV-infected mothers by infection and treatment status. *Pediatrics* 130, e1326–e1344. doi: 10.1542/peds.2012-0405

Lewis-de Los Angeles, C. P., Alpert, K. I., Williams, P. L., Malee, K., Huo, Y., Csernansky, J. G., et al. (2016). Deformed subcortical structures are related to past HIV disease severity in youth with perinatally acquired HIV infection. *J. Pediatric Infect. Dis. Soc.* 5, S6–S14. doi: 10.1093/jpids/piw051

Lewis-de Los Angeles, C. P., Williams, P. L., Huo, Y., Wang, S. D., Uban, K. A., Herting, M. M., et al. (2017). Lower total and regional grey matter brain volumes in youth with perinatally-acquired HIV infection: associations with HIV disease severity, substance use, and cognition. *Brain. Behav. Immun.* 62, 100–109. doi: 10.1016/j.bbi.2017.01.004

Madhi, S. A., Adrian, P., Cotton, M. F., McIntyre, J. A., Jean-Philippe, P., Meadows, S., et al. (2010). Effect of HIV infection status and anti-retroviral treatment on quantitative and qualitative antibody responses to pneumococcal conjugate vaccine in infants. *J. Infect. Dis.* 202, 355–361. doi: 10.1086/653704

Mbugua, K. K., Holmes, M. J., Cotton, M. F., Ratai, E.-M., Little, F., Hess, A. T., et al. (2016). HIV-associated CD4+/CD8+ depletion in infancy is associated with neurometabolic reductions in the basal ganglia at age 5 years despite early antiretroviral therapy. *AIDS* 30, 1353–1362. doi: 10.1097/QAD.0000000000001082

McClernon, D. R., Lanier, R., Gartner, S., Feaser, P., Pardo, C., a, Si Clair, M., et al. (2001). HIV in the brain: RNA levels and patterns of zidovudine resistance. *Neurology* 57, 1396–1401. doi: 10.1212/WNL.57.8.1396

Mehta, S., Grabowski, T. J., Trivedi, Y., and Damasio, H. (2003). Evaluation of voxel-based morphometry for focal lesion detection in individuals. *Neuroimage* 20, 1438–1454. doi: 10.1016/S1053-8119(03)00377-X

Miller, D. H., Barkhof, F., Frank, J. A., Parker, G. J. M., and Thompson, A. J. (2002). Measurement of atrophy in multiple sclerosis: pathological basis, methodological aspects and clinical relevance. *Brain* 125, 1676–1695. doi: 10.1093/brain/awf177

Mitchell, W. (2001). Neurological and developmental effects of HIV and AIDS in children and adolescents. *Ment. Retard. Dev. Disabil. Res. Rev.* 7, 211–216. doi: 10.1002/mrdd.1029

Morey, R. A., Petty, C. M., Xu, Y., Hayes, J. P., Wagner, H. R., Lewis, D. V., et al. (2009). A comparison of automated segmentation and manual tracing for quantifying hippocampal and amygdala volumes. *Neuroimage* 45, 855–866. doi: 10.1016/j.neuroimage.2008.12.033

Mustelak, K. A., and Fine, J. G. (2016). An updated systematic review of neuroimaging studies of children and adolescents with perinatally acquired HIV. *J. Pediatr. Neuropsychol.* 2, 34–49. doi: 10.1007/s40817-015-0009-1

Narayanan, P. L., Warton, C., Rosella Boonzaier, N., Molteno, C. D., Joseph, J., Jacobson, J. L., et al. (2016). Improved segmentation of cerebellar structures in children. *J. Neurosci. Methods* 262, 1–13. doi: 10.1016/j.jneumeth.2015.12.010

Oster, S., Christoffersen, P., Gundersen, H. J. G., Nielsen, J. O., Pakkenberg, B., and Pedersen, C. (1993). Cerebral atrophy in AIDS: a stereological study. *Acta Neuropathol.* 85, 617–622. doi: 10.1007/BF00334671

Patsalides, A. D., Wood, L. V., Atac, G. K., Sandifer, E., Butman, J. A., and Patronas, N. J. (2002). Cerebrovascular disease in HIV-infected pediatric patients: neuroimaging findings. *J. Roentgenol.* 179, 999–1003. doi: 10.2214/ajr.179.4.1790999

Pekny, M., and Pekna, M. (2016). Reactive gliosis in the pathogenesis of CNS diseases. *Biochim. Biophys. Acta Mol. Basis Dis.* 1862, 483–491. doi: 10.1016/j.bbadis.2015.11.014

Pérez-Cerdá, F., Sánchez-Gómez, M. V., and Matute, C. (2016). The link of inflammation and neurodegeneration in progressive multiple sclerosis. *Mult. Scler. Demyelinating Disord.* 1:9. doi: 10.1186/s40893-016-0012-0

Phillips, N., Amos, T., Kuo, C., Hoare, J., Ipser, J., Thomas, K. G. F., et al. (2016). HIV-associated cognitive impairment in perinatally infected children: a meta-analysis. *Pediatrics* 138, e20160893–e20160893. doi: 10.1542/peds.2016-0893

Pillai, S. K., Pond, S. L. K., Liu, Y., Good, B. M., Strain, M. C., Ellis, R. J., et al. (2006). Genetic attributes of cerebrospinal fluid-derived HIV-1 env. *Brain* 129, 1872–1883. doi: 10.1093/brain/awl136

Rosenzweig, I., Kempton, M. J., Crum, W. R., Glasser, M., Milosevic, M., Beniczky, S., et al. (2013). Hippocampal hypertrophy and sleep

apnea: a role for the ischemic preconditioning? *PLoS ONE* 8:e83173. doi: 10.1371/journal.pone.0083173

Sarma, M. K., Nagarajan, R., Keller, M. A., Kumar, R., Nielsen-Saines, K., Michalik, D. E., et al. (2014). Regional brain gray and white matter changes in perinatally HIV-infected adolescents. *Neuroimage Clin.* 4, 29–34. doi: 10.1016/j.nicl.2013.10.012

Selemon, L. D., Lidow, M. S., and Goldman-Rakic, P. S. (1999). Increased volume and glial density in primate prefrontal cortex associated with chronic antipsychotic drug exposure. *Biol. Psychiatry* 46, 161–172. doi: 10.1016/S0006-3223(99)00113-4

Shah, S. S., Zimmerman, R., a, Rorke, L. B., and Verzina, L. G. (1996). Cerebrovascular complications of HIV in children. *Am. J. Neuroradiol.* 17, 1913–1917.

Shanbhag, M. C., Rutstein, R. M., Zaoutis, T., Zhao, H., Chao, D., and Radcliffe, J. (2005). Neurocognitive functioning in pediatric human immunodeficiency virus infection: effects of combined therapy. *Arch. Pediatr. Adolesc. Med.* 159, 651–656. doi: 10.1001/archpedi.159.7.651

Strain, M. C., Letendre, S., Pillai, S. K., Russell, T., Ignacio, C. C., Günthard, H. F., et al. (2005). Genetic composition of human immunodeficiency virus type 1 in cerebrospinal fluid and blood without treatment and during failing antiretroviral therapy. *J. Virol.* 79, 1772–1788. doi: 10.1128/JVI.79.3.1772-1788.2005

Takemoto, J. K., Miller, T. L., Wang, J., Jacobson, D. L., Geffner, M. E., Van Dyke, R. B., et al. (2017). Insulin resistance in HIV-infected youth is associated with decreased mitochondrial respiration. *AIDS* 31, 15–23. doi: 10.1097/QAD.0000000000001299

Tamula, M. A. T., Wolters, P. L., Walsek, C., Zeichner, S., and Civitello, L. (2003). Cognitive decline with immunologic and virologic stability in four children with human immunodeficiency virus disease. *Pediatrics* 112, 679–684. doi: 10.1542/peds.112.3.679

Tardieu, M., Brunelle, F., Raybaud, C., Ball, W., Barret, B., Pautard, B., et al. (2005). Cerebral MR imaging in uninfected children born to HIV-seropositive mothers and perinatally exposed to zidovudine. *Am. J. Neuroradiol.* 26, 695–701.

Tardieu, M., Le Chenadec, J., Persoz, A., Meyer, L., Blanche, S., and Mayaux, M.-J. (2000). HIV-1-related encephalopathy in infants compared with children and adults. *Neurology* 54, 1089–1095. doi: 10.1212/WNL.54.5.1089

Thompson, P. M., Dutton, R., a, Hayashi, K. M., Lu, A., Lee, S. E., Lee, J. Y., et al. (2006). 3D mapping of ventricular and corpus callosum abnormalities in HIV/AIDS. *Neuroimage* 31, 12–23. doi: 10.1016/j.neuroimage.2005.11.043

Tisdall, M. D., Hess, A. T., Reuter, M., Meintjes, E. M., Fischl, B., and van der Kouwe, A. J. W. (2012). Volumetric navigators for prospective motion correction and selective reacquisition in neuroanatomical MRI. *Magn. Reson. Med.* 68, 389–399. doi: 10.1002/mrm.23228

Uban, K. A., Herting, M. M., Williams, P. L., Ajmera, T., Gautam, P., Huo, Y., et al. (2015). White matter microstructure among youth with perinatally acquired HIV is associated with disease severity. *AIDS* 29, 1035–1044. doi: 10.1097/QAD.0000000000000648

van Arnhem, L. A., Bunders, M. J., Scherpbier, H. J., Majoie, C. B. L. M., Reneman, L., Prinking, O., et al. (2013). Neurologic abnormalities in HIV-1 infected children in the era of combination antiretroviral therapy. *PLoS ONE* 8:e64398. doi: 10.1371/journal.pone.0064398

van der Kouwe, A. J. W., Benner, T., Salat, D. H., and Fischl, B. (2008). Brain morphometry with multiecho MPRAGE. *Neuroimage* 40, 559–569. doi: 10.1016/j.neuroimage.2007.12.025

van Rie, A., Harrington, P. R., Dow, A., and Robertson, K. (2007). Neurologic and neurodevelopmental manifestations of pediatric HIV/AIDS: a global perspective. *Eur. J. Paediatr. Neurol.* 11, 1–9. doi: 10.1016/j.ejpn.2006.10.006

Violari, A., Cotton, M. F., Gibb, D. M., Babiker, A. G., Steyn, J., Madhi, S. A., et al. (2008). Early antiretroviral therapy and mortality among HIV-infected infants. *N. Engl. J. Med.* 359, 2233–2244. doi: 10.1056/NEJMoa0800971

von Giesen, H. J., Niehues, T., Reumel, J., Haslinger, B. A., Ndagijimana, J., and Arendt, G. (2003). Delayed motor learning and psychomotor slowing in HIV-infected children. *Neuropediatrics* 34, 177–181. doi: 10.1055/s-2003-42205

Walsh, K. A., Megyesi, J. F., Wilson, J. X., Crukley, J., Laubach, V. E., and Hammond, R. R. (2004). Antioxidant protection from HIV-1 gp120-induced neuroglial toxicity. *J. Neuroinflammation* 1:8. doi: 10.1186/1742-2094-1-8

Whitehead, N., Potterton, J., and Coovadia, A. (2014). The neurodevelopment of HIV-infected infants on HAART compared to HIV-exposed but uninfected infants. *AIDS Care* 26, 497–504. doi: 10.1080/09540121.2013.841828

WHO (2013). *Consolidated Guidelines on the Use of Antiretroviral Drugs for Treating and Preventing HIV Infection Recommendations for a Public Health Approach.*

Woods, R. P. (2003). Multitracer: a java-based tool for anatomic delineation of grayscale volumetric images. *Neuroimage* 19, 1829–1834. doi: 10.1016/S1053-8119(03)00243-X

Yadav, S. K., Gupta, R. K., Garg, R. K., Venkatesh, V., Gupta, P. K., Singh, A. K., et al. (2017). Altered structural brain changes and neurocognitive performance in pediatric HIV. *Neuroimage Clin.* 14, 316–322. doi: 10.1016/j.nicl.2017.01.032

Yoon, U., Fonov, V. S., Perusse, D., Evans, A. C., and Brain Development Cooperative Group (2009). The effect of template choice on morphometric analysis of pediatric brain data. *Neuroimage* 45, 769–777. doi: 10.1016/j.neuroimage.2008.12.046

Conflict of Interest Statement: The authors declare that the research was conducted in the absence of any commercial or financial relationships that could be construed as a potential conflict of interest.

10.3 Appendix C: Mixed Effects Model Outcomes with BIC

Linear Model		Age at scan+ Dx +Sex + Age at scan:Dx							
		Controls			HIV+			Interaction Term	
		β_1	(SE)	*p*	β_1	(SE)	*p*	*p*	BIC
	L Caudate	**-68.10**	**21.45**	**0.002**	**-134.71**	**24.79**	**<0.001**	**0.045**	1828.28
	R Caudate	**-70.55**	**19.25**	**0.000**	**-139.14**	**22.57**	**<0.001**	**0.020**	1827.16
	L NA	-3.59	4.98	0.470	-6.53	5.76	0.260	0.700	1470.13
	R NA	**-10.20**	**5.86**	**0.090**	**-18.37**	**6.92**	**0.010**	0.370	1501.64
	CC	**-13.44**	**3.74**	**0.001**	**-9.43**	**4.31**	**0.030**	0.480	1377.40
	L Pu	5.03	16.04	0.760	**-122.46**	**18.45**	**<0.001**	**<0.001**	1747.18
	R Pu	-11.28	16.32	0.490	**-124.54**	**18.78**	**<0.001**	**<0.001**	1755.93
	L GP	**-27.70**	**12.90**	**0.035**	**-67.18**	**14.80**	**<0.001**	**0.047**	1643.67
	R GP	-45.33	12.79	<0.001	**-86.88**	**14.67**	**<0.001**	**0.036**	1642.44
Quadratic Model		Age at scan^2+age at scan+ Dx + Sex + Age at scan^2:Dx							
		Controls			HIV+			Interaction Term	
		β_1	(SE)	*p*	β_1	(SE)	*p*	*p*	BIC
	L Caudate	**60.18**	**10.04**	**<0.001**	**58.31**	**10.46**	**<0.001**	0.320	1803.25
	R Caudate	**50.24**	**9.33**	**<0.001**	**47.86**	**9.73**	**<0.001**	0.200	1807.70
	L NA	2.51	2.76	0.370	2.45	2.87	0.400	0.910	1475.68
	R NA	4.75	3.31	0.160	4.49	3.45	0.200	0.660	1505.89
	CC	**9.19**	**1.84**	**<0.001**	**9.78**	**1.92**	**<0.001**	**0.090**	1362.33
	L Pu	**20.32**	**9.02**	**0.030**	13.09	9.40	0.170	**<0.001**	1750.12
	R Pu	**28.33**	**8.89**	**0.002**	**22.38**	**9.26**	**0.018**	**<0.001**	1754.06
	L GP	29.46	6.73	<0.001	28.08	7.00	<0.001	0.250	1631.75
	R GP	33.47	6.38	<0.001	32.08	6.63	<0.001	0.220	1624.09
Cubic Model		Age at scan^3+Age at scan^2+Age at scan+Dx+Sex+Age at scan^3:Dx							
		Controls			HIV+			Interaction Term	
		β_1	(SE)	*p*	β_1	(SE)	*p*	*p*	BIC
	L Caudate	**60.18**	**10.04**	**<0.001**	**58.31**	**10.46**	**<0.001**	0.320	1803.25
	R Caudate	**50.24**	**9.33**	**<0.001**	**47.86**	**9.73**	**<0.001**	0.200	1807.70
	L NA	2.51	2.76	0.370	2.45	2.82	0.400	0.910	1475.68
	R NA	4.75	3.31	0.160	4.49	3.45	0.200	0.660	1505.89
	CC	**9.19**	**1.84**	**<0.001**	**9.78**	**1.92**	**<0.001**	**0.085**	1362.33
	L Pu	**20.32**	**9.02**	**0.027**	**13.09**	**9.40**	**0.170**	**<0.001**	1750.12
	R Pu	**28.33**	**8.89**	**0.002**	**22.38**	**9.26**	**0.018**	**<0.001**	1754.06
	L GP	**29.45**	**6.73**	**<0.001**	**28.07**	**7.00**	**<0.001**	0.250	1631.75
	R GP	**33.47**	**6.38**	**<0.001**	**32.08**	**6.63**	**<0.001**	0.220	1624.09
Logarithmic Model		Log(Age at scan)+Age at scan+Dx+Sex+Log(Age at scan):Dx+Age at scan:Dx							
		Controls			PHIV			Interaction Term	
		β_1	(SE)	*p*	β_1	(SE)	*p*	*p*	BIC
	L Caudate	**-12170.58**	**3170.03**	**<0.001**	**-20783.19**	**4339.11**	**<0.001**	0.113	**1769.2**
	R Caudate	**-9489.13**	**2924.68**	**0.002**	**-18330.58**	**4029.82**	**<0.001**	0.080	**1773.3**
	L NA	-83.56	881.12	0.925	-1659.95	1199.15	0.170	0.293	**1453.4**
	R NA	68.24	1036.14	0.948	**-3477.71**	**1411.95**	**0.016**	**0.046**	**1473.0**
	CC	**-2673.57**	**592.25**	**<0.001**	**-1844.80**	**799.64**	**0.024**	0.407	**1334.3**
	L Pu	902.37	2718.81	0.741	**-13694.30**	**3534.09**	**<0.001**	**0.001**	**1706.1**
	R Pu	-1140.89	2689.44	0.673	**-15855.21**	**3497.34**	**<0.001**	**0.001**	**1710.8**
	L GP	**-6247.21**	**2192.48**	**0.006**	**-9505.12**	**2827.39**	**0.001**	0.365	**1608.6**
	R GP	**-8604.64**	**2087.79**	**<0.001**	**-8489.11**	**2695.32**	**0.002**	0.973	**1593.2**

Values are unstandardised Betas
Bolded Values indicate significance at p<0.10
Strongest model fit indicated with bolded BIC value for each structure.